

General Disclaimer

One or more of the Following Statements may affect this Document

- This document has been reproduced from the best copy furnished by the organizational source. It is being released in the interest of making available as much information as possible.
- This document may contain data, which exceeds the sheet parameters. It was furnished in this condition by the organizational source and is the best copy available.
- This document may contain tone-on-tone or color graphs, charts and/or pictures, which have been reproduced in black and white.
- This document is paginated as submitted by the original source.
- Portions of this document are not fully legible due to the historical nature of some of the material. However, it is the best reproduction available from the original submission.

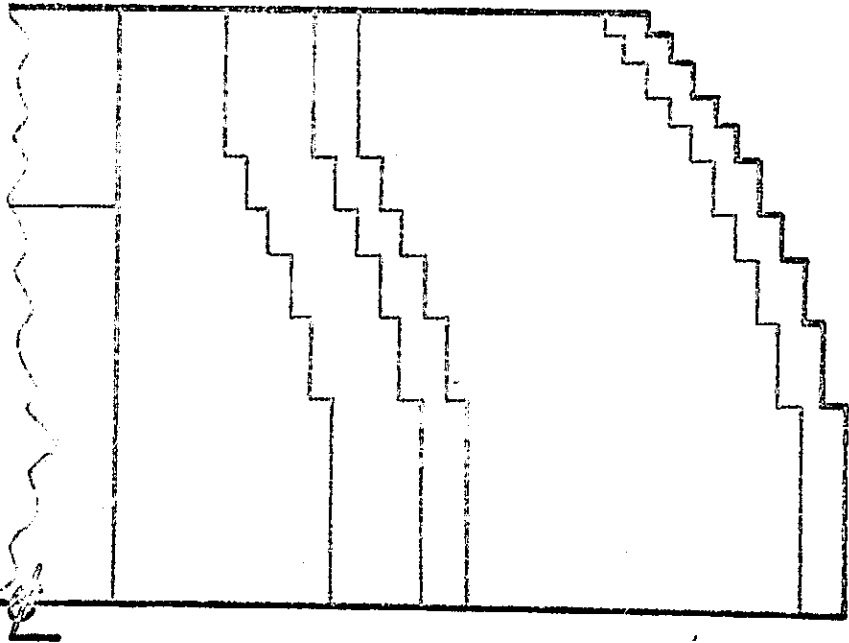
EVALUATION OF

$$K = \frac{Pe^{-\mu r}}{4\pi r^2}$$

$$\Delta \bar{N} + \sigma \bar{N} = S$$

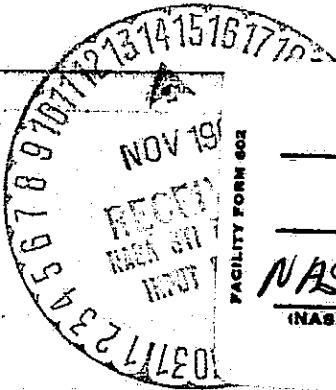
$$X = \frac{-\ln R}{\Sigma}$$

METHODS
FOR
COMPUTING



NUCLEAR ROCKET
RADIATION FIELDS

CONTRACT NAS 8-9500



N70-12633

(ACCESSION NUMBER)

128

(PAGES)

NASACR-102338

(NASA CR OR TMX OR AD NUMBER)

(THRU)

24

(CODE)

(CATEGORY)



LOCKHEED NUCLEAR PRODUCTS

Lockheed-Georgia Company -- A Division of Lockheed Aircraft Corporation

ER 8236

EVALUATION OF METHODS
FOR COMPUTING
NUCLEAR ROCKET RADIATION FIELDS
NAS 8-9500
TASK 2.10

Prepared For:
GEORGE C. MARSHALL SPACE FLIGHT CENTER

Prepared By:
LOCKHEED GEORGIA NUCLEAR LABORATORY

LOCKHEED GEORGIA NUCLEAR LABORATORY
Lockheed-Georgia Company - A Division of Lockheed Aircraft Corporation

If this document is supplied under the requirements of a United States Government contract, the following legend shall apply unless the letter U appears in the coding box.

This data is furnished under a United States Government contract and only those portions hereof which are marked (for example, by circling, underscoring or otherwise) and indicated as being subject to this legend shall not be released outside the Government (except to foreign governments, subject to these same limitations), nor be disclosed, used, or duplicated, for procurement or manufacturing purposes, except as otherwise authorized by contract, without the permission of Lockheed-Georgia Company, A Division of Lockheed Aircraft Corporation, Marietta, Georgia. This legend shall be marked on any reproduction hereon in whole or in part.

The "otherwise marking" and "indicated portions" as used above shall mean this statement and include all details or manufacture contained herein respectively.

Contract NAS 8-9500

Code U

FOREWORD

This document is submitted to the George C. Marshall Space Flight Center, Huntsville, Alabama, by the Lockheed-Georgia Company, Marietta, Georgia. This report contains final results of analyses performed in satisfaction of Task 2.10 of Contract NAS 8-9500. Work was performed by the Lockheed-Georgia Company under an interdivisional contract arrangement with the Lockheed Missiles and Space Company, the prime contractor for this contract.

The report describes critical evaluations of a series of computer programs suitable for theoretical predictions of radiation fields in RIFT vehicles and other nuclear rocket systems. Ten computer programs covering point-kernel, discrete ordinates and Monte Carlo methods have been examined as a part of this study.

TABLE OF CONTENTS

	Page
FOREWORD	i
TABLE OF CONTENTS	iii
LIST OF FIGURES	v
 1.0 INTRODUCTION	 1
 2.0 OPERATIONAL CHARACTERISTICS OF SELECTED CODES	 5
2.1 POINT-KERNEL METHOD	5
2.1.1 14-0 And 14-1 Programs	5
2.1.2 QAD-P5 And QAD-IV Programs	8
2.2 DISCRETE ORDINATES METHOD	10
2.2.1 DDK Program	10
2.2.2 DTK Program	12
2.3 MONTE CARLO METHOD	12
2.3.1 18-0 Program	12
2.3.2 MCS Program	20
2.3.3 MCG Program	23
2.3.4 O5R Program	24
2.4 PROGRAM COMPARISON	26
2.4.1 Detail And Direct Usefulness Of Output	26
2.4.2 Generality Of Problems Which May Be Treated	28
2.4.3 Operational Problems	28
2.4.4 Program Running Time	31
 3.0 COMPARATIVE ACCURACY	 37
3.1 PROBLEMS TREATED	37
3.2 COMPARISON OF GAMMA RAY COMPUTATIONS	47

PRECEDING PAGE BLANK NOT FILLED

TABLE OF CONTENTS
(Continued)

	Page
3.3 COMPARISON OF NEUTRON COMPUTATIONS	64
4.0 SUMMARY	99
5.0 CONCLUSIONS	101
6.0 RECOMMENDATIONS	103
APPENDIX A BASIC CROSS SECTION DATA	105

LIST OF FIGURES

Figures		Page
FIGURE 1	RELATIONSHIP OF PROGRAM 18-0 AND AUXILIARY PROGRAMS	16
FIGURE 2	PROGRAM OUTPUT	27
FIGURE 3	FEATURES OF POINT KERNEL PROGRAMS	29
FIGURE 4	FEATURES OF MONTE CARLO PROGRAMS	30
FIGURE 5	COMPUTER TIME - POINT KERNEL	33
FIGURE 6	COMPUTER TIME - DISCRETE ORDINATES	34
FIGURE 7	COMPUTER TIME - MONTE CARLO	35
FIGURE 8	CONFIGURATION A	38
FIGURE 9	SHIELD MODELS	39
FIGURE 10	REGIONAL COMPOSITIONS - g/cm^3	41
FIGURE 11	FISSION DISTRIBUTION (RELATIVE UNITS)	42
FIGURE 12	GAMMA SOURCE SPECTRUM	43
FIGURE 13	PROPELLANT TANK MODEL GAMMA	44
FIGURE 14	PROPELLANT TANK MODEL NEUTRON	45
FIGURE 15	CONFIGURATION B APPROXIMATIONS	46
FIGURE 16	GAMMA DOSE RATE ($Z = 93 \rightarrow 338 \text{ CM}$)	48
FIGURE 17	GAMMA DOSE RATE ($Z = 157.5 \text{ CM}$)	49
FIGURE 18	GAMMA DOSE RATE ($Z = 178 \text{ CM}$)	50
FIGURE 19	GAMMA DOSE RATE ($Z = 192 \text{ CM}$)	51
FIGURE 20	GAMMA FORWARD CURRENT ($Z = 157.5 \text{ CM}$)	53
FIGURE 21	GAMMA FORWARD CURRENT ($Z = 178 \text{ CM}$)	54
FIGURE 22	GAMMA FORWARD CURRENT ($Z = 182 \text{ CM}$)	55
FIGURE 23	CONFIGURATION B, GAMMA DOSE RATE ($Z = 183.9 \text{ CM}$)	56
FIGURE 24	SHIELD GAMMA HEATING, CONFIGURATION A	58
FIGURE 25	GAMMA SPECTRA, AXIAL BIAS ($Z = 192 \text{ CM}$, $R = 0 \rightarrow 39 \text{ CM}$)	59

LIST OF FIGURES (Continued)

Figures		Page
FIGURE 26	GAMMA LEAKAGE CURRENT ON RADIAL BOUNDARY (R = 66 CM)	60
FIGURE 27	GAMMA DOSE RATE ON RADIAL BOUNDARY (R = 66 CM)	61
FIGURE 28	GAMMA SPECTRA, RADIAL BIAS (R = 66 CM, Z = 50→80 CM)	63
FIGURE 29	PROPELLANT GAMMA ENERGY DEPOSITION (WATTS)	65
FIGURE 30	GAMMA DOSE RATE, PROPELLANT TANK TOP (Z = 1729 CM)	66
FIGURE 31	NEUTRON DOSE RATE (Z = 93 CM)	67
FIGURE 32	NEUTRON DOSE RATE (Z = 164 CM)	68
FIGURE 33	NEUTRON DOSE RATE (Z = 184 CM)	69
FIGURE 34	NEUTRON DOSE RATE (Z = 260 CM)	70
FIGURE 35	NEUTRON DOSE RATE (Z = 338 CM)	71
FIGURE 36	NEUTRON FLUX (Z = 93 CM)	74
FIGURE 37	NEUTRON DOSE RATE (Z = 164 CM)	75
FIGURE 38	NEUTRON DOSE RATE (Z = 183.9 CM)	76
FIGURE 39	NEUTRON FLUX AND FORWARD CURRENT (Z = 165 CM)	77
FIGURE 40	NEUTRON FLUX AND FORWARD CURRENT (Z = 183.9 CM)	78
FIGURE 41	NEUTRON FLUX AND FORWARD CURRENT (Z = 192 CM)	79
FIGURE 42	RADIATIVE CAPTURE EVENTS	80
FIGURE 43	CONFIGURATION B, NEUTRON DOSE RATE (Z = 184 CM)	82
FIGURE 44	CONFIGURATION B, NEUTRON DOSE RATE (Z = 183.9 CM)	83

LIST OF FIGURES (Continued)

Figures	Page
FIGURE 45 CONFIGURATION B, NEUTRON DOSE RATE (Z = 338 CM)	84
FIGURE 46 SHIELD NEUTRON HEATING, CONFIGURATION A	85
FIGURE 47 NEUTRON SPECTRA	87
FIGURE 48 NEUTRON SPECTRA NORMALIZED AT 3 MeV	88
FIGURE 49 NEUTRON FLUX AND CURRENT ON RADIAL BOUNDARY (R = 66 CM)	89
FIGURE 50 NEUTRON DOSE RATE (R = 124 CM)	91
FIGURE 51 NEUTRON SPECTRA NORMALIZED AT 3 MeV	92
FIGURE 52 NEUTRON HEATING AT PROPELLANT TANK EDGE	93
FIGURE 53 NEUTRON HEATING PARALLEL TO TANK AXIS (R = 490 CM)	94
FIGURE 54 PROPELLANT NEUTRON ENERGY DEPOSITION (WATTS)	96
FIGURE 55 NEUTRON DOSE RATE, PROPELLANT TANK TOP (Z = 1729 CM)	97




1.0 INTRODUCTION

Prior to commencement of the work reported here, discrepancies had been noted among theoretical predictions of radiation fields in RIFT vehicles and other nuclear rocket systems. These discrepancies were substantially larger than might have been expected on the basis of published results for elementary configurations. Since the design analyses were made by several contractors, assignment of the cause of differences was seldom feasible; usually the computational technique, basic data, and model of the system configuration had been varied simultaneously. Hence a critical evaluation of pertinent computer programs, emphasizing usefulness in future analysis and design of nuclear rocket systems, appeared highly desirable. The description and results of such an evaluation are presented in this report.

The analyses undertaken are intended to be quite general in scope, subject to the restriction that only methods directly applicable to nuclear rocket design analyses are treated. Thus only the gross features of vehicle and engine design are preserved, to the minimum extent believed capable of representing the fundamental difficulties encountered in practical design problems. On the other hand, the problems treated are more difficult than those usually treated in comparison of methods. Several methods and codes of theoretical importance are omitted because of inability to treat even a crude representation of a nuclear rocket.

The point-kernel, discrete ordinates* and Monte Carlo methods have most commonly been applied in nuclear rocket studies, and a preliminary survey of available codes disclosed no cogent reason for expanding this list. Particular codes selected for

*The general term "discrete ordinates" is used here in preference to " S_n Method" because in some of the early literature the latter implies a particular angular quadrature which is now seldom used and because in one-dimensional codes a P_n or DP_n quadrature may be substituted.



investigation included, initially, the following:

Point-kernel programs 14-0 (and 14-1), QAD-P5 (and QAD-IV), C-17;
Discrete ordinates programs DDK and DTK; and
Monte Carlo programs 18-0, MCS and MCG, O5R, COHORT.

The C-17 Program was deleted after cursory examination disclosed no apparent advantage over the later QAD programs. The O5R Program became generally available quite late in the contract period and hence did not receive the emphasis it otherwise would have merited. Revisions of the promising COHORT Program, currently in progress, have prevented its inclusion. The remaining Monte Carlo programs, however, appear representative of specialized (18-0) and flexible (MCS/MCG) Monte Carlo techniques.

The criteria adopted for code evaluation are:

- Type and detail of data obtainable;
- Flexibility for treatment of system configuration, radiation sources, and types of radiation interaction;
- Computer running time and time required for problem preparation;
- Relative difficulty of operation; and
- Comparative accuracy of output.

The first four criteria are treated in Section 2.0 of the present report, together with such abbreviated code descriptions as appear necessary for intelligibility of results. The last, and clearly most difficult, criterion is treated in Section 3.0, which includes a description of the test problems treated. It should be noted that a set of "standard" microscopic cross sections, listed in Appendix A, were assumed for all except point-kernel computations. Thus differences among corresponding computations

reflect, primarily, differences in radiation transport model and generality of geometric representation.

2.0 OPERATIONAL CHARACTERISTICS OF SELECTED CODES

In the following discussion, a general familiarity with point-kernel, discrete ordinates and Monte Carlo techniques is presumed. Salient characteristics of specific codes are described in a subsection for each method; the fullest available descriptions and operating instructions are referenced throughout the text. A comparison of operational features of the several codes concludes this section.

2.1 POINT-KERNEL METHOD

2.1.1 14-0 And 14-1 Programs

The 14-series programs, Reference 1, are the last in a series of point-kernel programs initiated by the ANP Division of the General Electric Company. The versions of these programs used in the present study were coded in FAP language for the IBM-7090/7094 Computer and modified by Lockheed for compatibility with the FORTRAN II monitor system. The sole difference between 14-0 and 14-1 is in their treatment of the spatial distribution of radiation sources (or reactor power). 14-0 requires separable axial and radial distribution functions, fitted piecewise by cosine or exponential functions, with the results normalized to the desired reactor power; 14-1 requires the power per unit volume as direct input for each R-Z ring of source points. For both codes the number of sources in each ring may vary with R. Power distributions must be input as absolute quantities since the programs have no self-normalization capability.

These programs treat cylindrical source regions or any degenerate form (point, plane, or line) thereof. Multiple source regions and up to six gamma source types (different gamma source spectra) may be treated. Thus a system incorporating clustered reactors can be treated as a single problem, as can systems involving production of secondary gamma radiation from several different materials.

PRECEDING PAGE BLANK NOT FILMED.

System configuration must be approximated by regions generated through certain allowed rotations or translations of quadrilaterals. The generation of regions by rotation is restricted to rotation of trapezoids about the system Z-axis, or any axis parallel thereto. Translation must be parallel to either the X, Y, or Z axis. The specification of system geometry consists of a series of "master regions", each of which may contain a set of smaller "basic regions". The penetration distance through each material along the line of sight is obtained by a stepping routine with a specific step size associated with each master region. A large percentage of the total computing time is spent on this stepping procedure, making it imperative that the master region step sizes be chosen with care.

One of the principal operational difficulties encountered in using the 14-series is an error stop resulting from calculation of "negative path lengths". In all cases observed, the difficulty arose in stepping across a conical surface generated by rotation of a trapezoid. While the basic cause remains unknown, a minor modification of the input geometric parameters always proved sufficient to alleviate the problem.

The 14-series neutron calculation emphasizes a modified Albert-Welton attenuation kernel. For the present analyses, coefficients for this kernel were taken from Reference 2. These represent a semi-empirical fit to bulk-shielding data obtained using the Battelle Memorial Institute source plate. The broad-beam fast neutron removal cross-sections for non-hydrogeneous materials were also taken from Reference 2. An alternate kernel is allowed in the 14-1 series programs, to be applied to each source-detector path which encounters less than a preselected amount of hydrogen. This alternate kernel may be fitted to moments method data for non-hydrogeneous infinite media. Adjustment of the leading coefficient for detectors located in vacua is, of course, possible.

As an option, an estimate of neutron differential number flux may be computed. This calculation uses a bivariate polynomial fitting of NDA moments-method results. The

calculated differential number flux is normalized, internally, to the Albert-Welton dose rate. With some difficulty such data may be converted to energy deposition in an arbitrary medium. Because of the tediousness of this procedure, however, it was applied at only a few points for the present computations. The ratio of energy deposition to tissue dose, assumed constant for neighboring points, was applied as a correction to the Albert-Welton kernel, or occasionally to the computed tissue response. In this approximate form, however, computation of multiple responses is relatively easy.

The treatment of gamma rays consists of an exponential attenuation, combined with a third-degree polynomial buildup factor. The 14-series allows the option of using Kalos' formulae for buildup in two-layer media (either light-heavy or heavy-light), but for the present study only the single layer form with the buildup based on a light material (water) was used. Gamma ray total attenuation coefficients were taken from Reference 3. The coefficients of the buildup polynomial were taken from Reference 4. The programs also contain capability for computing gamma ray energy flux based on a bivariate polynomial fit to moments-method data. As for neutrons, only a single gamma ray response is provided by the programs. Since the gamma ray calculation is multi-group, conversion to different responses by hand is tedious. Hence, for computation of energy deposition in several detector materials, these programs are relatively inconvenient.

Preparation of a problem for the 14-series programs involves no particular difficulties. Setting up the geometry usually consists of preparing a scale drawing of a section through the system, dividing it into trapezoids and rectangles, and reading the coordinates of the corners of these figures for input to the program. Experience shows that trapezoidal representation should be used sparingly, in order to avoid the error stop described earlier. Linear absorption coefficients are required, often necessitating manual correction of available mass absorption data. Consistent with the linear attenuation coefficients, region compositions are given as volume fractions of

each material in the system; again, this may be slightly less convenient than specifying compositions directly in gm/cm^3 of each material in a region. The most time-consuming task in the preparation of a 14-0 problem is the fitting and normalization of the power distribution. A small auxiliary computer program for normalization of this function reduced the amount of hand calculation required, but this program is not generally available. In their basic form, the 14-series makes no provision for this calculation.

2.1.2 QAD-P5 And QAD-IV Programs

At the commencement of the present study, QAD-IV and QAD-P5, Reference 5, were the latest in a series of point-kernel programs developed by the Los Alamos Scientific Laboratories. The versions used in this study are written in the FORTRAN II programming language, although FORTRAN IV versions have also been written. In effect, QAD-IV is a simplified, and hence faster, modification of QAD-P5. The following description applies to both, except as noted.

QAD treats a single source-region, which must be cylindrical in the case of QAD-IV, and a single gamma-source spectrum. Spatial distribution must be approximated by separable functions of R and Z, with the same number of source points in each ring. The separate R and Z functions may either be specified as point functions or fitted by cosines. Piecewise fitting, however, is not permissible. In either, normalization to specified power level or total source strength is accomplished internally. Unlike 14-0, the equivalent source points treated lie at the center of the source cells, rather than at the corners.

The QAD geometry routine can treat complex configurations comprising numerous regions bounded by planes or certain quadric surfaces. Allowable quadric surfaces are those symmetric about one of the three major axes, although some care is required to preclude unwanted reflections. Path lengths through successive regions along a line of sight are computed directly without iterative stepping. Appreciable savings of

computer time are possible by judicious ordering of input describing the regions and boundaries and by specification for each region of the region most likely to be next entered. Further, boundaries not intersected by any source-detector path need not be described.

The most significant differences between the QAD versions lies in the treatment of neutron transmission. Both compute an Albert-Welton kernel estimate of tissue dose (or other response), but QAD-P5 emphasizes additional data not available with QAD-IV. These data comprise neutron flux, energy flux, number spectrum, tissue dose rate, and energy deposition in up to four arbitrarily chosen materials. Computation is based on an input library of transmitted spectra, as computed by the moments method for five different media. Interpolation for depth of penetration is accomplished according to the total removal cross section for each source-detector path. Up to five estimates for each output quantity may be obtained, one for each equivalent medium. For some detector points within a complex configuration, selection of a plausible weighted average could be most perplexing.

Treatment of gamma radiation transmission is similar to that of 14-0 except that two-layer buildup functions are precluded. QAD-P5 output is more complete, however, comprising uncollided and total dose rate, energy deposition in up to four other materials, an approximate energy flux, and buildup factors for these quantities. For the present computations, absorption coefficients and buildup factors were identically those used with 14-0.

Preparation of a problem for QAD is easily accomplished. Self-normalization of the source (where total power is an input quantity) and use of mass attenuation coefficients and material compositions in mass per unit volume result in reduced preparation times. Perhaps the most difficult task is the fitting of second-degree boundary surfaces. Use of the FORTRAN language, and incorporation of numerous subroutines, make QAD particularly adaptable to modification should this appear desirable.

2.2 DISCRETE ORDINATES METHOD

The modus operandi of the two dimensional DDK and one dimensional DTK discrete S_n codes developed at the Los Alamos Scientific Laboratory, is fully described in Reference 6. Reference 7 gives complete, though informal, operating instructions. Both codes are written in the FLOCO language and suffer the disadvantage of incompatibility with the IBM-7094 monitor; however a FORTRAN version of DDK, Reference 8, prepared at the Oak Ridge National Laboratory is expected to be generally available in the near future.

2.2.1 DDK Program

The output from DDK of principal interest for present purposes comprises neutron fluxes at each point of a rectangular mesh lying in the R-Z plane. Total flux and partial fluxes, corresponding to the energy groups specified, are obtained. Computation of other measures of radiation intensity depends upon hand calculation or preparation of a simple satellite code. The latter approach appears particularly attractive since DDK can, at option, output fluxes on either magnetic tape or punch cards. One convenient feature of the output is the preparation of maps of the point mesh, coded by region symbol and by index of material composition. A limited output at the conclusion of each outer iteration is useful in estimating the degree of convergence achieved. Total leakage currents across outer boundaries of a system are also output.

Flexibility for approximation of complex configurations is severely limited by the inherent imposition of axial symmetry and a rectangular R-Z mesh. Thus boundaries of non-cylindrical regions must be approximated by step-functions. Since the FLOCO system allocates storage at the time of execution, the maximum mesh size is indeterminate; however, slightly over 800 points seem to be a practical limit. This limitation may be eased somewhat by specification of a plane of specular reflection when appropriate. Neutron sources may be treated either as constant for specified mesh points or as the natural consequence of fission events. In most of the present computations,

the latter approach was taken, in conjunction with an iterative search for system reactivity. In either method the specification of source spectrum must correspond to the group structure selected.

The fictitious neutron reactions treated are transport, production (fission), absorption, and group-to-group transfer (optionally including up-scatter). Since almost any set of real reactions can be approximated within the above framework, flexibility in treatment of reaction type can be considered only in terms of accuracy of the approximation. For present purposes a set of 15-group cross sections was prepared. Except for hydrogen, the "standard" cross sections used for Monte Carlo computations were averaged for each energy group, weighted by a representative neutron spectrum which had earlier been computed as part of the RIFT vehicle design effort. Fortunately the weighting function proved to be close to the presently computed spectra down to energies of a few eV. "Hot" and "cold" cross sections, corresponding to different thermal bases in the core and shield, were used for materials appearing in both regions. The anisotropic hydrogen cross sections used were taken from a Los Alamos compilation of 18-group cross sections due to C. Mills, truncated for the raised thermal base.

An S_4 quadrature due to Lee, Reference 6, was used throughout except for one minor S_2 computation. Computations prior to commencement of the present study had resulted in fair agreement ($\sim 5\%$) between S_4 and S_6 flux estimates for a NERVA engine, excepting low energy fluxes in highly absorbing regions where the optical mesh-width was unduly coarse. Hence, investigation of higher S_n approximations seemed relatively infertile.

Initial preparation of DDK problems is complicated only by uncertainty whether data storage is adequate for a large problem. Once over this hurdle, several computations of a few iterations each may be required for final adjustment of mesh spacing. If group fluxes at adjacent mesh points vary by a factor much larger than two, the corresponding difference equation fails locally and convergence to a useful solution

cannot be expected. Some of the effort expended can be retrieved, however, by outputting results of preliminary iterations on tape for use in starting successive iterations.

It has been suggested that computer time may be saved by using a low order, e.g. S_2 , approximation for early iterations. But a saving is by no means certain. When applied to one configuration, described in Section 3, the S_2 approximation proved wholly inadequate in the vicinity of stepped boundaries, and a net loss probably resulted.

2.2.2 DTK Program

Usage of this program differs from that of DDK primarily in the obvious details contingent upon the dimension of the point mesh. Slab, cylindrical or spherical configurations may be treated; a diffusion approximation of transverse leakage is provided optionally. Output is more complete than for DDK. Angular flux-distributions and neutron reaction rates may be obtained for preselected mesh points.

2.3 MONTE CARLO METHOD

2.3.1 18-0 Program

18-0, Reference 9, is a specialized Monte Carlo computer program designed to investigate and determine nuclear heating rates and neutron and gamma leakage distributions in energy and angle for cylindrically symmetric reactor-shield systems. The program provides only as much geometry and importance sampling capability as were needed for analysis of GE-ANPD reactor-shield systems. Specialization in these areas provided a more efficient code for intended applications than the more general purpose Monte Carlo codes. Because this specialization is largely applicable to the treatment of nuclear rocket vehicle configuration, the program is included in the present study.

The program is coded in FAP language for the IBM-7090/7094 computer. Up to 7 magnetic tapes are required in its use.

Two reactor description capabilities are provided by the program. The shield region geometry routine can be utilized to describe reactors that can be approximated by contiguous regions of homogeneous composition which possess cylindrical symmetry about the reactor-shield assembly axis. A reactor geometry subroutine, separate from the shield geometry subroutine, is provided in the program for the description of reactors with off-axis cylindrical fuel tubes. In the present investigation this geometry routine was not used. The portion of a reactor-shield assembly is described by regions which are formed by rotation of a class of simply connected quadrilaterals about the reactor-shield assembly axis. Each region is composed of a homogeneous mixture of the basic materials of which the region is composed.

The spatial and energy coordinates of source neutrons and protons are generated by an auxiliary code, Program 20-0, which places the source particle parameters on tape for use as input to Program 18-0. Direction cosines of a source particle are chosen by Program 18-0 from an isotropic distribution in the laboratory system.

A collision event is selected by random sampling from the appropriate discrete distributions for all neutron or gamma ray events allowed in the program. Neutron events treated by the program are:

- Elastic scattering,
- Inelastic scattering,
- Radiative capture,
- Neutron capture with alpha emission,
- $n, 2n$ reaction in beryllium, and
- Absorption with no secondary emission.

Photon events treated by the program are:

- Compton scattering,
- Absorption (photoelectric and pair production), and
- Photoneutron reaction.

The angular distribution of elastically scattered neutrons may be isotropic or anisotropic in the center-of-mass system at the discretion of the user. Inelastically scattered neutrons, neutrons from the $(n, 2n)$ reaction and secondary photons are treated by 18-0 to be emitted isotropically in the laboratory system.

Angular distribution of scattered photons is computed by the Klein-Nishina formula. The angular distribution of photoneutrons is described by a second degree polynomial in the cosine of the polar scattering angle in the center-of-mass system.

Bias sampling techniques of splitting and Russian roulette on region and energy for neutrons and on region for photons are optionally allowed in the program; these techniques are the only importance sampling capabilities included in the program.

Output available from the program for each shield region includes:

- Neutron and gamma energy deposition,
- Neutron and gamma particles suffering energy cut-off,
- Neutron and gamma particle currents across specified boundaries,
- Number of neutron and gamma particles absorbed,
- Number of (n, α) reactions,
- Number of (n, γ) reactions, and
- Number of inelastic scattering events.

Also included in the output is the neutron and gamma energy-angle leakage distribution for a point source equivalent to the assembly, or, optionally a tape record of the

parameters of escaping particles. In addition a tape record of generated secondary particles may form part of the output when desired. Program 18-0 will accept an escape or secondary particle tape and continue the history of each particle listed as long as the program region description is compatible with the region number and weight of the escape or secondary particle. Use of the escape tape as a source of output data requires the use of an auxiliary routine, Program 20-8, which analyzes the escape tape and computes leakage current as a function of energy and angle emitted from specified surface areas of the reactor shield assembly.

Program 18-0 requires extensive and sometimes redundant information about the reactor and shield configuration, source data and interaction probabilities to operate efficiently. Preparation of this information in a form acceptable to Program 18-0 is greatly facilitated by a series of eight satellite programs, References 10 through 17, which perform numerous calculations on basic data available from the problem and/or from standard sources. A brief description of each satellite program, its relation to 18-0 and any difficulties in its use are summarized below. A block diagram depicting the relationship of each program to Program 18-0 and to each other (if any) is shown in Figure 1.

Satellite program 20-2 approximates the energy dependence of the cross section for a specified event by discontinuous straight line segments across arbitrarily specified energy groups. Input preparation for Program 20-2 is basically a straightforward compilation of point cross section data for each event, and output from the program is available on punched cards suitable for input to Program 18-0 and Program 20-3.

Program 20-3 computes the total macroscopic cross section and collision probabilities for a material composition given the densities, atomic weights, volume fractions, and microscopic cross sections (computed in 20-2) of all constituent materials. Input preparation for the program is fairly easy with the punched card output of 20-2; however, the order of cross section input data on material and collision type does require

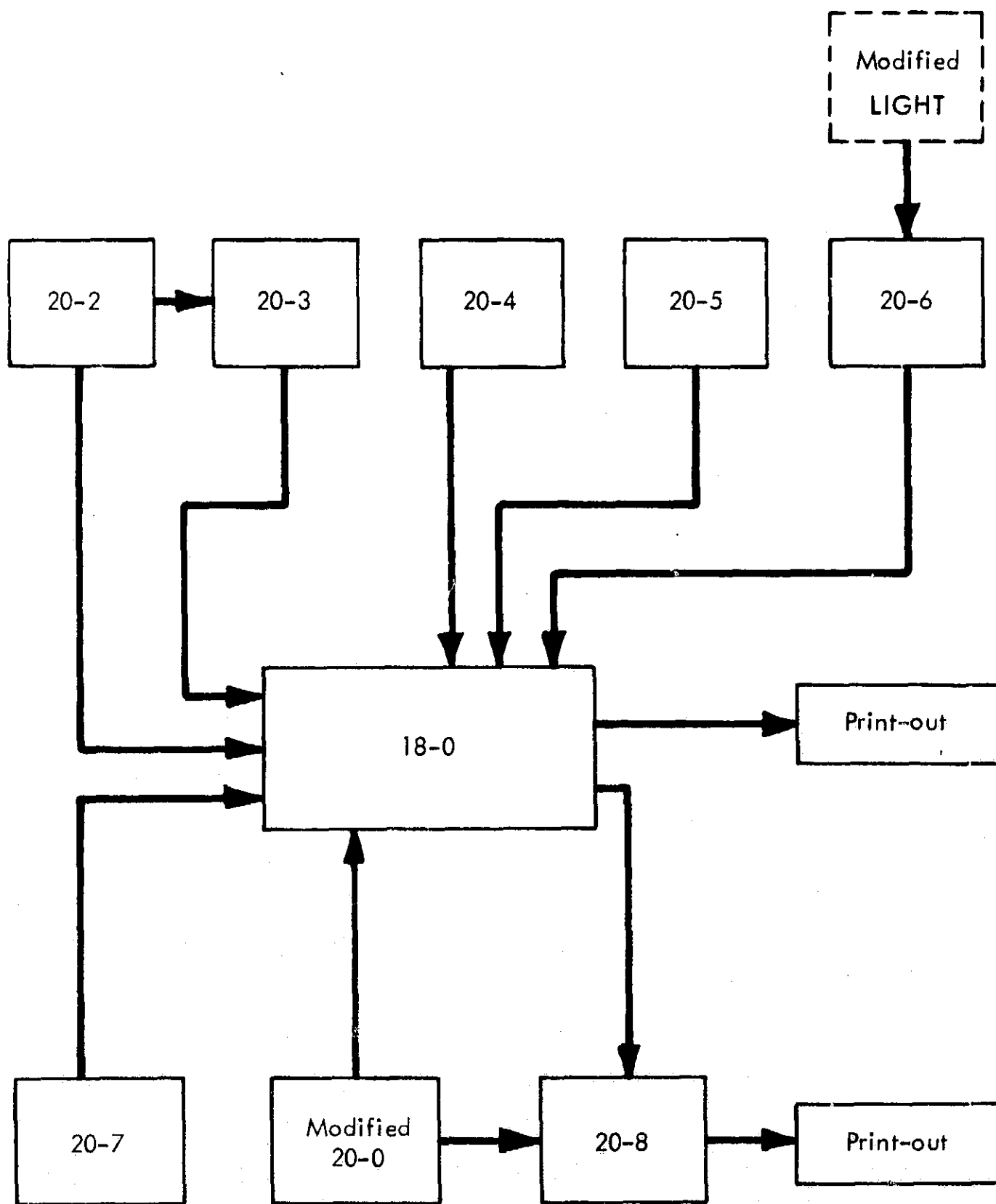


FIGURE 1 RELATIONSHIP OF PROGRAM 18-0 AND AUXILIARY PROGRAMS

special care to avoid errors. Output from the program is available on punched cards suitable for input to Program 18-0.

Program 20-4 averages input differential scattering cross sections over arbitrarily spaced energy groups to obtain group averaged angular distribution data. These data are prepared in the form of cumulative probability tables and are punched on cards suitable for use in Program 18-0.

In Program 18-0 the post collision energy of a neutron undergoing inelastic scattering and the number and energies of subsequent gamma rays from the reaction are determined by one of two schemes. Choice of the scheme used is determined by the separation of the incident neutron energy into collisions of high or low energy. High energy inelastic scattering data required by 18-0 are cumulative probability tables for the energy spectra of the scattered neutrons. Program 20-5 utilizes the evaporation model of nuclear reactions to determine these cumulative probability distributions for energy spectra of inelastically scattered neutrons and places the distribution data on punched cards for input to Program 18-0.

Low energy inelastic scattering data required by 18-0 requires a detailed description of the energy level structure and associated excitation and transition probabilities for the residual nucleus. This information is partially supplied by Program 20-6, which computes excitation and transition probabilities for excited states of the residual nucleus from an inelastic scattering reaction given the relative gamma transition intensities that occur in the process and the energy level structure of the nucleus. For many excited nuclei, and in particular for those of the present investigation, the relative intensity data of gamma transitions are not available. To circumvent this lack of data a special modification of a program called LIGHT, Reference 18, (developed by Lockheed for space radiation shielding studies) was used to approximate the gamma transition intensities.

The LIGHT code estimates gamma spectra resulting from inelastic nucleon-nucleus collisions. These computations are based upon a simple statistical model of the nucleus supplemented by a knowledge of low-lying nuclear levels.

Two methods of describing the shield configuration geometry are available. One method is by direct card input to 18-0. In the other method the geometry input to 18-0 can be simplified by using auxiliary Program 20-7. Input to Program 20-7 is less complex and the amount of input is reduced by about 45% from the amount of direct input required by 18-0 to describe a shield configuration. Program 20-7 performs numerous adjustments and calculations on its input data and produces as primary output a binary deck of cards to be inserted in the 18-0 binary deck.

Considerable difficulty was encountered, however, when using 20-7 to describe very simple shield configurations. The reason for the failure of 20-7 to handle simple configurations was not determined. For simple configurations, however, direct input data cards to 18-0 can be used and can be prepared in a reasonably short time.

The Monte Carlo source program used in the present investigation is an extensive modification of the General Electric Program 20-0, which computes and writes on-tape source particle parameters to be used as input for Program 18-0. In the modified program particle coordinates are chosen by a random method from power density distributions in a systematic fashion that determines the number of particles to be started from specified volume elements, which make up a cylindrical core. Particle energy is also chosen by a random method from a spectral distribution, and provision is made in the program for splitting on region and energy to conform to the needs of Program 18-0.

Occasionally in the use of the source program, output tapes with an erroneous record gap were produced although the program had indicated that a normal tape had been prepared. Subsequent use of the tape by 18-0 would cause a program stop or sometimes

would give erroneous results due to a shortage in the number of particle parameter records processed by 18-0. Recent modifications on the 20-0 program have corrected this intermittent tape error.

Although not used for preparation of input data for 18-0, another program, 20-8, is briefly described here for completeness of the 18-0 satellite program series. Program 20-8 interprets and analyzes Program 20-0 source particle output tapes or Program 18-0 escape particle tapes. Source tapes produced by Program 20-0 may be analyzed to determine the number of particles generated in specified core volume elements and energy groups. This option of 20-8 was not used since the modified version of 20-0 computes and prints out this data directly. As another option an output escape tape from 18-0 may be analyzed to determine the number of particles leaving the reactor-shield assembly through specified surface areas with energy and direction lying in specified energy-angle bins. Leakage currents are then computed from these data. This option was used extensively in the present investigation to compute leakage current across specified boundaries.

The principle difficulty encountered in the use of 20-8 was the uncovering of a discrepancy between the 20-8 leakage current (when normalized to current count) and the current count as tallied directly by 18-0. This discrepancy was found to be due to an error in solid angle as computed by 20-8. Since no source deck was available for easy program change, compensation for the error was made by a multiplicative factor in the 20-8 input.

In the event of a program stop due to an input or program error, Program 18-0 will in most cases print out an error indicator. This serves as a valuable aid in recognizing and locating the type of error encountered. The most frequent and troublesome error encountered in the operation of 18-0 in the present investigation was tape error, especially in the output escape tape.

Program 18-0 also has as an option a feature to write all pertinent information in the computer memory on tape after every specified number of particle parameter records have been run. This memory dump is a safety factor against possible loss of computer time due to machine error or power failure. The information on the memory dump tape can be retrieved by using a restart option of the program. Since, in the present investigation, all source particles were processed in relatively small batches (2,000 to 4,000), no large computer time was ever at stake and the memory dump option was not used.

The addition or alteration of input data to a problem to which 18-0 is applied is straightforward; however, changes in energy grouping, cross section or material requires the rerun of several or all of the auxiliary programs described above. Changes in geometry, statistical weights, source distributions and controls are fairly simple and involve only the source or geometry program and 18-0 itself.

Coding changes and/or modifications to the 18-0 program have been difficult because the only form of the program available at this installation was a non-relocatable binary deck. Several changes and additions to the original binary deck were required, however, to make the program operational on the FORTRAN monitor system as used at the Lockheed-Georgia Company.

2.3.2 MCS Program

Computer program MCS, Reference 19, is a general Monte Carlo neutron shielding calculation, written in the FLOCO coding system, Reference 20, for the IBM 7090 computer. MCS is capable of treating an arbitrary three dimensional configuration of first and second degree surfaces. A maximum of 432 surfaces forming 2048 cells is allowed. If the problem possesses complete reflection symmetry in some plane, the geometry specification may be simplified by defining that plane to be a reflecting plane. A particle attempting to cross such a reflecting plane will be specularly reflected. A source routine must be prepared by the user; therefore, the type of

source treated is limited in complexity only by the user's ingenuity. Computed data, which are routinely output, are limited to collision densities as a function of cell and energy. Other quantities desired as output are dependent upon the writing of special tally routines as described in Reference 19. These routines, as well as the source routine, must be written in FLOCO. The FLOCO instructions are in most cases identical to FAP; dissimilarities and FLOCO card formats are defined in Reference 20. A programmer with previous FAP experience can make the transition to FLOCO with little difficulty.

Actual generation of source particles for MCS for the present study was done with Program 20-0 described previously. The source tape from 20-0 was rewritten in a form acceptable to the FLOCO tape-read routine and the MCS source routine simply read the particles one at a time directly from this tape.

The output of quantities accumulated by special tally routines is automatically taken care of by the MCS program as described in Reference 19. Thus, by use of special tally routines, almost any quantity of interest may be obtained. In particular, a routine prepared for the present work was used to tally flux and current across selected surfaces and energy deposition in selected cells. MCS automatically computes and prints the relative error associated with any quantity output by a special tally routine.

A useful feature of MCS is its ability to accumulate the results of several runs of small batches of source particles on the problem tape. After each run, the accumulated results up to that time are printed along with the relative errors. This allows one to observe the results at intermediate points and to run in small batches until the desired relative error is obtained.

The reactions considered by MCS include elastic scattering, inelastic scattering, $(n, 2n)$, fission, and absorption. In practice, particles are not absorbed but, as a technique

for variance reduction, scattered with appropriate reduction in statistical weight. Other variance reduction techniques allowed by MCS are biasing on energy and region, and the exponential transformation for transmission through thick shields. The non-absorption feature is automatic, each of the others is optional. For the present study, all the above techniques were employed with the exception of the exponential transformation. Histories are terminated by cut-off on specified limits of energy, weight, and time. These limits are constant throughout the system. A value for thermal energy is specified for each cell, and particle energy is not allowed to fall below this value.

An initiating program, MCA, is used to process the geometrical, nuclear, and material data for use by the MCS. This program, also written in FLOCO, runs fairly quickly, and prepares a "problem tape" for use by the MCS. This problem tape can be altered, for geometrical changes only, by use of a second initiating program, MCI. Thus, after setting up a library of element data on tape with MCA, the "problem tape" can be edited by MCI to alter the geometry with a resultant savings in machine time over that required for rerun of MCA.

All nuclear cross sections are read in at discrete energy points in MCA. The number of elements and the number of energies per element are limited only by core storage available since FLOCO assigns storage at the time of loading for both data and all subroutines. Discrete energy cross section information eliminates the need for any group averaging. Further, the energies corresponding to these discrete points may vary with element allowing the use of many points for elements with numerous resonances and few points for elements with smoothly varying cross sections. Interpolation within the energy points is linear with \sqrt{E} . If E is greater than the largest specified E , the cross section values at E_{\max} are assumed to apply. For E smaller than the smallest specified E , the elastic cross section is taken to be that at E_{\min} , the absorption cross section is extrapolated proportional to $1/\sqrt{E}$, and the total cross section is optionally taken to be that at E_{\min} or extrapolated proportional to $1/\sqrt{E}$. Fitting the equations for second-degree surfaces is, as with QAD, one of the more

time-consuming tasks in setting up the data for MCA-MCS. Writing the FLOCO source and special tally routines is the area where most difficulties are likely to arise. An experienced programmer will, however, be able to perform this task after a short period of practice.

Perhaps the most serious difficulty encountered in the use of these programs at Lockheed-Georgia was that imposed by the incompatibility of FLOCO with the FORTRAN monitor system. FLOCO binary cards are row binary and must be read into the computer on-line. This led to running these programs only at night and results in a penalizing long lead-time even for short check-out runs.

2.3.3 MCG Program

The MCG Program, Reference 21, is the gamma counterpart of MCS. All comments made concerning geometry and the FLOCO system in reference to MCS apply equally here. Source and special tally routines may also be written for MCG although energy deposition is automatically output as a function of cell. For any specified subset of the set of surfaces comprising the geometry, fluxes and/or currents across these surfaces may also be automatically obtained.

The program treats Compton scattering, absorption (photoelectric effect) and pair-production. In the current study pair-production was included with absorption. When pair-production is considered, it is assumed that the energy loss by the incoming photon in creating the pair is local, and the two resulting one-half MeV gammas are followed further. The program was designed primarily to treat photons in the energy range from 10 keV to 12 MeV.

The biasing techniques available in MCG are identical to those described for MCS. An additional feature is the provision for varying the energy cut-off with cell.

MCG has two initiating programs - MCF corresponding to MCA for set-up of both

geometry and element data, and MCE corresponding to MCI for altering the geometry only. As with MCA, cross section data is input for a set of discrete energies for each element. MCG also has the small-batch capability described for MCS.

2.3.4 O5R Program

The O5R Program, Reference 22, is a flexible Monte Carlo neutron transport program and is intended to be applicable to a wide range of reactor and shielding problems. Perhaps the most distinctive feature of the program is its detailed representation of cross section data. In this representation the energy range from 77.13 MeV to 0.07×10^{-3} eV is divided into 40 supergroups, each a factor of 2 apart, and each supergroup is divided into n subgroups where n is any power of 2 from 1 to 512. O5R stores in the computer memory only the cross sections for a single supergroup and processes batches of neutrons (200 - 2000) through the range of the supergroup. Cross sections for the next lower supergroup are then read in from tape and the process repeated.

The program is written in FORTRAN 63 for the CDC-1604-A computer and in FORTRAN II, version 3 for the IBM-7090/7094 computer. A number of O5R subroutines are written in CODAP for the CDC-1604-A machine and in FAP for the IBM-7090/7094 computer.

A general geometry routine in O5R permits the treatment of complicated configurations. As many as 16 media are permitted and boundaries may be either planes or quadric surfaces, arbitrarily oriented and intersecting in arbitrary fashion. The geometry routine also permits the division of a configuration into arbitrarily bounded regions for the application of weight standards. Within each region and for specified energy groups both splitting and Russian roulette are allowed.

Fast and/or thermal fissioning are permitted in appropriate systems, and O5R treats a variety of neutron scattering collisions. Absorption of neutron particles is not permitted; instead, the probability of absorption is accounted for by the statistical

weight reduction of a particle at each collision. Anisotropic scattering, utilizing a technique for selecting from anisotropic distributions which gives the same accuracy as a straightforward selection from a Legendre expansion but requires less computer time, is permitted.

Generation of the initial parameters for neutrons is accomplished by a subroutine SOURCE which must be written by the user and included with the O5R Program. The user must supply a subroutine (KINNEY) for determining the energy and scattering angle of inelastically scattered neutrons where these have importance in a problem.

Included in the O5R package are a number of random variable generating routines and a program for performing a variety of manipulations with cross sections. The cross section program includes routines for preparing master tapes, performing cross section arithmetic and preparing cross section data in the form needed by O5R.

No analysis is performed by O5R. Instead, its output consists of one or more "collision" tapes which contain, for every collision, any or all of 34 distinct parameters describing the event. Analysis of these tapes to extract and/or compute the information desired is done by separate routines which must be written by the user.

In the O5R system, the user is required to supply point values of microscopic cross sections at arbitrary energy points. A cross section routine, XSECT, which is run separately from O5R, performs various manipulations on the point cross section data and prepares tapes containing data in the form required by O5R. XSECT contains nine codes for the processing of cross section data. A brief description is given below of three of these cross section codes which are necessary in preparing data required by O5R.

Code 1 reads point cross sections and/or Legendre expansion coefficients and writes them on a master cross section tape in a form convenient for further processing. A

special program called LEGENDRE (separate from XSECT) calculates the Legendre coefficients from input differential cross sections as a function of angle and energy and punches them on cards in a form suitable for loading by Code 1. Code 6 uses the master cross section tape as input and operates on this basic data to obtain for each medium in the problem the parameters and probabilities needed by O5R for the running of a problem. The output of Code 6 is the O5R system data tape, which is a basic input tape to O5R. Code 8 prepares from the master cross section tape the so-called "phi tape" which contains data necessary to the employment of the Coveyou technique for the selection of the cosine of a scattering angle from an anisotropic angular scattering distribution.

The "package" required to run a problem with O5R consists of a system data tape, a phi tape, an O5R input data deck, a geometry routine input deck, suitable subroutines SOURCE and KINNEY, and the O5R program deck. All of these items with the exception of SOURCE and KINNEY have been prepared for the Configuration A of the present investigation.

2.4 PROGRAM COMPARISON

Comparison of the programs investigated is summarized below in terms of each of the stated criteria except accuracy.

2.4.1 Detail And Direct Usefulness Of Output

The types of data which may be computed by each program are tabulated in Figure 2. An X indicates that a quantity is directly output by the program, at least optionally. A C indicates that a quantity is available in less useful form, since further computation by hand or by specialized satellite code is required. An asterisk indicates direct output, but only with the inconvenience of preparing a subroutine if not already available. The Monte Carlo is best suited to computation of quantities averaged over discrete intervals; statistical estimation routines could be prepared. In addition to

DATA	CODE								
	14-0,14-1	QAD IV	QAD-P5	DTK	DDK	18-0	MCS**	MCG**	05R
NEUTRON • ENERGY • DEPOSITION (DOSE)	X	X	X	X	C	X	*		*
• FLUX	C		X	X	X		*		*
• CURRENT						C	*		*
• SPECTRA	X		X	X	X	X,C	*		*
• ANGLE				X		C	*		*
• ACTIVITY				X	C	C	*		*
• COLLISION DENSITY									
• SOURCE				X	X		X		*
GAMMA • ENERGY • DESPOSITION (DOSE)	X	X	X			X		X	
• FLUX								X	
• CURRENT						C		X	
• SPECTRA						X,C		X	
• ANGLE						C		*	
• BUILD UP		X	X						
SYSTEM WEIGHT	X								

X - Calculated Internally

*Special Analysis Subroutines Prepared By The User Permit Complete Output Flexibility

**Error Estimate Always Computed

C - Calculated Externally

FIGURE 2 PROGRAM OUTPUT

printed output, tape output to allow for interrupted operation or satellite input is available with all programs listed excepting point kernel.

2.4.2 Generality Of Problems Which May Be Treated

Flexibility of each program for treatment of system configuration, source distribution and type of radiation interaction are summarized below. Salient features of the point kernel and Monte Carlo programs are tabulated in Figures 3 and 4, respectively. The discrete ordinates program DTK has specifications similar to DDK except that it is one-dimensional. Features of the latter are summarized below.

Boundaries: Orthogonal two dimensional mesh, including $R, Z; R, \theta; X, Y$.

Boundary Conditions: Absorptive, specularly reflective, periodic.

Neutron Reactions*: Transport, production, absorption, group transfer.

Scattering: Isotropic, backward, forward.

Flux Description: Discrete direction and energy.

Iteration Modes: Reactivity, invariant source, critical dimension, critical fuel loading, period.

Starting Option: Fission distribution, flux.

Computer Language: FLOCO

2.4.3 Operational Problems

Several problems arising in the use of the various programs are of interest in evaluation of methods, since they lengthen the span required for computation. Among these are:

Anomalous error stop from 14-0 geometry routine;

Overflow of 18-0 latent particle storage;

*Corresponding gamma cross sections can be derived.

FEATURE	CODE				
	14-0	14-1	QAD IV	QAD - P5	
BOUNDARIES	CONICAL & PLANAR	CONICAL & PLANAR	QUADRIC	QUADRIC	
Power Distribution Input	Cosine	X	X	X	
	Exponential	X			
	Point		X	X	
Radial Variation Of Source Point Array	X	X			
Self-Normalization Of Power			X	X	
Multiple Source Regions	X	X			
Multiple Gamma Source Spectra	X	X			
Variation Of Power Distribution With θ			X	X	
Modified Albert-Welton For Neutrons	X	X	X	X	
Alternate Non-Hydrogenous Kernel For Neutrons	X	X			
Moments Method Spectra For Neutrons	X	X		X	
Moments Method Dose And Multiple Heating For Neutrons				X	
Single Layer Build Up For Gammas	X	X	X	X	
Two Layer Build Up For Gammas	X	X			
Multiple Dose And Heating Responses For Gammas				X	
System Weight (By Material)	X	X			
Programming Language	FAP	FAP	FORTAN II	FORTAN I&IV	

FIGURE 3 FEATURES OF POINT KERNEL PROGRAMS

FEATURE	CODE		
	18-0	MCS, MCG	05R*
BOUNDARIES	CONICAL & PLANAR	GENERAL QUADRIC	GENERAL QUADRIC
EVENTS NEUTRON	(n, n) , (n, n') (n, γ) (n, α) , $(n, 2n)$ ABSORPTION	(n, n) , (n, n') $(n, 2n)$, (n, f)	(n, n) , (n, n') $(n, 2n)$ (n, x) (n, f)
GAMMA	COMPTON ABSORPTION PHOTONEUTRON	COMPTON PHOTOELECTRIC PAIR PRODUCTION	
SAMPLE BIASING	REGION ENERGY*	REGION ENERGY EXPONENTIAL NON-ABSORPTION	REGION ENERGY SCATTER ANGLE NON-ABSORPTION
PROGRAMMING LANGUAGE	FAP	FLOCO	FORTAN II, 63 FAP

* NEUTRON ONLY

FIGURE 4 FEATURES OF MONTE CARLO PROGRAMS

Error stop on exceeding variable DDK input storage;
Preliminary computation for establishment of discrete ordinates mesh; and
Preliminary computation of Monte Carlo importance.

2.4.4 Program Running Time

Generally, the running times are proportionate to the sophistication of the radiation transport model, increasing from point kernel, through discrete ordinates, to Monte Carlo. So many options are available for treatment of a given problem with a given method, however, that no direct comparison is possible. The approach taken is to establish a plausible measure of effectiveness for each type of program, then observe its range as problems of different complexity are treated. From these ranges, some intuition of running times for problems of similar "complexity" may be gained. The measures chosen are:

Point Kernel: Source point x detector points/time in msec (SD/ms).

Discrete Ordinates: Outer iterations x mesh points x energy groups/time (IMG/ms).

Monte Carlo: $1/\text{relative error squared} \times \text{time}$ ($1/E^2 t$).

Results for some of the computations made are shown in Figures 5, 6, and 7. In the first two figures, A and B refer to configurations defined in Section 3.1; the numbers appended in Figure 6 refer to the number of energy groups.

So simple a scheme must have pitfalls. A few are noted here. QAD requires more source points than 14-0 in order to meet a given requirement for maximum spacing. Furthermore the efficiency, predictably, decreases with the size of the problem, as illustrated by the parenthetical number in Figure 5. A difficulty unique to S_n is the variability of time required per outer iteration, the required number of inner iterations is difficult to estimate, however. The drawback with the Monte Carlo measure is that the measure itself is a statistic, whose significance is open to question.

The advantage of energy biasing for energy deposition computations seem clear, however.

DATA	CODE	TIME (ms/SD)	
		CONFIGURATION A	CONFIGURATION B
DOSE	QAD IV	13	
	14-0	23	
SPECTRUM	QAD - P5*	36 (43)	43
	14-0	36	66

*Number Of Doses = $1 + 2 \times 2$

FIGURE 5 COMPUTER TIME - POINT KERNEL

CODE	PROBLEM	ITERATION (I)	min/I	MESH (M)	ms/IMG
DTK	A-15 Axial	13	0.5	59	40
	A-15 Radial	7	0.14	14	40
DDK	A-15	11	14	11 x 51	100
	A-4	8	2 ⁺	17 x 46	30
	B-15	9	10	11 x 51	70
	B-4	5*	6 ⁺	17 x 46	120

*Nonconvergent

⁺ Inner Iterations - B4:A4 > 2:1

FIGURE 6 COMPUTER TIME - DISCRETE ORDINATES

Configuration	Computation	Program	Source Particles	7094 Time t(min.)	Relative Error E	Measure Of Effectiveness $1/E^2 t$
Neutron Axial Bias	Leakage Current At Pressure Vessel Head, R = 0 - 39 CM	18-0*	14000	76	.17	.46
		MCS	6000	73	.19	.38
Neutron Radial Bias	Leakage Current At Reactor Side Z = 80 - 110 CM	18-0	8000	17	.12	4.1
		MCS	2000	31	.10	3.2
Gamma Axial Bias	Volume Heating Upper Shield Support R = 0 - 39 CM	18-0	14000	38	.42	.15
		MCG (1)	8002	29	.40	.22
		MCG (2)	7999	77	.12	.90
	Leakage Current At Pressure Vessel Head, R = 56 - 66 CM	18-0	14000	38	.42	.15
		MCG (1)	8002	29	.41	.21
		MCG (2)	7999	77	.30	.14
Gamma Radial Bias	Volume Heating Propellant Tank Volume #1	18-0	14000	60	.40	.10
		MCG (1)	8000	51	.35	.16
	Leakage Current At Reactor Side Z = 50 - 80 CM	18-0	12000	34	.10	2.9
		MCG (1)	4000	31	.16	1.3

*18-0 Time Includes 20-8 Time MCG (1) - Region Biasing Only MCG (2) - Region And Energy Biasing

FIGURE 7 COMPUTER TIME - MONTE CARLO

3.0 COMPARATIVE ACCURACY

The relative flexibility, speed and convenience of a program, as discussed in the preceding section, are unavailing if its accuracy is unacceptable. As always, the final arbiter of accuracy must be the preservation of experimental appearances. Two factors, however, militated against such direct approach in the present instance. Experimental data on transmission through shielding and propellant was unavailable. Available data, from the KIWI test series, is complicated by factors whose quantitative examination lies beyond the scope of the present study. Consequently, accuracy must be evaluated by consensus of several methods and by computed statistical deviations, with occasional recourse to qualitative theoretical considerations.

The quantities usually most critical in design problems are energy deposition (or dose rate) and flux; comparison of these is emphasized. Spectra, more pertinent to an understanding of fundamentals, were also computed extensively. Since the 18-0 Program cannot compute flux, current is used as one basis of comparison with MCG and MCS. Most of the comparisons shown imply a substantial amount of hand adjustment of computer output. Included are normalization of DDK and Monte Carlo data to standard power, volume averaging of point energy depositions for comparability with Monte Carlo output, and computing mean values and relative errors from separate 18-0 runs.

3.1 PROBLEMS TREATED

Two configurations representative of a reactor-shield assembly are used for method comparison. A section of the first, a strictly cylindrical geometry designated Configuration A, is shown in Figure 8. Most of the computations treat this configuration. A slightly more difficult configuration, used to check errors due to approximations of quadric boundaries, is compared with Configuration A in Figure 9. Designated "B", this configuration incorporates five spherical boundaries, each having a 105 cm radius of curvature. Radius composition, and edge thickness are identical for

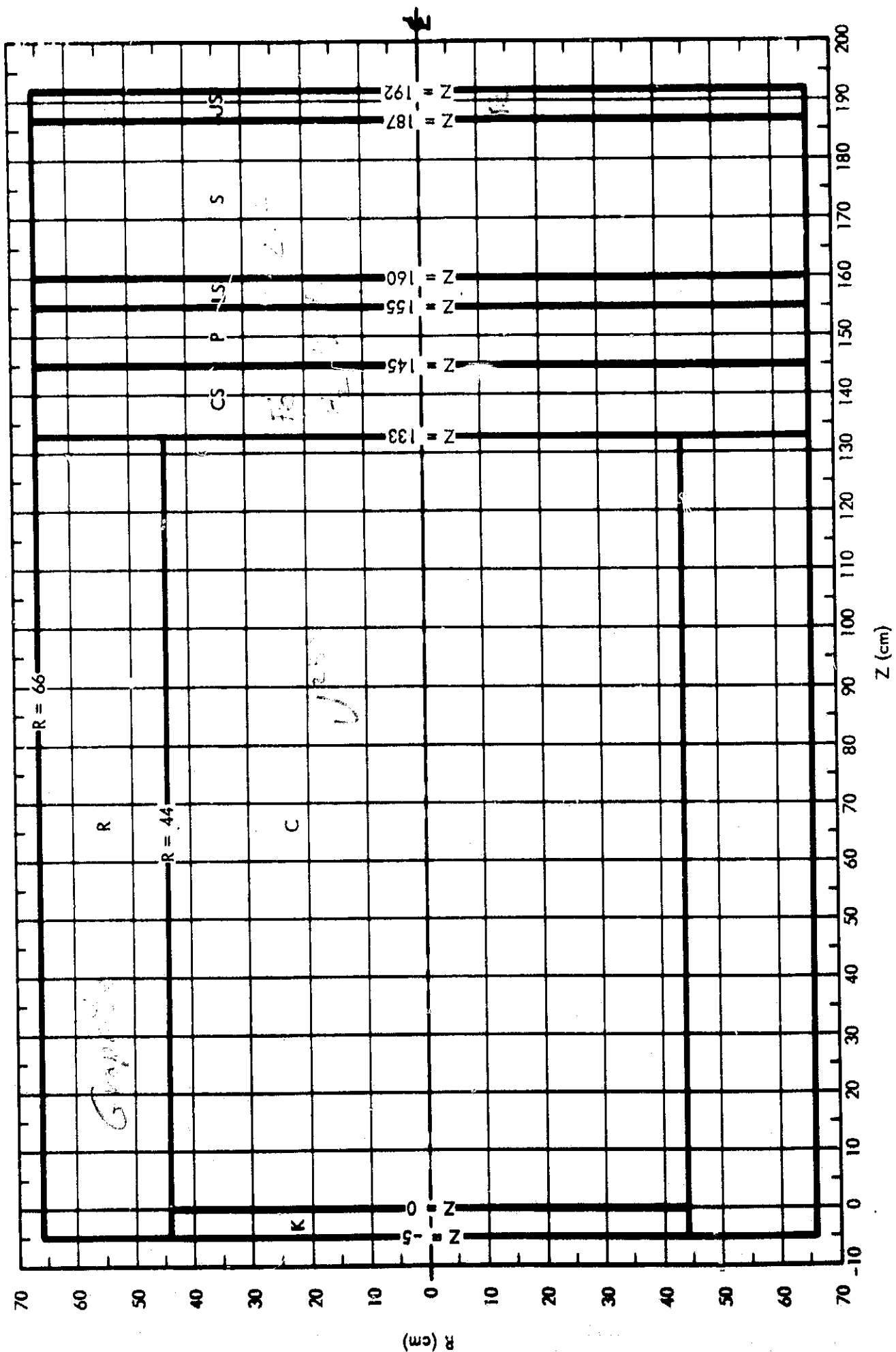


FIGURE 8 CONFIGURATION A

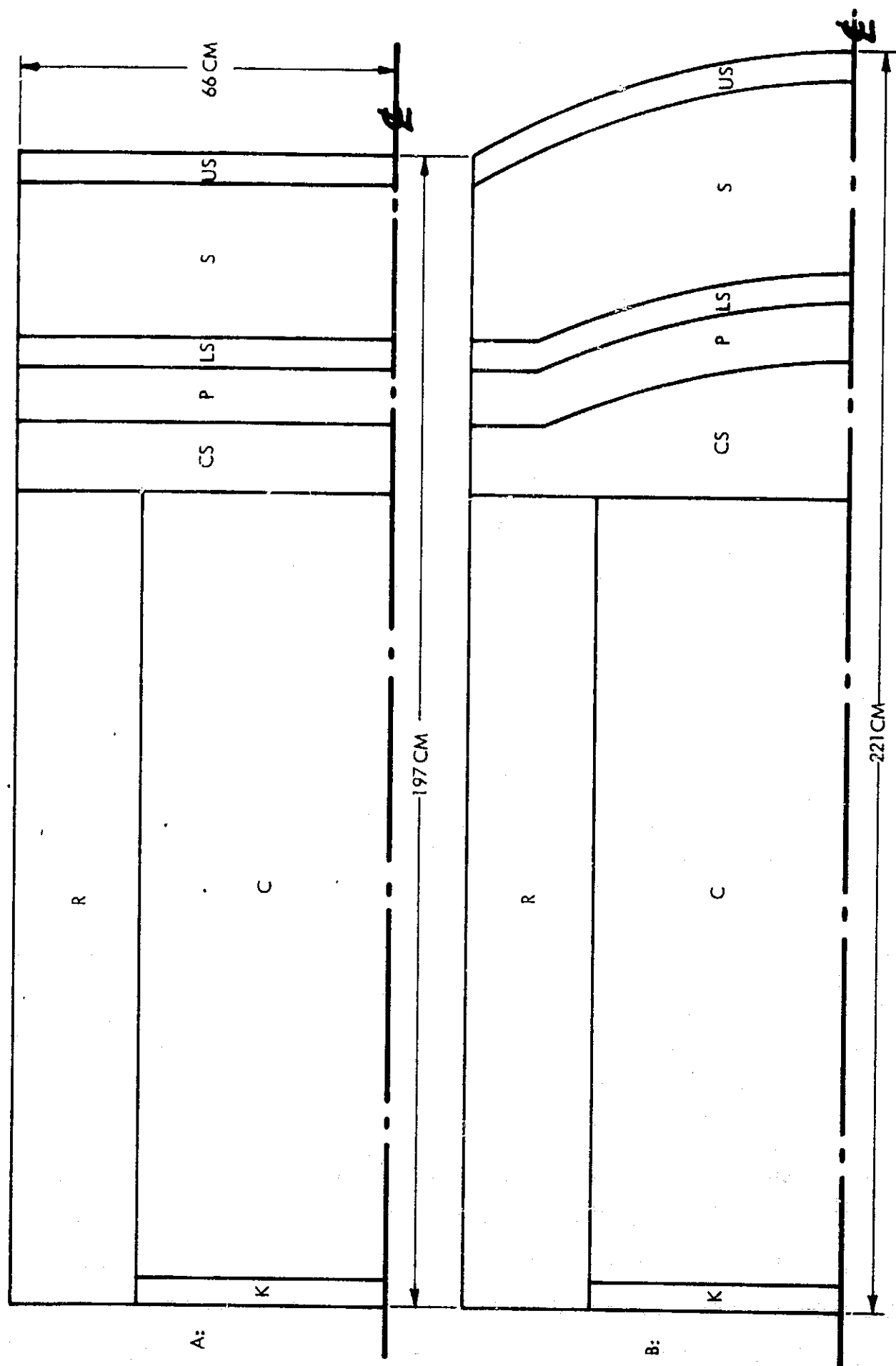


FIGURE 9 SHIELD MODELS

corresponding regions in each configuration. Regional compositions are tabulated in Figure 10.

The reactor power distribution obtained during a 15-group S_4 computation for Configuration A was used throughout in establishing radiation sources for point kernel and Monte Carlo computations. This distribution is tabulated in Figure 11. All radiation intensities computed are normalized to a nominal power of 1,000 megawatts. The California fission spectrum was assumed for source neutrons. The gamma source spectrum used for both point kernel and Monte Carlo programs was generated for a carbon-uranium core and included prompt fission gammas, short-term fission product decay gammas, and radiative capture in the core materials. This spectrum is shown in Figure 12.

The tank contour assumed for computation of energy deposition in propellant is shown to scale in Figures 13 and 14, together with its size and orientation with respect to Configuration A. Hydrogen density and tank wall thickness treated are, respectively, 0.0692 g/cm^3 and 0.25 cm of iron. The numbered areas represent regions in which Monte Carlo estimates of gamma and neutron energy deposition were tallied. Axial thicknesses of these regions are 100 and 18 cm, respectively. The broken lines normal to the system axis represent propellant levels assumed in computation of intensities at the tank top. Three radial surface elements shown on the tank top are used for this Monte Carlo tally.

As implied earlier, Configuration B can only be approximated by the geometry routines of DDK, 14-0 and 18-0. The approximations used with DDK and 14-0 are shown in Figure 15 as Configurations B-1 and B-2, respectively. (In B-2 the curved lines mask one edge of the adjacent trapezoids.) The approximation used with 18-0 is similar to B-2, except that general quadrilaterals are used to advantage, and that statistical weighting requirements limit the axial dimensions.

Two independent sets of region weights are used with Configuration A, depending

MATERIAL.	REGION							
	K	C	R	CS	P	LS	S	US
H		.0005		.004	.01			
LiH							.54	
C	1.7	1.3	1.2					
Fe		.11		2.		7.	1.2	7.
U ²³⁵		.2						
TOTAL	1.7	1.6	1.2	2.	.01	7.	1.7	7.

FIGURE 10 REGIONAL COMPOSITIONS - g/cm³

Z (CM) R (CM)	0 - 5	5 - 25	25 - 65	65 - 115	115 - 131	131 - 133
0 - 30	6.08 (-7)	1.04 (-6)	1.80 (-6)	1.71 (-6)	1.01 (-6)	8.39 (-7)
30 - 36	4.82 (-7)	8.30 (-7)	1.44 (-6)	1.36 (-6)	8.16 (-7)	6.83 (-7)
36 - 39	4.42 (-7)	7.67 (-7)	1.33 (-6)	1.27 (-6)	7.60 (-7)	6.32 (-7)
39 - 42	4.45 (-7)	7.91 (-7)	1.37 (-6)	1.31 (-6)	7.88 (-7)	6.32 (-7)
42 - 43	4.67 (-7)	8.59 (-7)	1.49 (-6)	1.43 (-6)	8.58 (-7)	6.58 (-7)
43 - 44	5.07 (-7)	9.58 (-7)	1.66 (-6)	1.60 (-6)	9.58 (-7)	7.09 (-7)

FIGURE 11 FISSION DISTRIBUTION (RELATIVE UNITS)

Energy (MeV)	Photons/Fission • MeV
.10	14.7
.30	11.8
.50	9.46
.70	7.59
1.0	5.46
1.5	3.15
2.0	1.82
2.5	1.05
3.0	.605
3.5	.349
4.0	.202
5.0	.0688
6.0	.0230
7.0	.00905
8.0	.00410

FIGURE 12 GAMMA SOURCE SPECTRUM

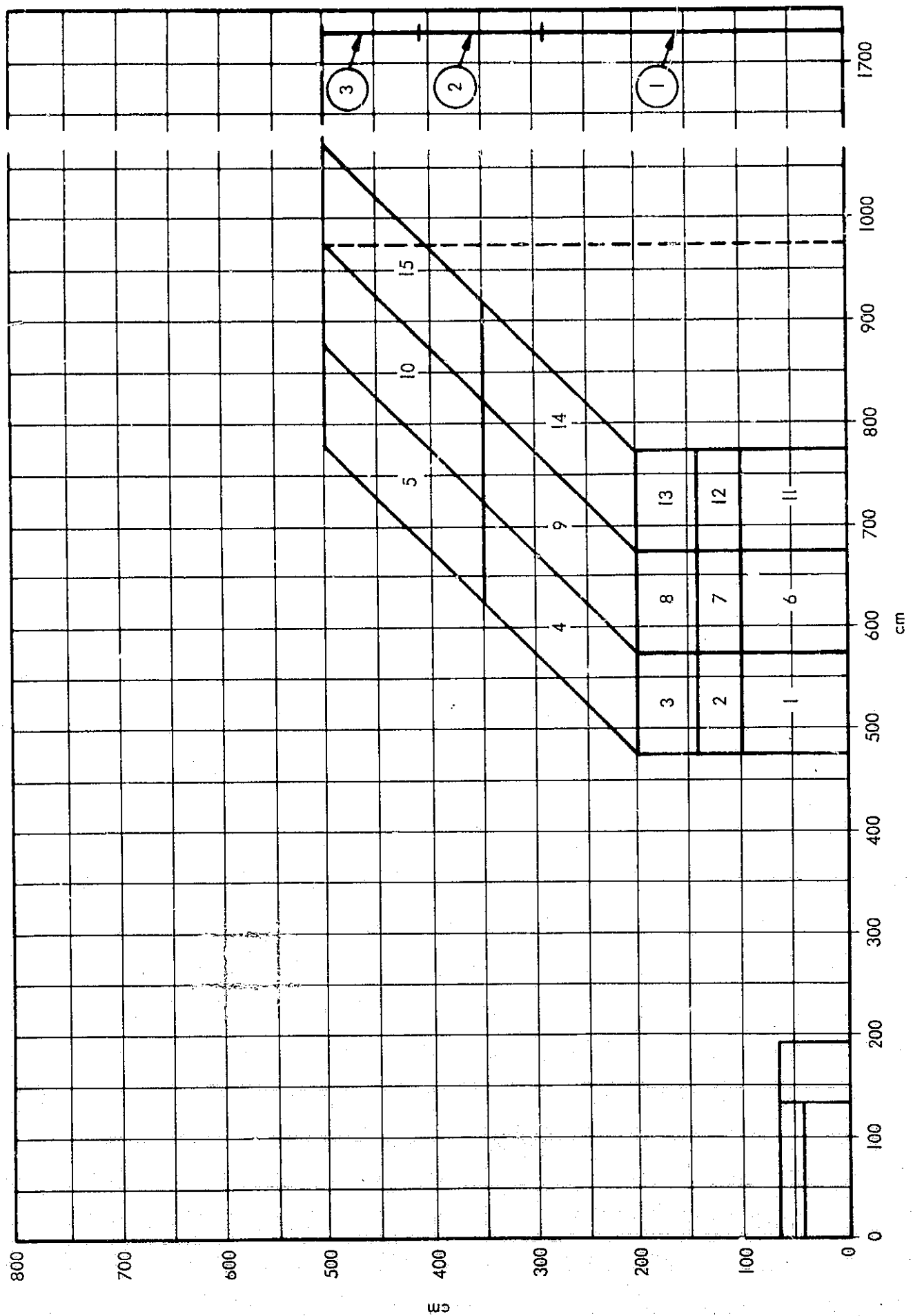


FIGURE 13 PROPELLANT TANK MODEL GAMMA

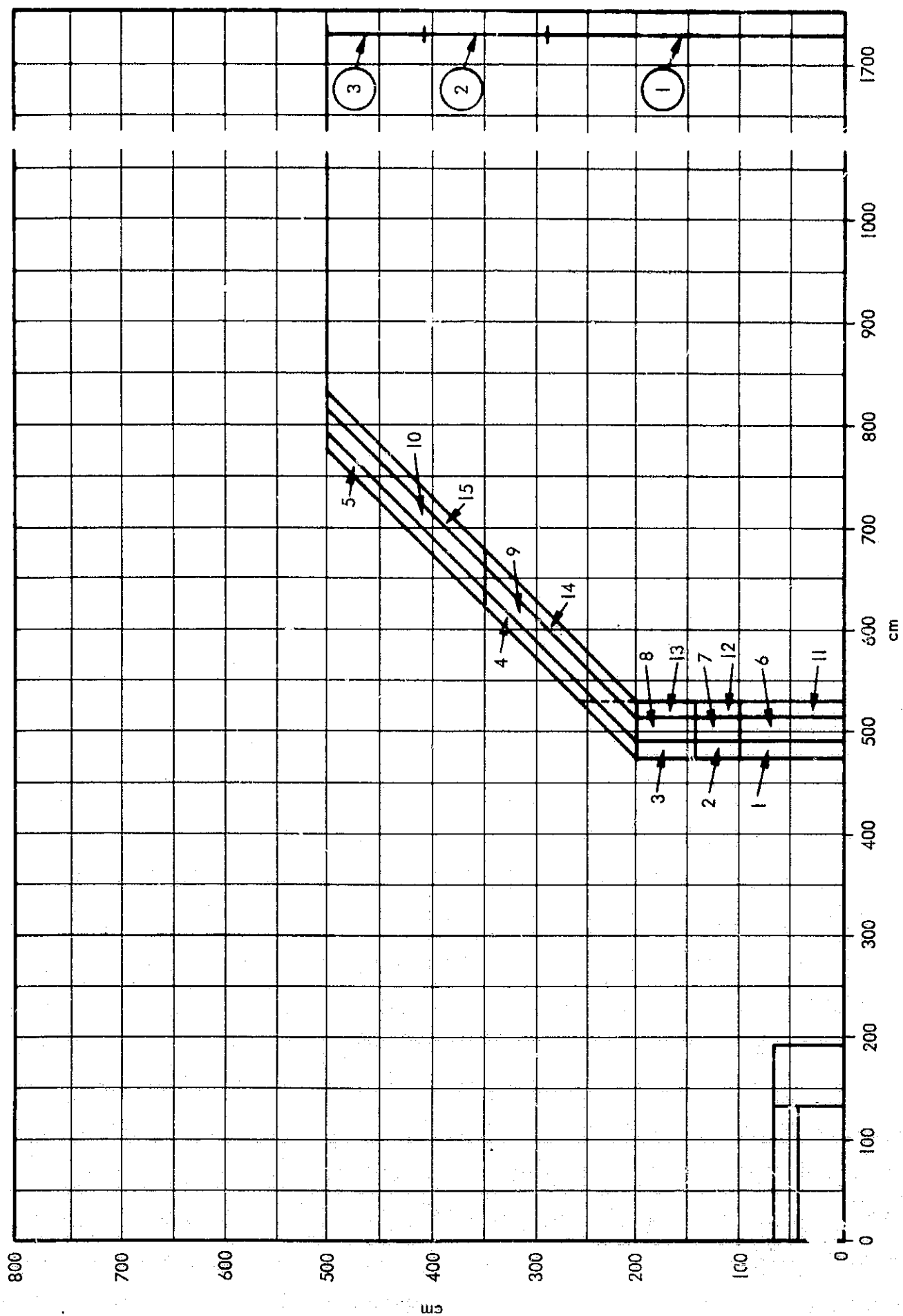
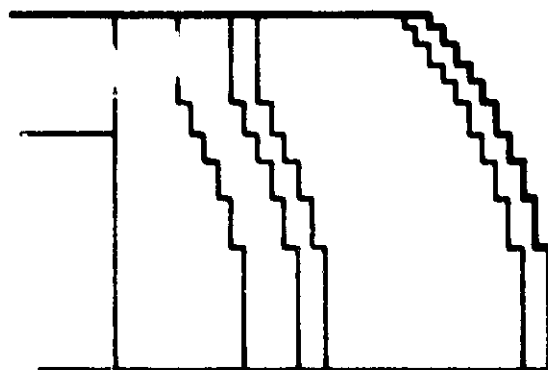
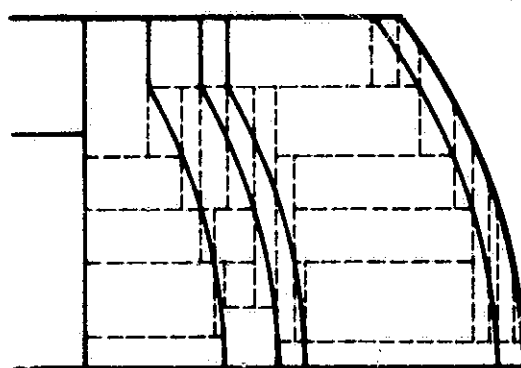


FIGURE 14 PROPELLANT TANK MODEL NEUTRON



B-1



B-2

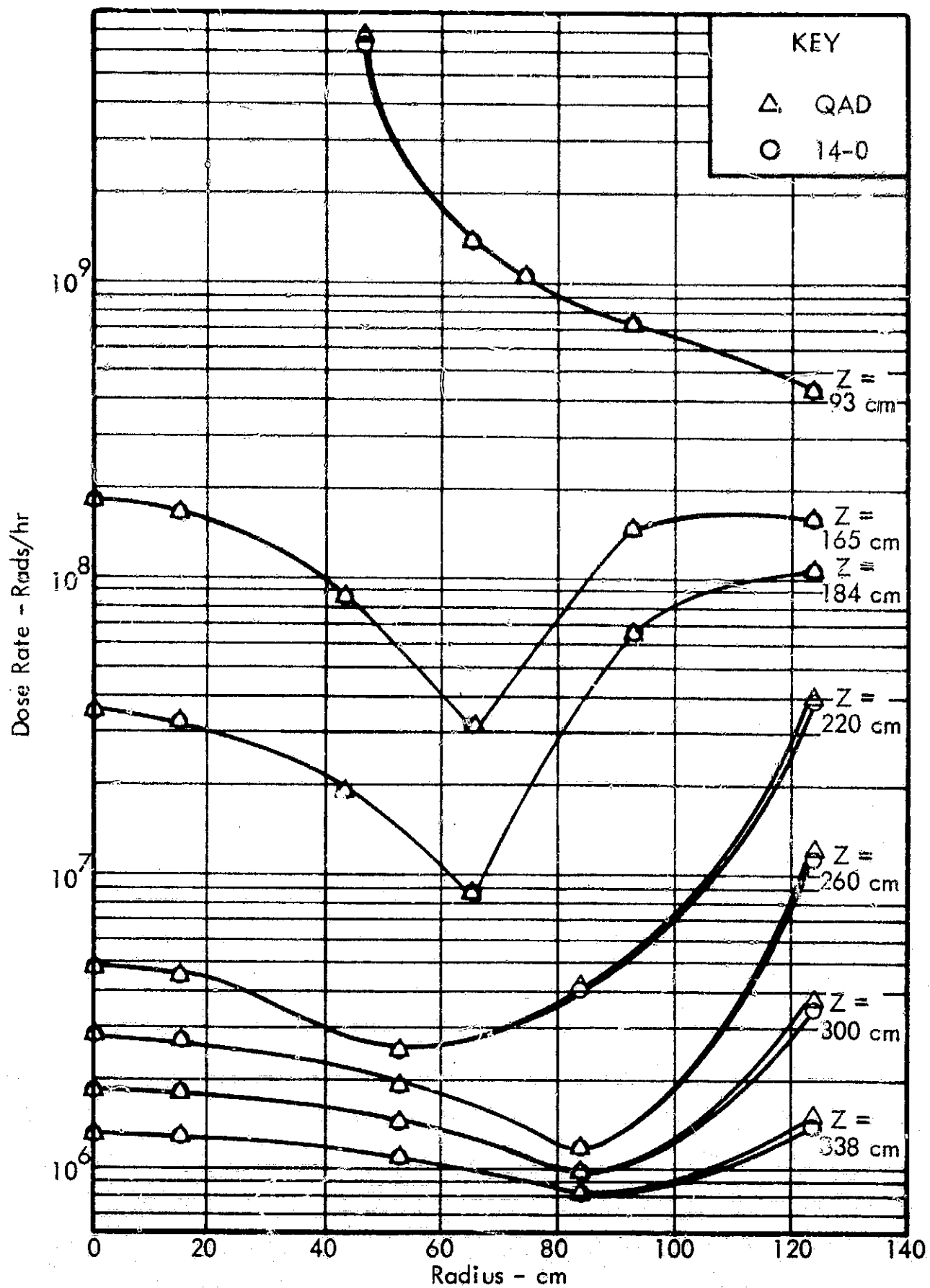
FIGURE 15 CONFIGURATION B APPROXIMATIONS

upon whether leakage through the cylindrical or planar boundary is to be emphasized. In either case particle density is held roughly constant over the system, while splitting approximately 2: 1 at successive boundaries. The one exception to this scheme is in establishing weights in reflector region R for the radial biasing of particles. Particle current leaving the reflector is more than ten times entering current, in order to provide a significant number of leakage particles directed toward the propellant tank. Neutron importance is set proportionate to energy. Program 18-0 does not permit gamma energy weighting; MCG is here used both unweighted and proportionately weighted. In most cases, preliminary runs of about 2, 000 particles were used to refine initial weight guesses. While the above scheme is hardly optimum for computation of any one datum, it seems fairly effective for tallying varied data from one set of histories.

3.2 COMPARISON OF GAMMA RAY COMPUTATIONS

Data are presented, where possible, in order of increasing attenuation. Point kernel estimates of tissue dose rate, representative of energy absorption in any material of low atomic number, are shown in Figure 16, for the vicinity of the Configuration A shield. Discontinuities at the radial shield boundary are readily apparent in the two traverses which intersect the shield; other traverses do not intersect the shield regions. The QAD points are presumed to apply to both versions; however, only a few were checked with QAD-IV to establish the expected identity, and determine computer time. The slight discrepancies between QAD and 14-0 are readily explicable in terms of the differences in source point treatment, described in Section 2.

Correspondence between point kernel and MCG Monte Carlo estimates of tissue dose rate at three penetration depths is shown in Figures 17, 18, and 19. The MCG dose rates are hand computed from tallied flux spectra, although a more sophisticated tally routine is easily prepared if multiple cases are desired. The error limits shown are internally computed relative errors, plotted such that their abscissas approximately



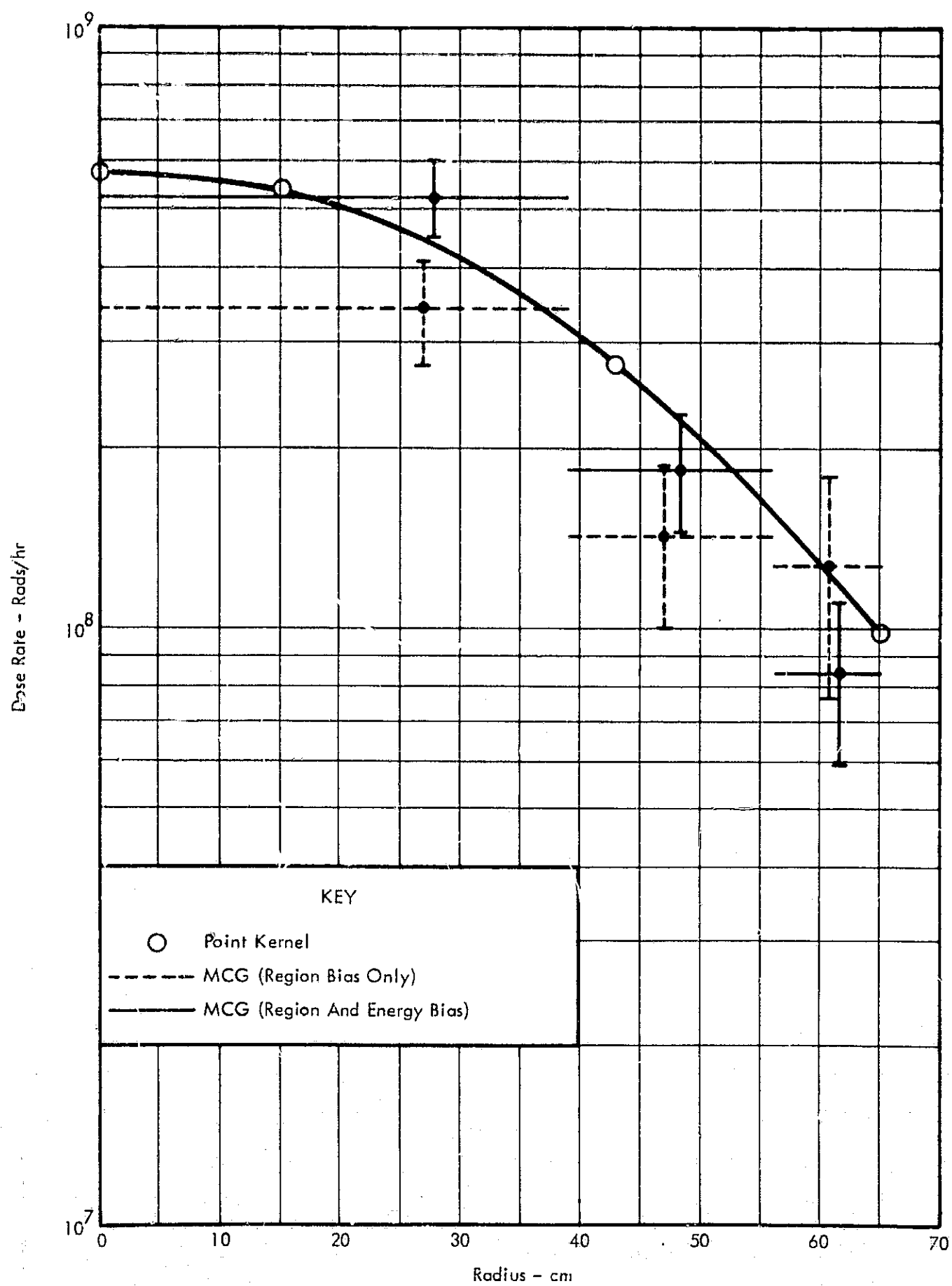


FIGURE 17 GAMMA DOSE RATE (Z = 157.5 CM)

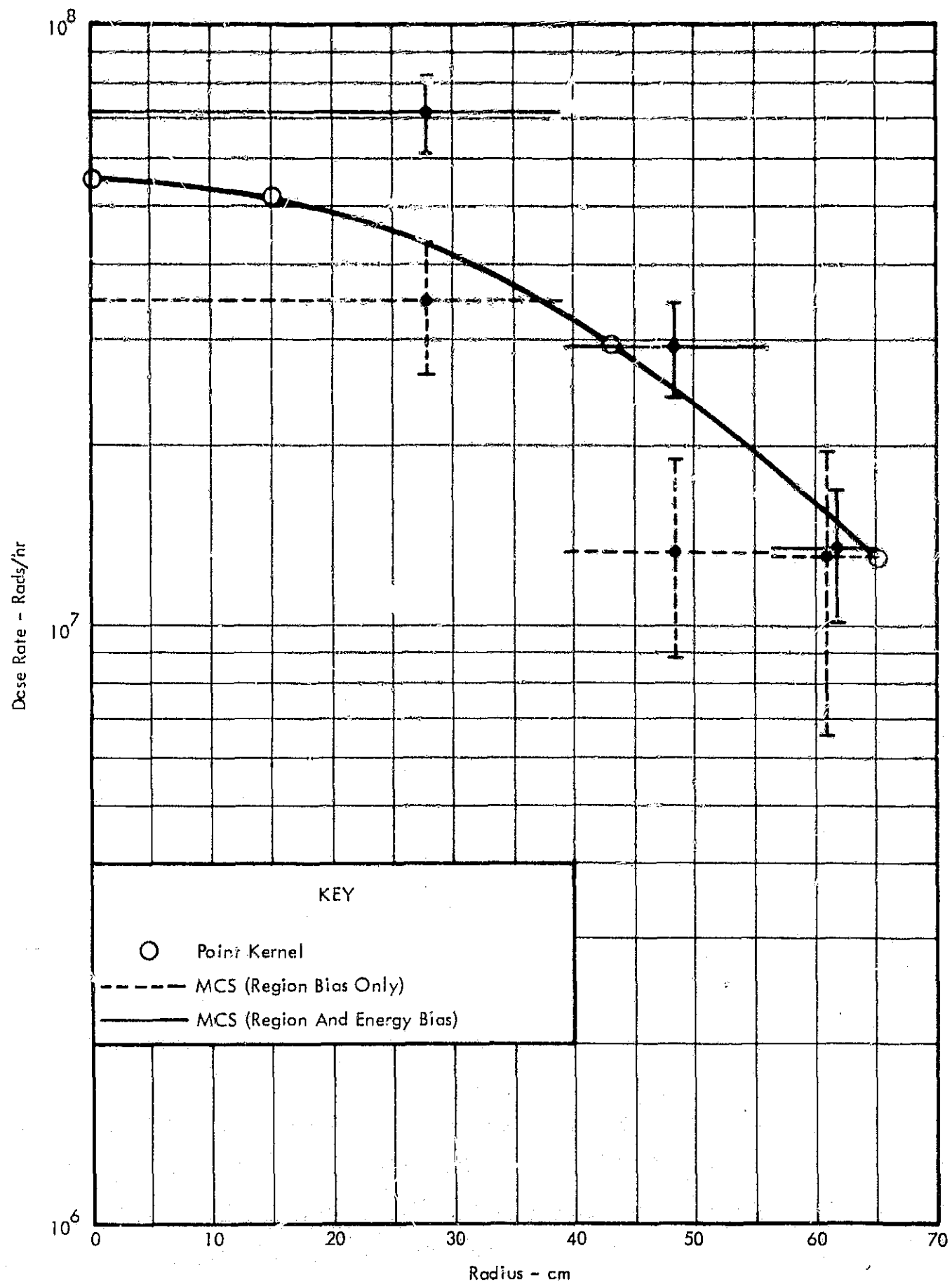


FIGURE 18 GAMMA DOSE RATE ($z = 178$ CM)

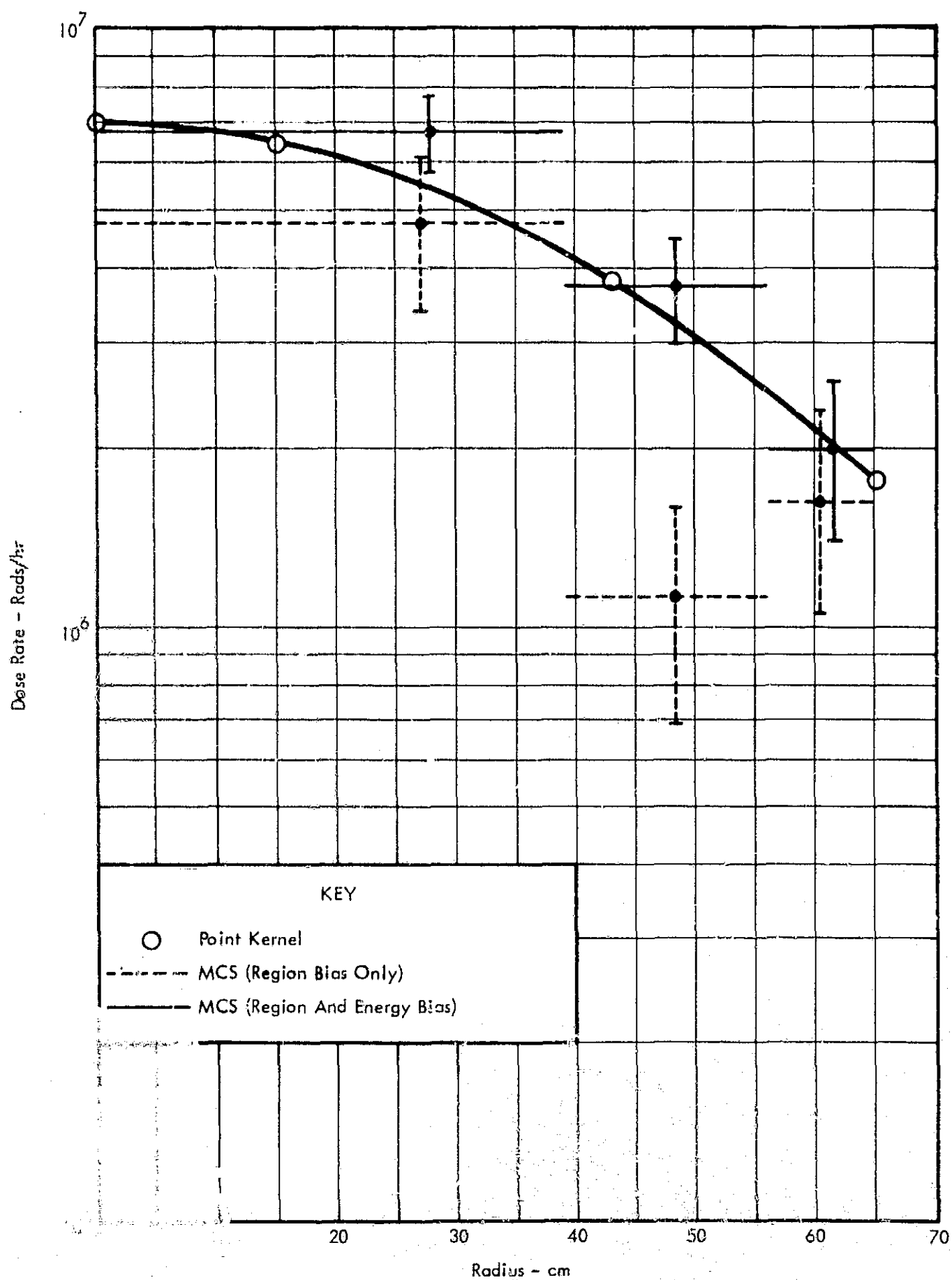


FIGURE 19 GAMMA DOSE RATE (Z = 192 CM)

halve the tally surfaces. It will be noted that the unbiased data for the second tally ring show increasing discrepancy with increasing penetration. No cause is apparent other than statistical fluctuation, a supposition supported by the very large error estimate and by results of the energy-biased computation. With the above possible exception, no statistically significant discrepancy can be demonstrated between point kernel and Monte Carlo gamma data at an attenuation of some few hundred.* Additional histories, would, of course, be highly desirable.

The 18-0 and MCG Programs are compared, over the same Configuration A shield regions, in Figures 20, 21, and 22. A convenient basis for comparison here is forward current, J_+ , since 18-0 does not compute flux. The previously noted anomaly in the unbiased MCG data is repeated here, since the same histories are involved. The relative error of the 18-0 data increases more rapidly with penetration depth, perhaps due to loss of particles by absorption. Again the statistics are insufficient to disclose discrepancies, if such exist.

So far only Configuration A has been mentioned. Three estimates of gamma dose rate along a traverse through the Configuration B shield are shown in Figure 23. The 18-0 dose rates are estimated from computed values of energy deposition in shield annuli predominantly composed of LiH. Two liberties are taken in this procedure, neither of which results in a large correction factor. First, energy deposition per gram of shield material, for each annular region and energy group, is interpolated to the plane $Z = 183.9$ cm., using slopes estimated by QAD-P5. Second, energy deposition in the shield material for each group is converted to the equivalent deposition in tissue. Excepting the axial 18-0 region, the agreement of curve shapes is remarkably good. The systematic 20% discrepancy between 14-0 and QAD was also observed on other traverses through the shield. In view of the agreement displayed in

*An earlier plot of this data which received a limited circulation showed a much larger discrepancy. It is embarrassing to report that this resulted from normalization to source particles, rather than source photons.

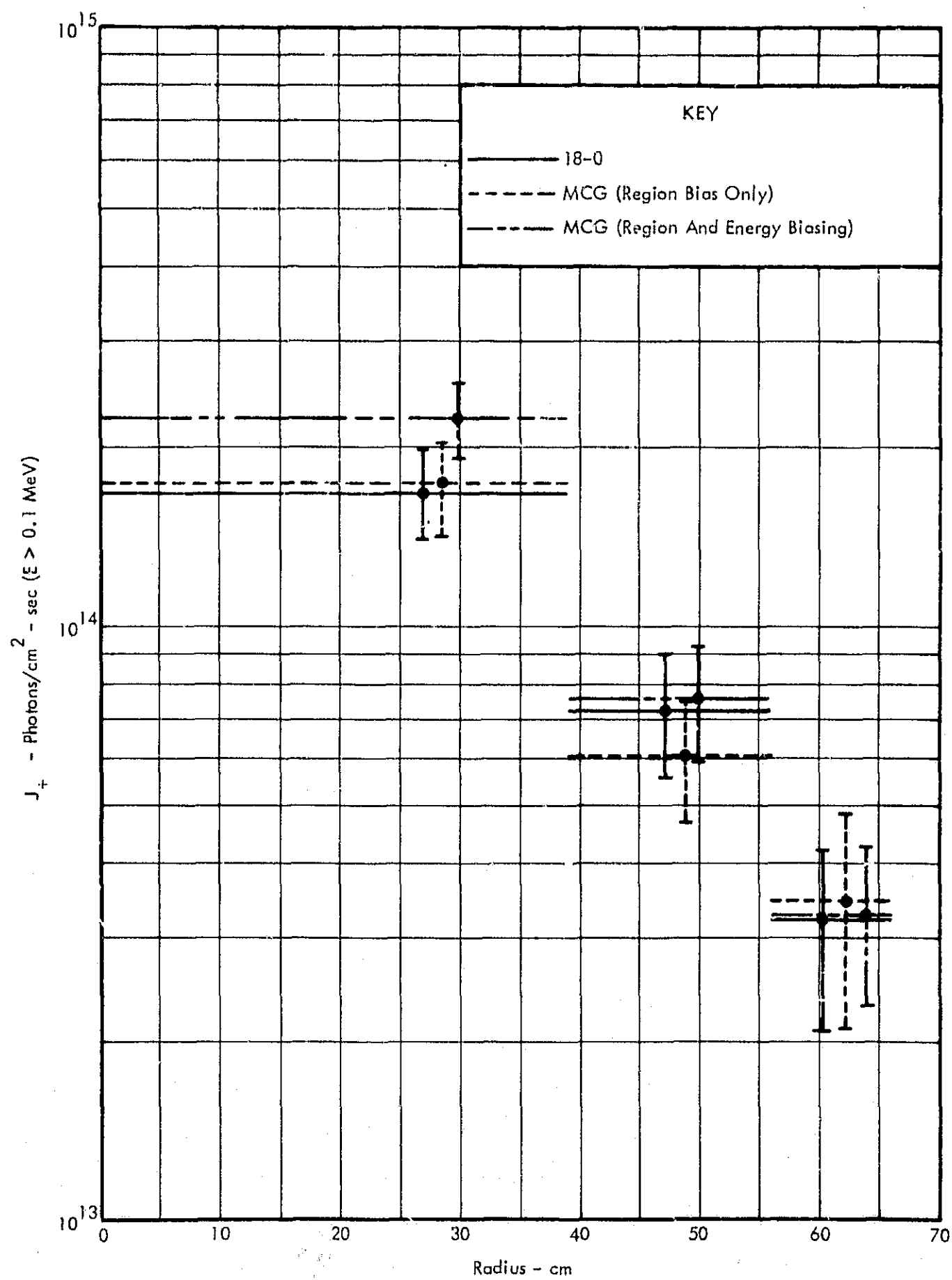


FIGURE 20 GAMMA FORWARD CURRENT (Z = 157.5 CM)

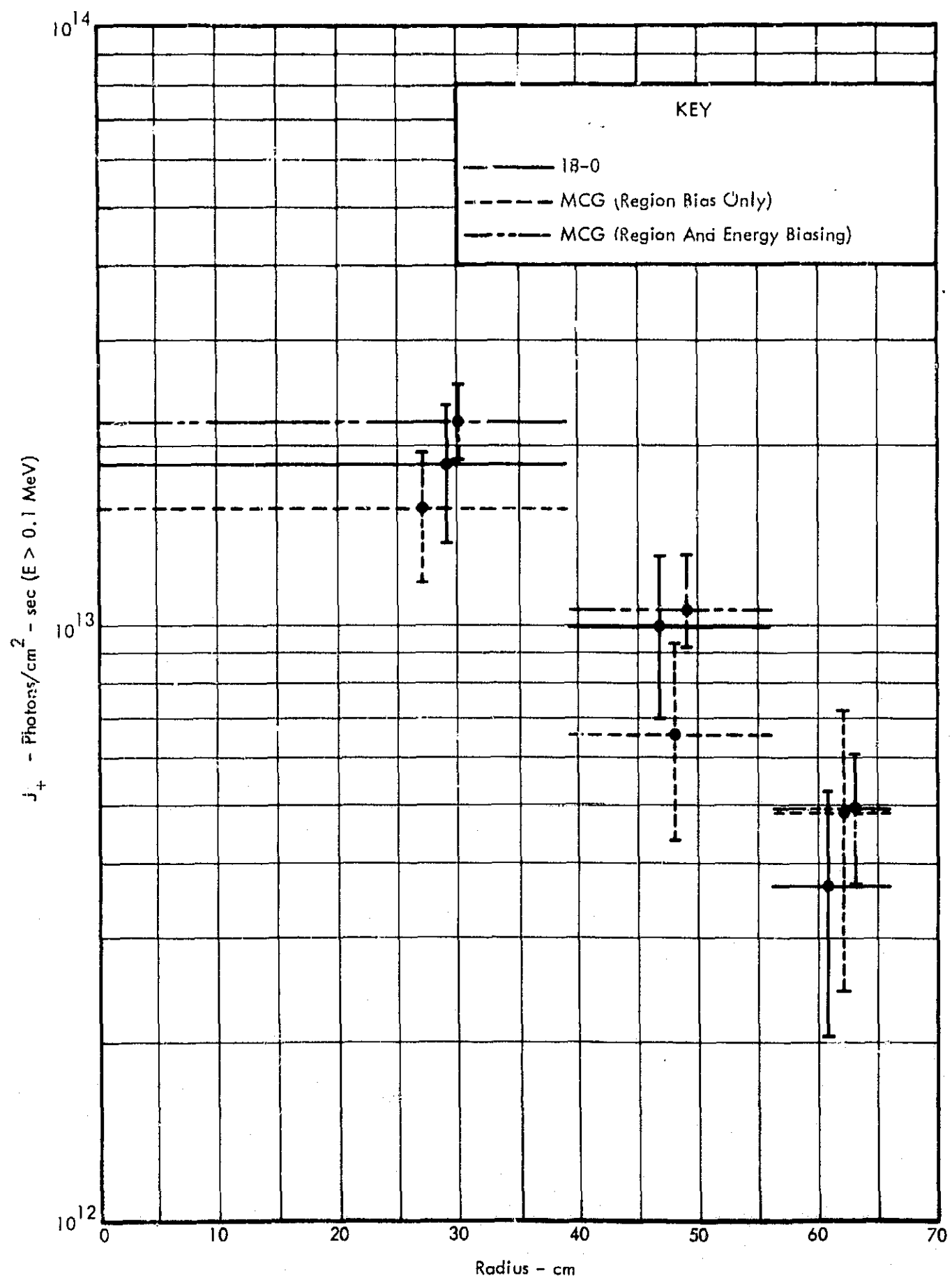


FIGURE 21 GAMMA FORWARD CURRENT (Z = 178 CM)

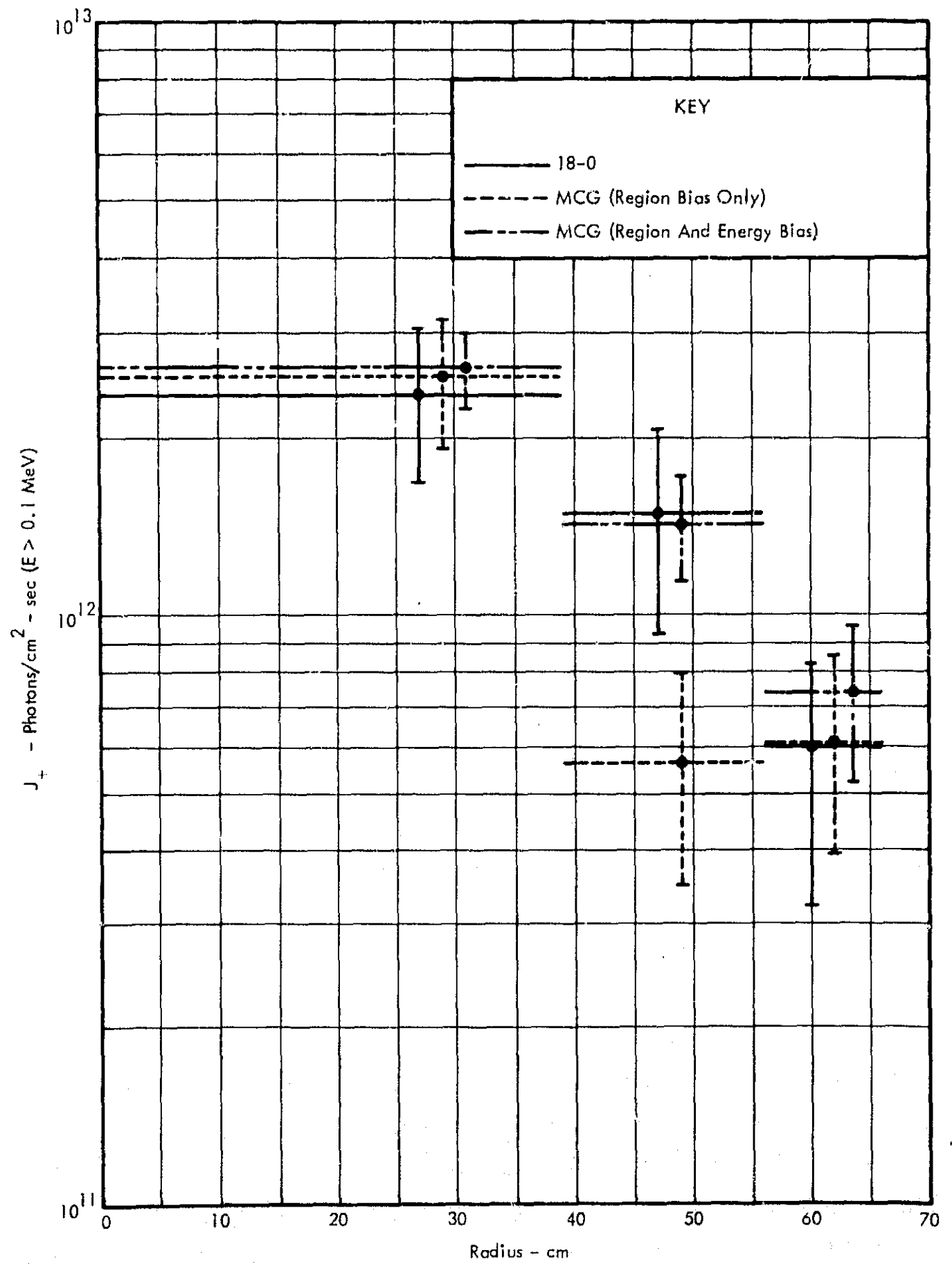


FIGURE 22 GAMMA FORWARD CURRENT (Z = 192 CM)

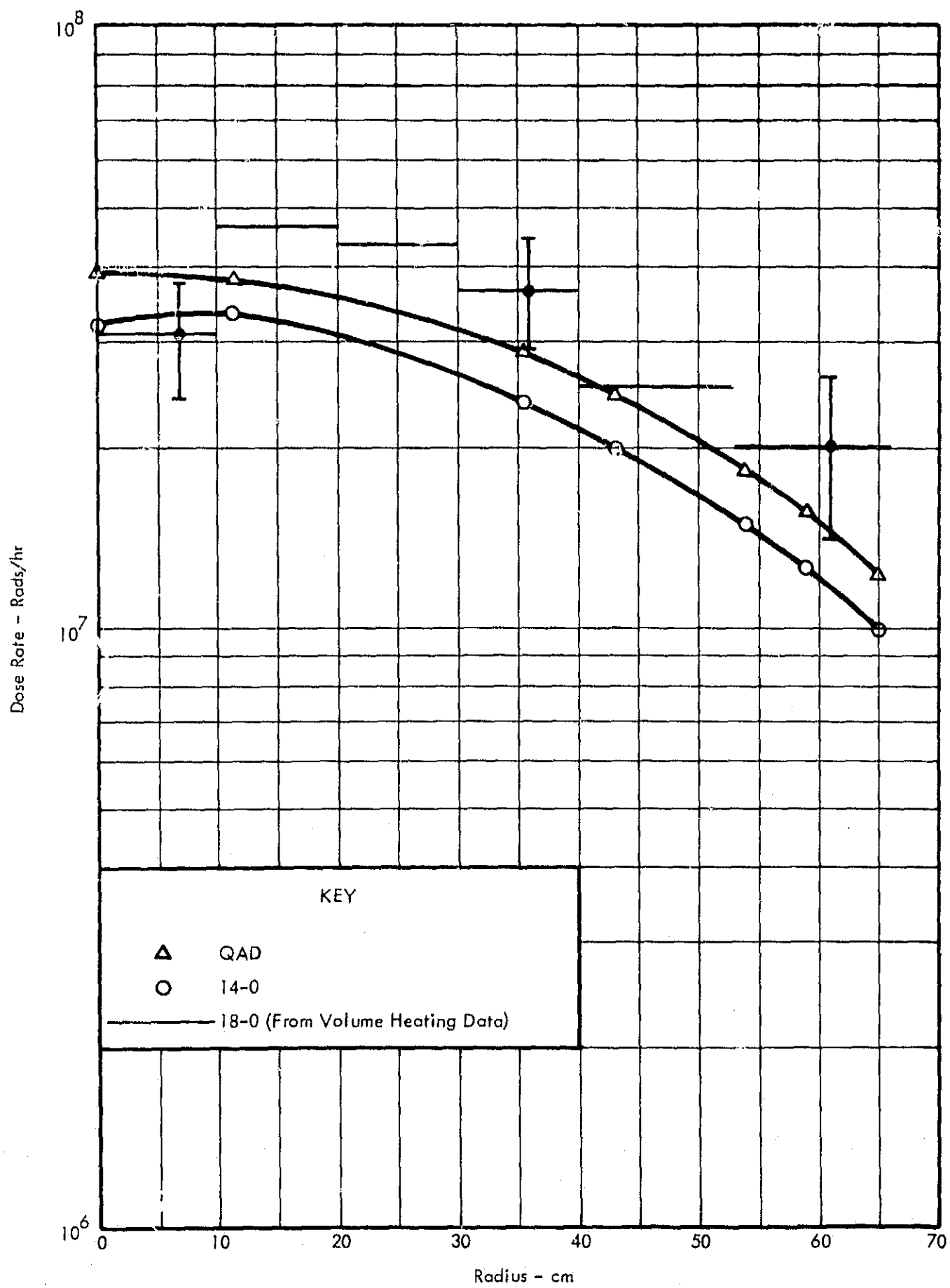


FIGURE 23 CONFIGURATION B, GAMMA DOSE RATE (Z = 183.9 CM)

Figure 16, cause must be assigned to the geometric approximation required by 14-0. In one sense this comparison is unfair, because many configurations encountered in practice must be compromised by QAD also.

Computations of total gamma energy deposition in selected regions of Configuration A are shown in Figure 24. Most of the 14-0 data, representative of QAD also, were obtained by numerical integration over a 3×5 mesh. Statistically significant differences appear between point kernel and the more accurate Monte Carlo data; however, the discrepancy is nowhere greater than a factor of two and is usually much less. Agreement among Monte Carlo data, excepting the unbiased MCG data for 39-56 cm radius, is surprisingly good considering that some of the errors are larger than would normally be considered acceptable.

The computed errors, together with running times shown in Figure 7, indicate the usefulness of the MCG capability for sample biasing on energy. The reason becomes clearer upon examination of Figure 25, showing spectra of photons penetrating the shield. The biased spectrum indicates fairly good sampling up to 4 MeV, and a few particles of energy up to 8 MeV (not shown) were treated. The unbiased sampling is questionable at 2 MeV and no particles are treated above 5 and 6 MeV, respectively, for the MCG and 18-0. It should be noted that some of the narrower of the 25 energy groups treated are combined for presentation in the figure.

To this point, only Monte Carlo computations biased to emphasize transmission parallel to the system axis have been shown. Some results of biasing for radial transmission are shown in Figures 26 and 27. As might be expected for the low attenuation, statistical error is substantially less than within the shield. The point kernel data agree with Monte Carlo to within $\sim 40\%$, also better than within the shield. It is unclear whether this is due to the lesser attenuation, or to the buildup factors used. Buildup characteristic of water is assumed to apply throughout, despite the iron present in the shield.

Component	Axial Limits (CM)	Computer Program	Energy Deposition (Watts)					
			Radial Limits (CM)					
			0-39		39-56		56-66	
			Heating	Relative Error %	Heating	Relative Error %	Heating	Relative Error %
Core Support	139 145	MCG (1) MCG (2) 18-0	2.4(5)	9.0	8.1(4)	16	3.3(4)	33
			2.8(5)	4.5	9.6(4)	6.7	2.8(4)	11
			2.6(5)	10	1.1(5)	27	4.7(4)	35
Lower Shield Support	155 157.5	MCG (1) MCG (2) 18-0	1.4(5)	10	6.3(4)	17	4.0(4)	27
			1.8(5)	5.0	7.6(4)	7.0	2.8(4)	10
			1.6(5)	10	8.1(4)	18	2.4(4)	28
Shield	160 169	MCG (1) MCG (2) 18-0 14-0	2.3(4)	15	1.2(4)	22	6.3(3)	28
			3.5(4)	6.9	1.6(4)	8.6	5.0(3)	12
			3.0(4)	13	1.5(4)	28	5.8(3)	50
			2.0(4)	—	1.2(4)	—	4.8(3)	—
Shield	178 187	MCG (1) MCG (2) 18-0 14-0	5.2(3)	21	2.5(3)	23	1.5(3)	38
			7.6(3)	9.4	4.4(3)	11	1.8(3)	12
			6.9(3)	24	5.0(3)	33	1.8(3)	45
			5.3(3)	—	3.8(3)	—	9.3(2)	—
Upper Shield Support	189.5 192	MCG (1) MCG (2) 18-0	1.7(3)	40	4.7(2)	23	5.5(2)	40
			2.4(3)	12	1.4(3)	13	5.7(2)	14
			2.2(3)	42	1.6(3)	35	5.9(2)	55

MCG (1) - Region Biasing Only

MCG (2) - Region And Energy Biasing

FIGURE 24 SHIELD GAMMA HEATING, CONFIGURATION A

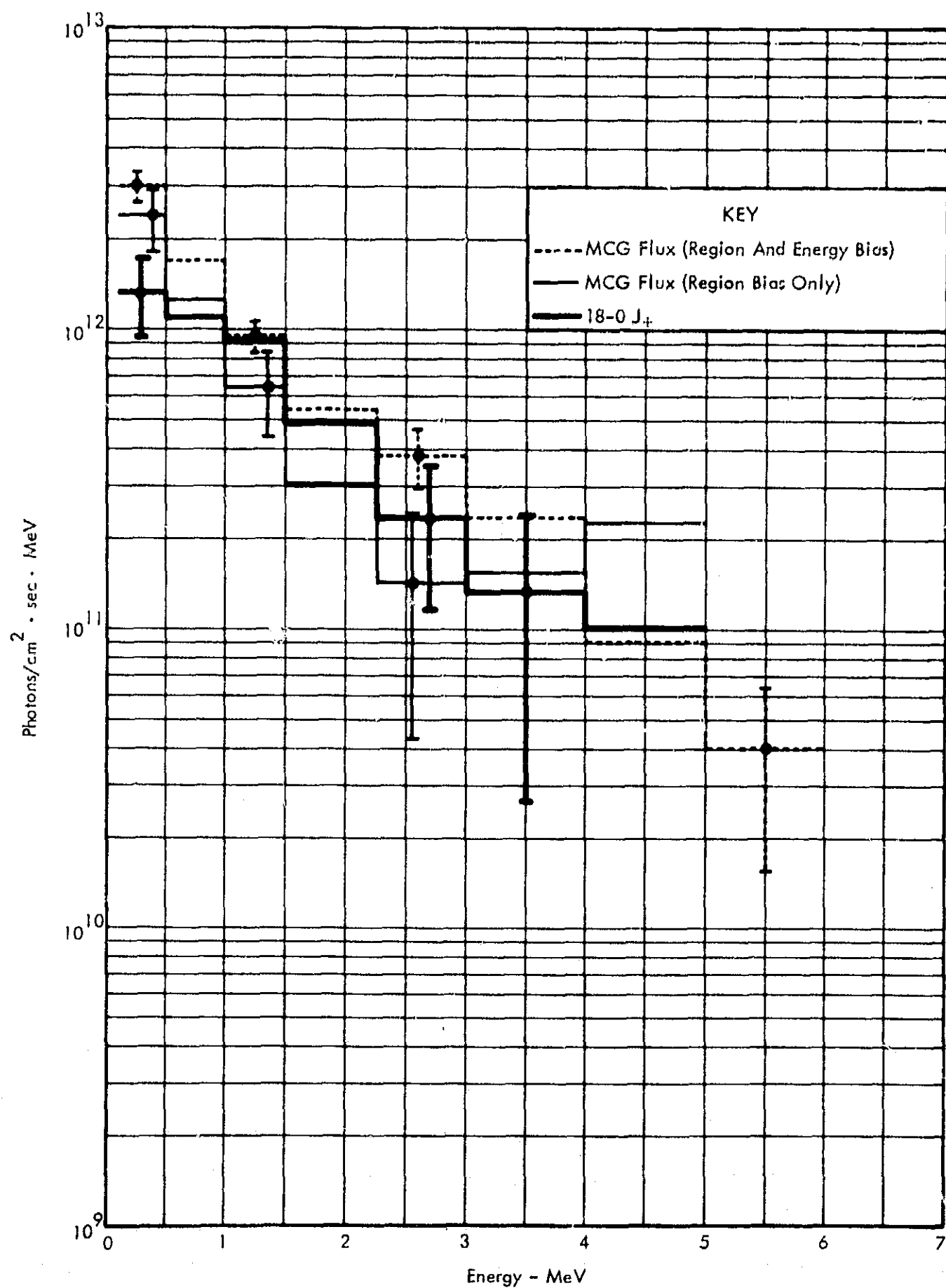


FIGURE 25 GAMMA SPECTRA, AXIAL BIAS (Z = 192 CM, R = 0→39 CM)

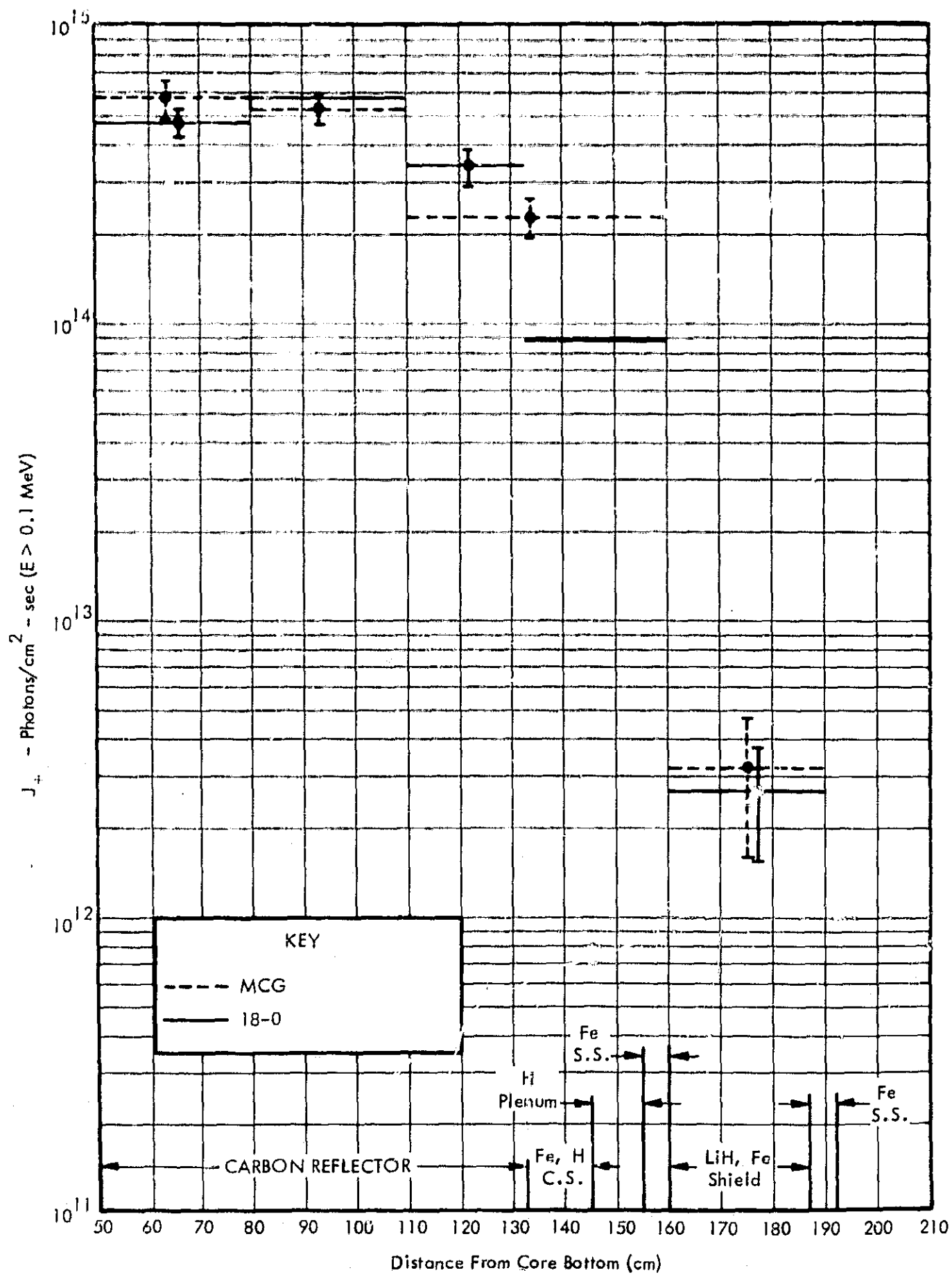


FIGURE 26 GAMMA LEAKAGE CURRENT ON RADIAL BOUNDARY (R = 66 CM)

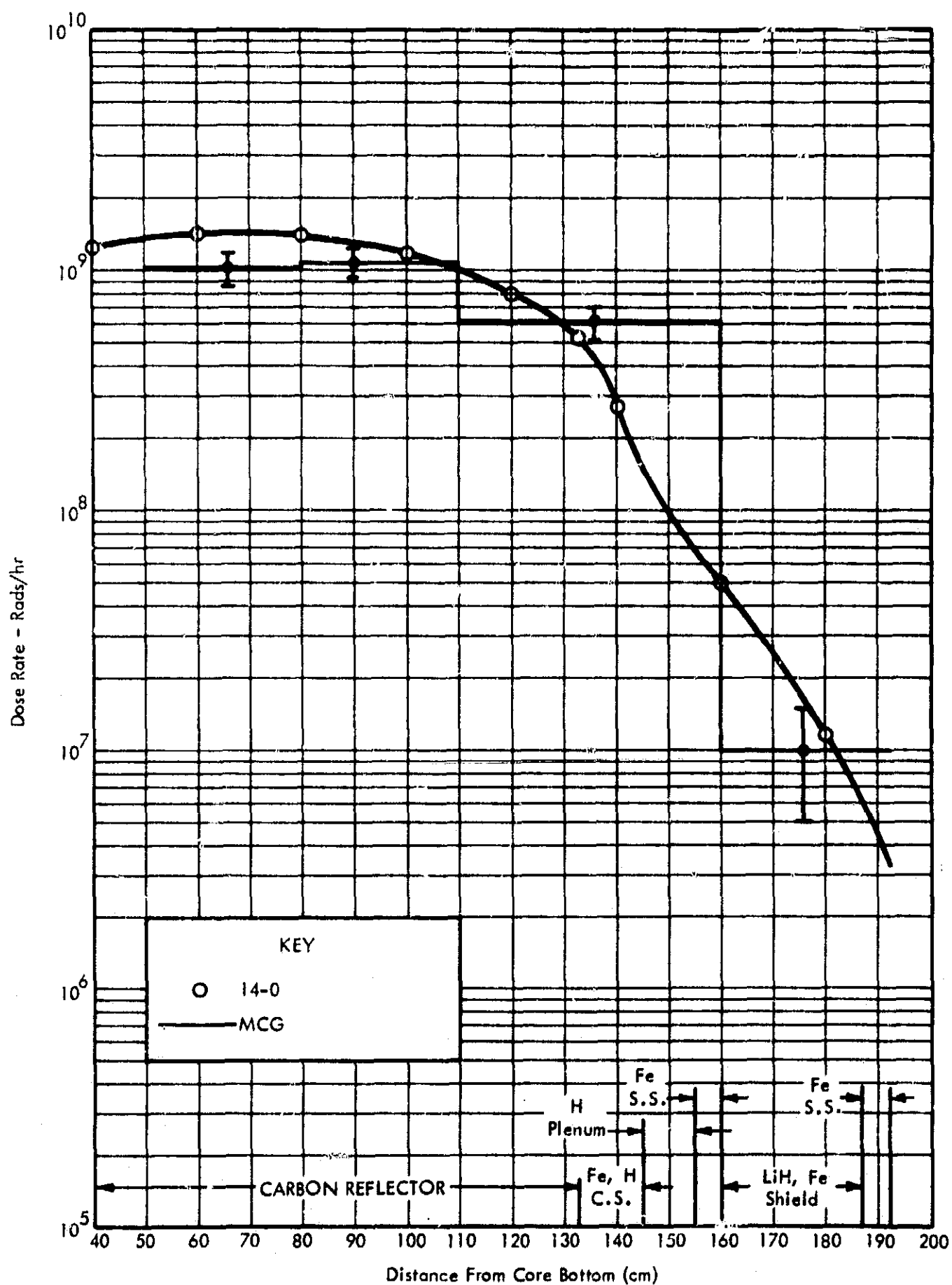


FIGURE 27 GAMMA DOSE RATE ON RADIAL BOUNDARY (R = 66 CM)

Computed spectra of photons escaping the reflector are shown in Figure 28. As before, narrow energy bands are combined. Sampling is fair up to 3 or 4 MeV, which probably covers the range of importance in estimating propellant heating. A few statistically insignificant particles of energy up to 7 MeV are omitted here. The discrepancy below 0.5 MeV may be partly attributable to the diffuse angular distribution characteristic of this energy range, with consequent effect on the ratio of flux and current.

Energy depositions in propellant are tabulated in Figure 29; region boundaries are defined in Figure 13. While it is unfortunate that time did not permit following the energy-biased MCG histories into the tank, the fortuitous agreement shown in Figure 24 lends credence to the axially biased 18-0 data, despite the large relative errors shown. The importance, even near the centerline, of radiation escaping through the reflector is apparent. Although a minimal core-tank separation was deliberately selected to emphasize this problem, it seems certain to remain a major design consideration at any practical separation. This is particularly true in view of the critical effect on propellant convection of heating in Regions 4 and 5. The radially biased data for Regions 1, 6, and 11 are due to scattering in either the reflector or the tank, since no direct transmission is allowed by the computational technique used. The point kernel data shown were obtained by summation over a mesh of at least 3 axial by 5 radial points, with a maximum error thought to be less than 10%. Agreement with Monte Carlo is as good as within the shield, except in Region 11 where the Monte Carlo datum is meaningless.

Dose rates at the top of the propellant tank, a design consideration because of potential radiation damage to vehicle components, are compared in Figure 30. The 18-0 dose rates shown are obtained from current spectrum and flux-to-dose conversion factors for each energy band, implying equivalence of flux and current. This approximation is at least partially justifiable on grounds of distance collimation. Liquid level in the tank is shown by the dashed line in Figure 13. Hence an attenuation due to

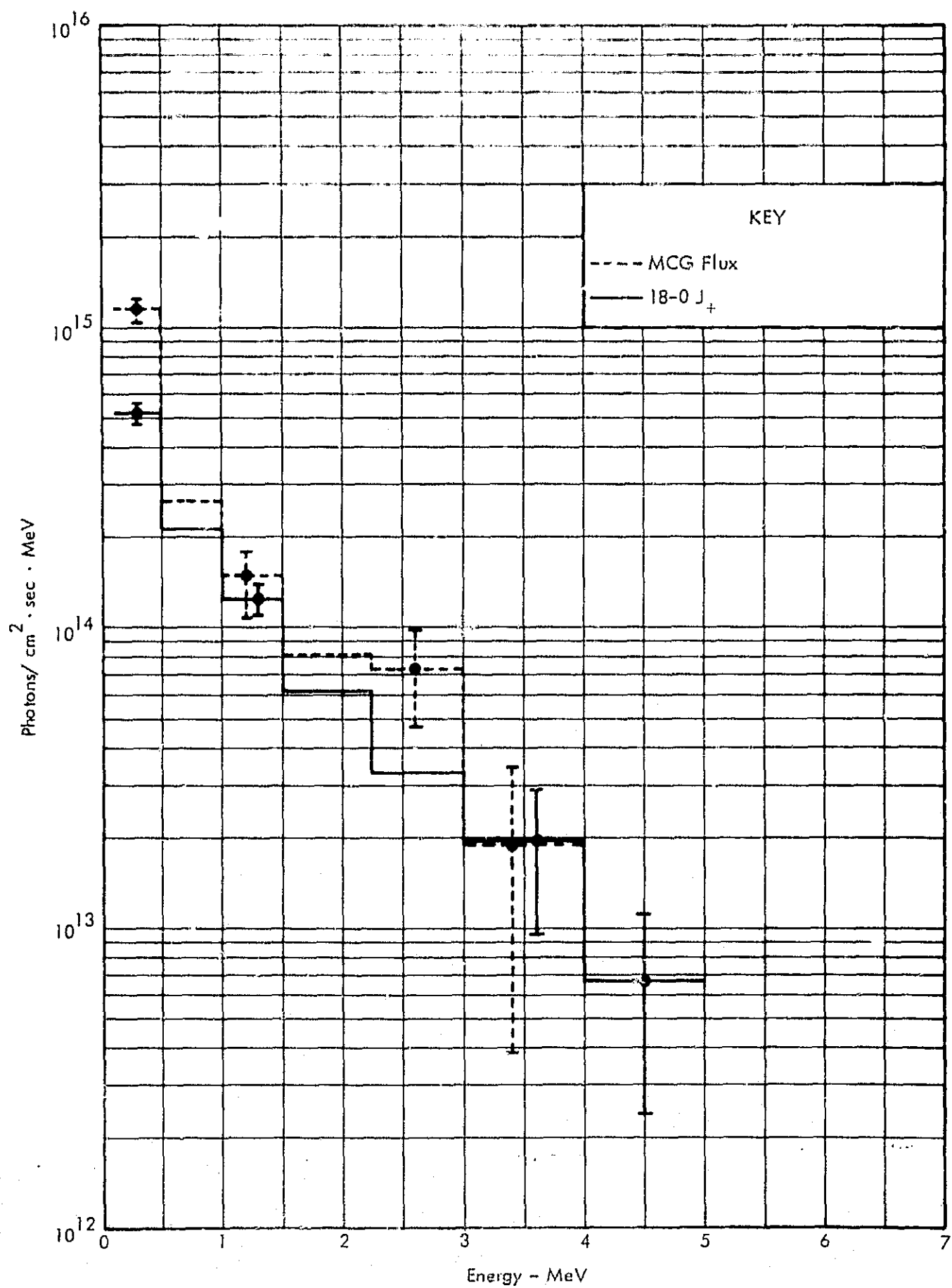


FIGURE 28 GAMMA SPECTRA, RADIAL BIAS (R = 66 CM, Z = 50 → 80 CM)

propellant, of between 10 and 100 may be inferred from Figure 29. The quantity most frequently of interest is total dose summed over the tank drain cycle. Since most of this sum is attributable to the end of the cycle, the attenuation treated is about the largest which need be known with great precision. Factor of two agreement between point kernel and Monte Carlo dose predictions may reasonably be expected, therefore, for regions above a propellant tank. The rise at the end of the 14-0 curve is due to source-detector paths which by-pass the shield. Since radiation emitted over the entire liquid surface must in fact contribute to dose at each point, as suggested by the Monte Carlo data, local irregularities in point kernel data at the tank top must be deemed fictitious.

3.3 COMPARISON OF NEUTRON COMPUTATIONS

The schema used in comparison of gamma data is now applied to neutron data. Description of adjustments of computer output, to a common basis of comparison, will not be repeated. Data shown refer to Configuration A, unless otherwise stated. Additional complications arise, however, with the introduction of multiple point kernel estimates, and of discrete ordinates data. From the nature of the latter method, source distribution is slightly different for each individual computation. The standard source, described in Section 3.1, was obtained in a 15-group computation for Configuration A. A reflecting plane through the core was introduced to conserve mesh points for treatment of exterior regions. The error which could be introduced by this difference appears to be about 10 to 15% for the 4-group data, relative to 15-group. Some of this difficulty could have been avoided by use of the "fixed source" option of DDK. A trial computation with DTK indicated a tripling of computer time per group treated, more than could be allotted for discrete ordinates computations.

Figures 31, 32, 33, 34, and 35 show dose rates in and near the shield, as estimated by DDK and the several point kernel options described in Section 2.0. The DDK curves are a composite of two computations, 15-group interior and 4-group data

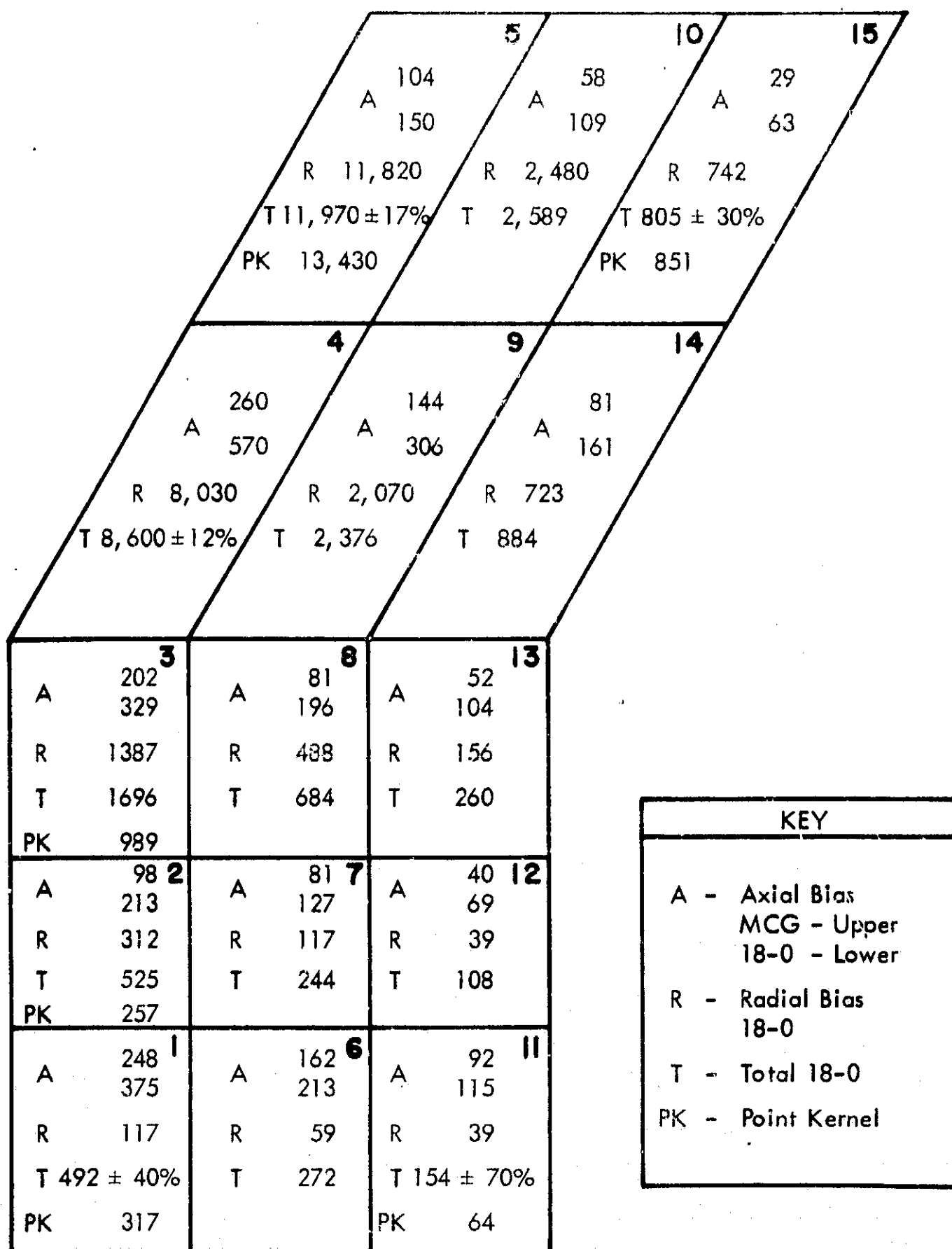


FIGURE 29 PROPELLANT GAMMA ENERGY DEPOSITION (WATTS)

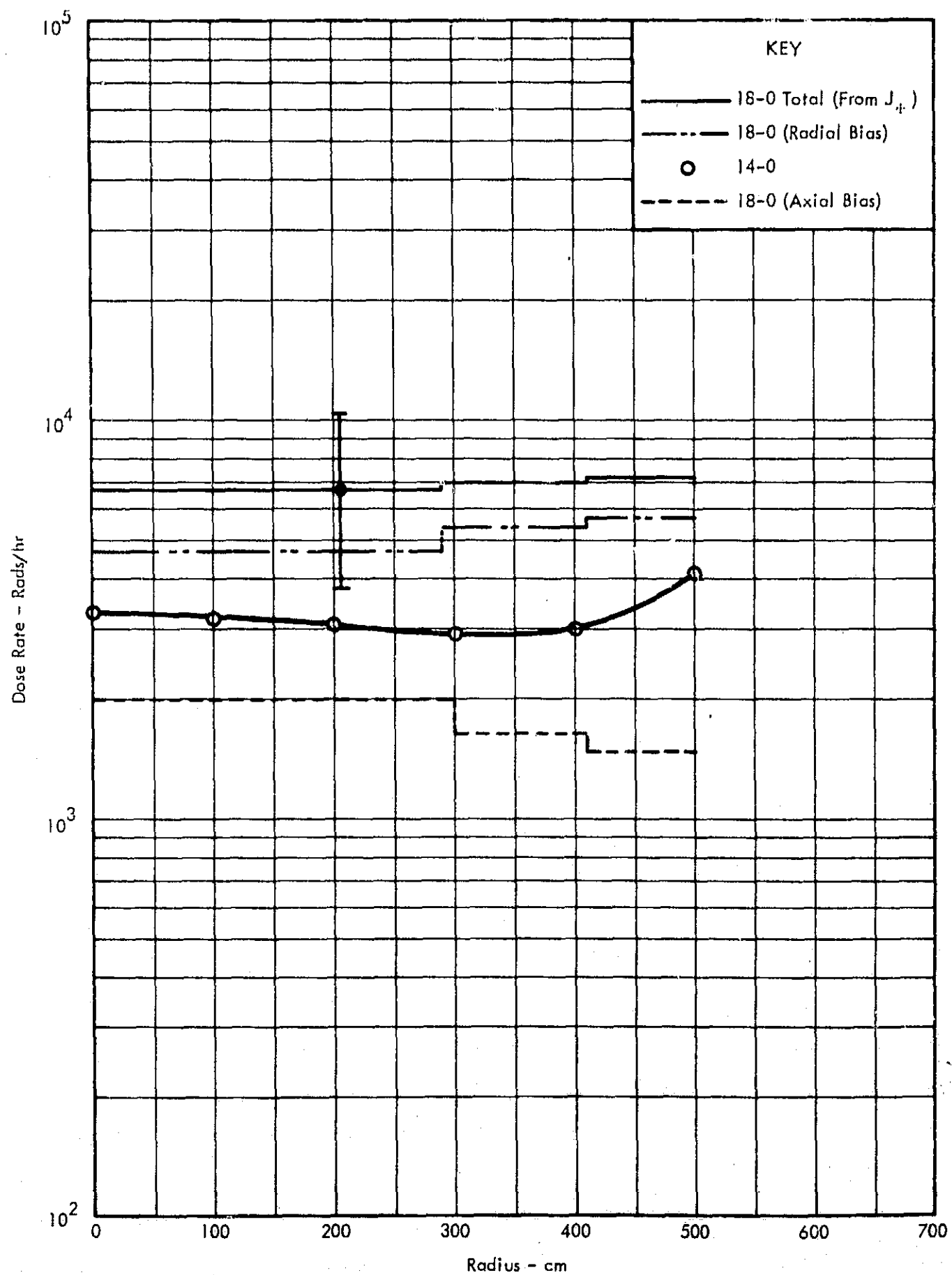


FIGURE 30 GAMMA DOSE RATE, PROPELLANT TANK TOP ($Z = 1729$ CM)

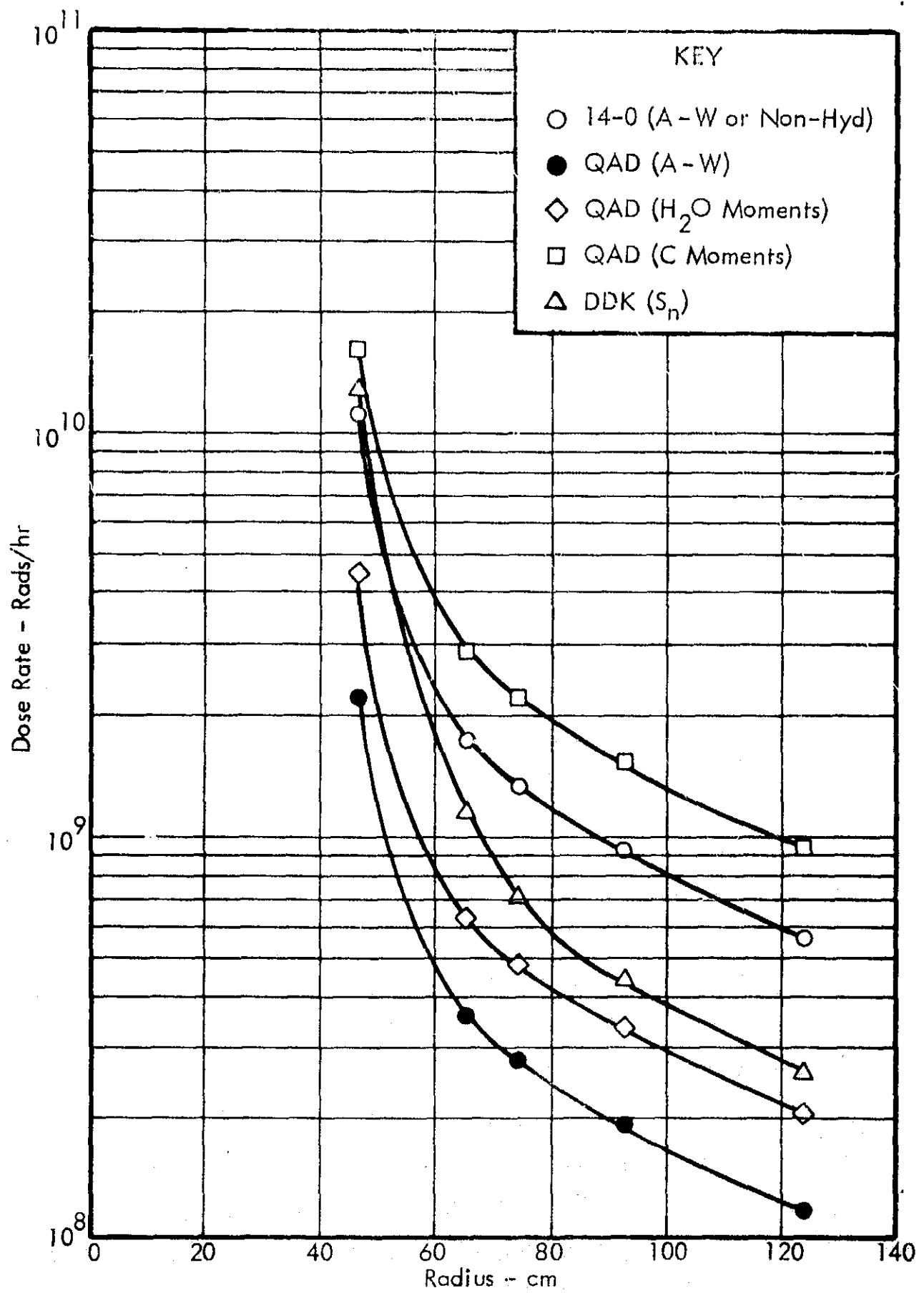


FIGURE 31 NEUTRON DOSE RATE (Z = 93 CM)

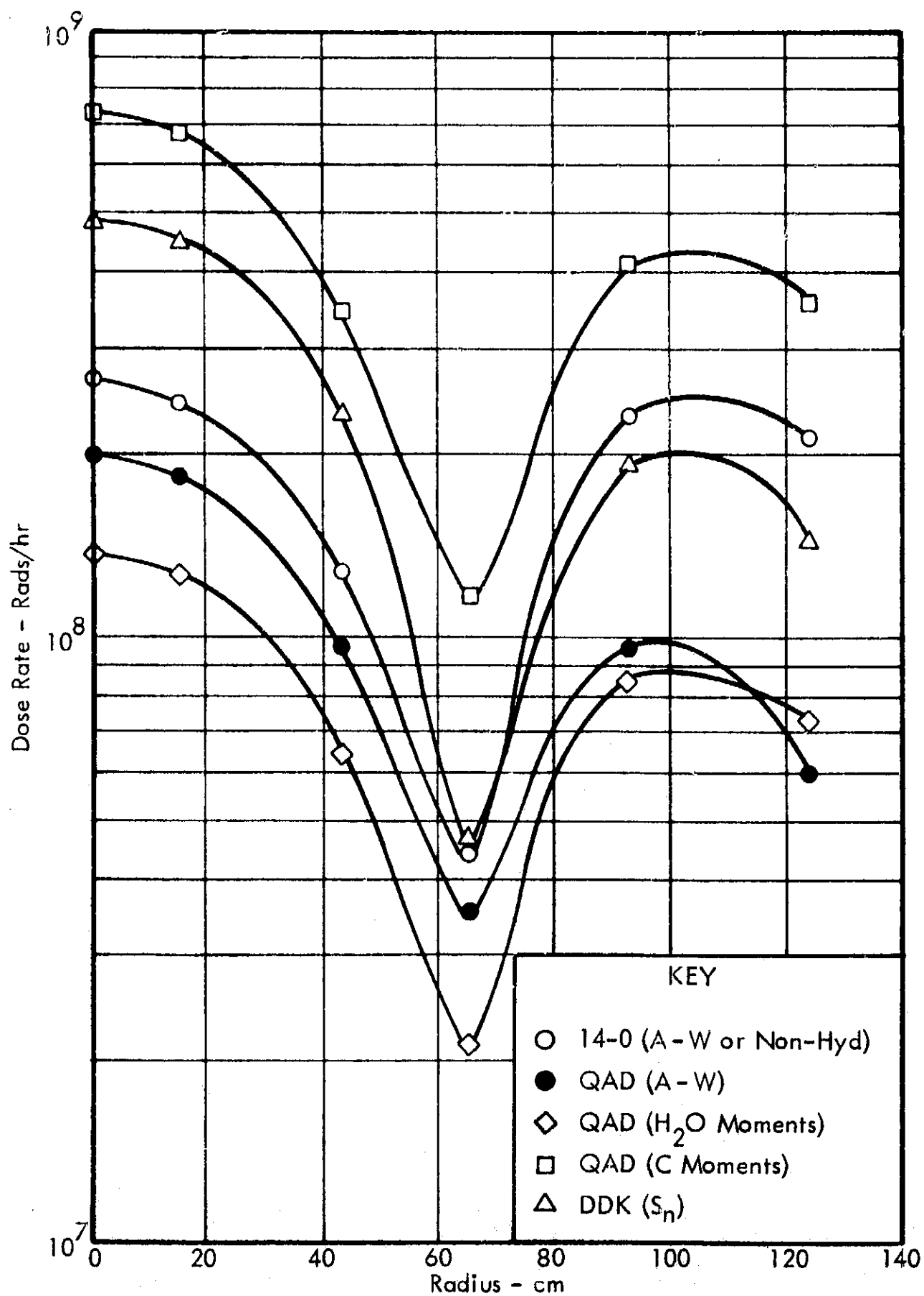


FIGURE 32 NEUTRON DOSE RATE ($Z = 164$ CM)

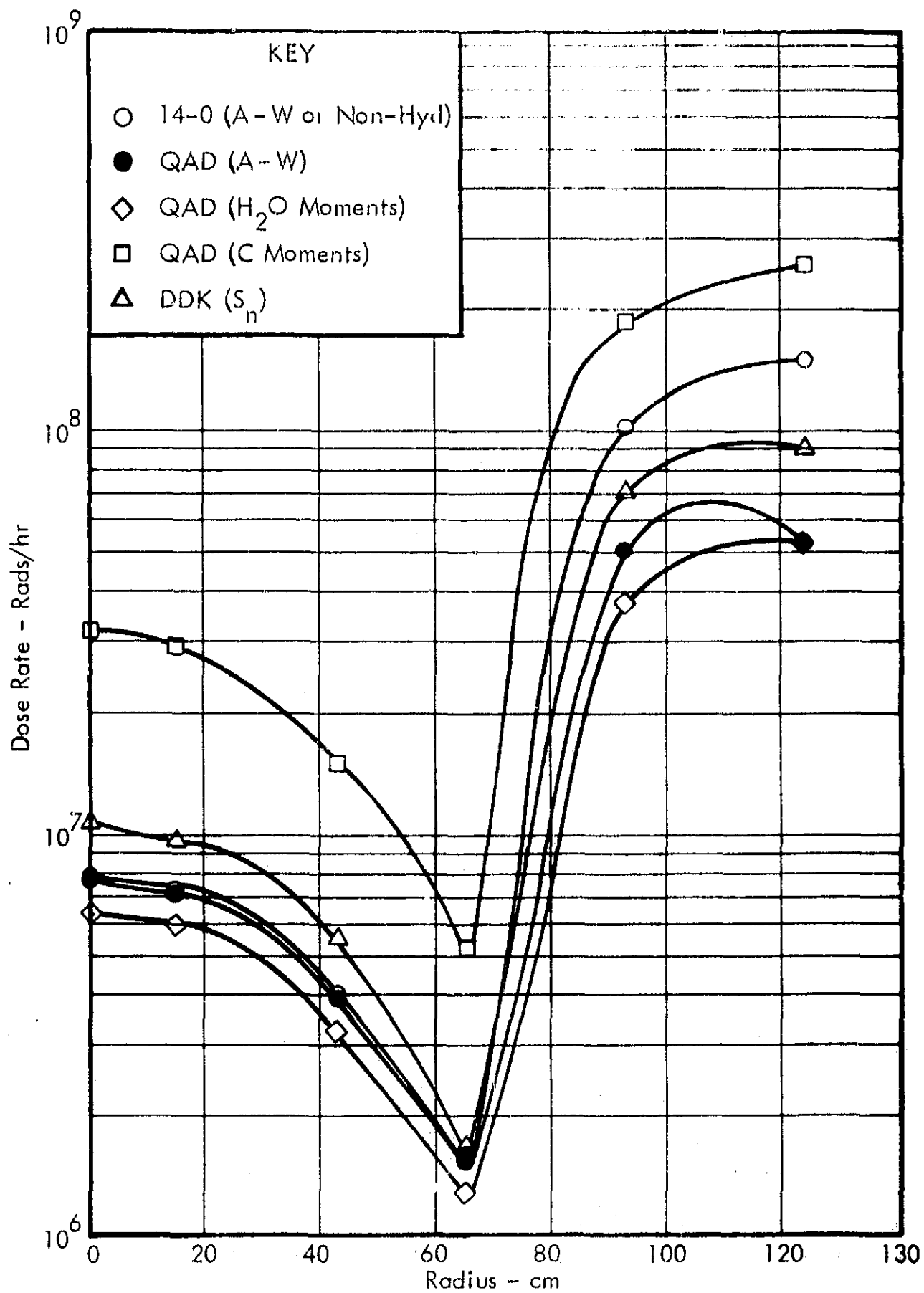


FIGURE 33 NEUTRON DOSE RATE (Z = 184 CM)

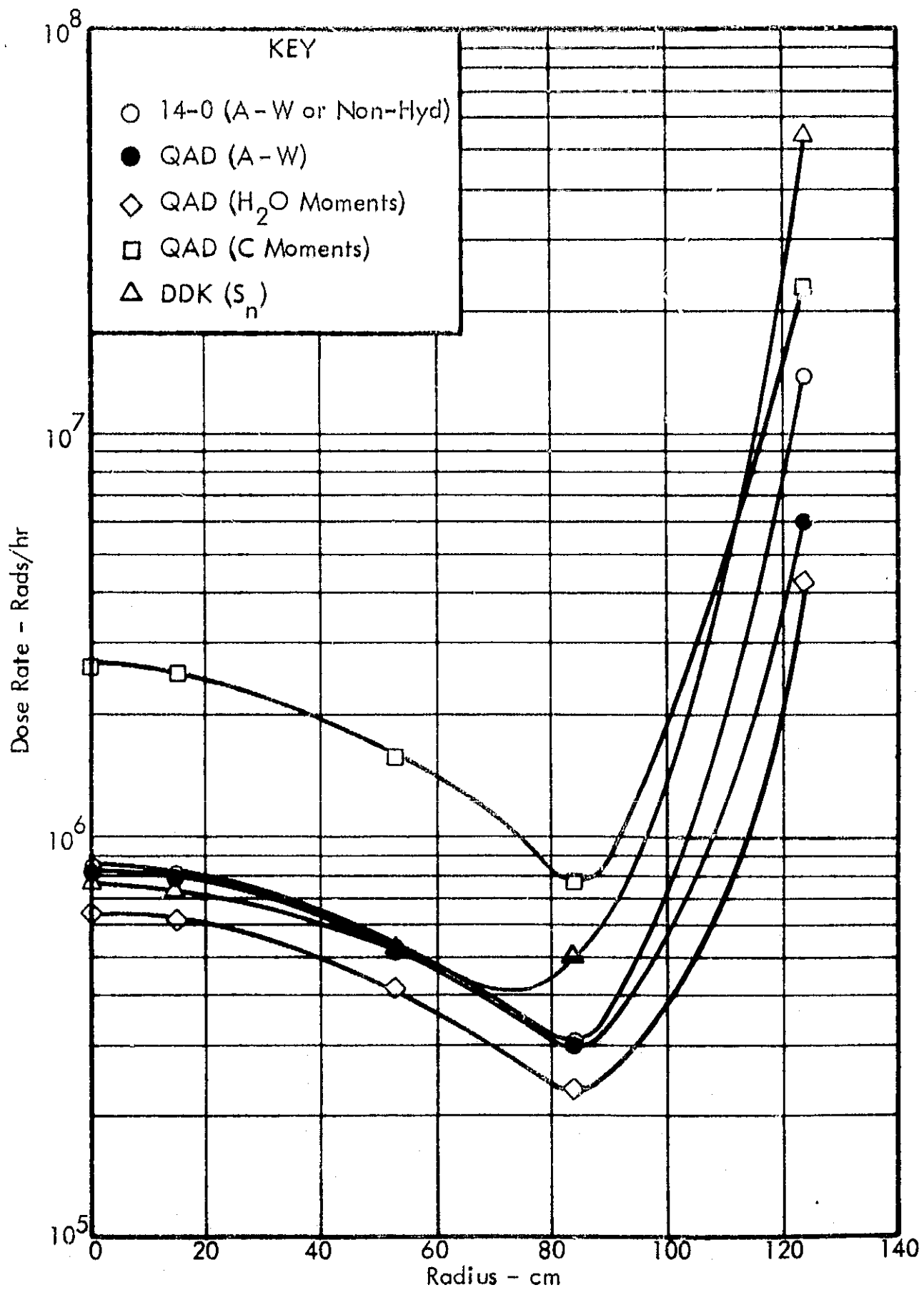


FIGURE 34 NEUTRON DOSE RATE (Z = 260 CM)

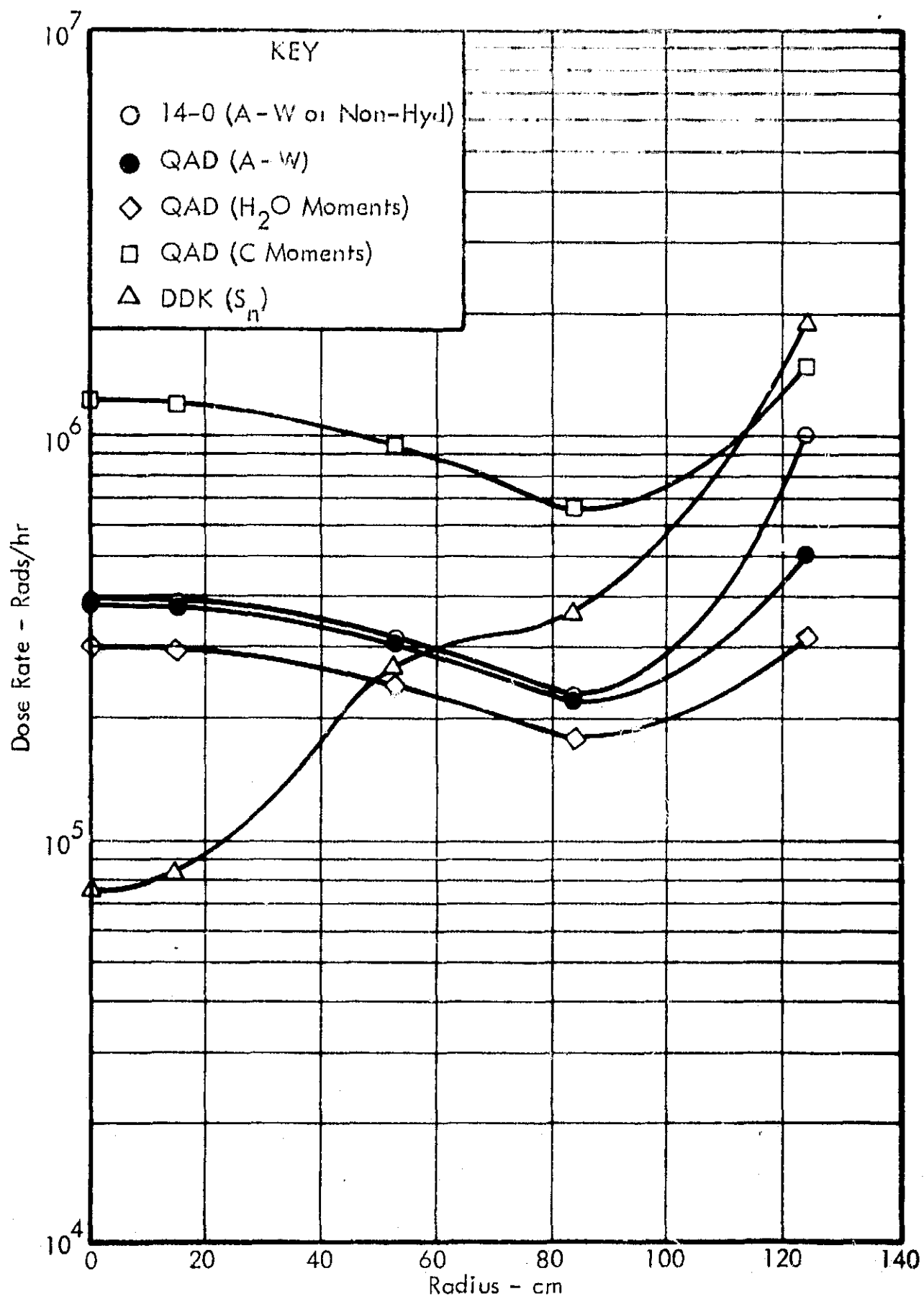


FIGURE 35 NEUTRON DOSE RATE ($Z = 338$ CM)

exterior to the shield. For both, more mesh points were computed than are depicted in the figures. Though hardly outstanding, the agreement is not as bad as it might appear at first glance.

The two lowest curves in Figures 31 and 32, corresponding to modified Albert-Welton and water moments-method kernels, are probably inapplicable due to the scarcity of hydrogen between source and detector. At $Z = 93$ cm, near the forward edge of the core, the QAD carbon-moments and the 14-0 kernels agree to within a factor of two. Here the source points contributing most to the 14-0 dose rate estimates are presumably treated by the non-hydrogenous kernel routine. At $Z = 164$ cm, near the rear boundary of the LiH shield region, more of the 14-0 source points are treated by the modified Albert-Welton routine, at least within the shield. Thus, up to 66 cm radius, the 14-0 data agrees more closely with the Albert-Welton estimate of QAD. Outside the shield, less hydrogen is encountered along most source-detector paths, and the 14-0 data remains nearer the carbon kernel estimate.

Near the forward boundary of the LiH region the 14-0, QAD Albert-Welton, and QAD water-moments kernels agree very well within the shield, as shown in Figure 33. Such difference as exists between the first two of these can only be the result of differences in source point mesh. Outside the shield, the materials traversed by the source-detector paths remain as for the preceding figures, and the carbon-moments kernel or 14-0 kernel are presumably most accurate. The situation several feet forward of the shield, shown in Figures 34 and 35 is somewhat similar except that the maximum dose rates occur at greater radii. The relatively rapid rise of the DDK data exterior to the shield may indicate the effect of scattering within the reflector; this possibility will be considered later.

If it be assumed that the discrete ordinates computation is a suitable standard of comparison as suggested by theory but not necessarily by subsequent comparison with Monte Carlo data, then either point kernel code is accurate to a factor of two within

the shield. Outside the shield, the situation is clouded by the small number of energy groups used with DDK. Furthermore, the DDK iteration did not converge for a few points at the edge of the mesh. This problem is illustrated by the dip at $R = 0$ in Figure 34. Further iteration and/or mesh adjustment did not appear profitable, since treatment of the 338×120 cm cylindrical space about Configuration A very nearly exhausted the DDK data storage capacity.

Fluxes corresponding to the dose rates described above are shown in Figure 36. Similarity with the corresponding dose rate curves, Figure 31, is obvious. This similarity continued to all axial traverses examined, up to and including $Z = 338$ cm. A comparison of 15-group and 4-group fluxes is shown. It remains unclear why agreement was consistently better at the Configuration A boundary.

Some of the dose rate estimates previously shown are now compared with Monte Carlo results. At the rear edge of the lithium hydride region, Figure 37, the QAD carbon-moments data is in substantially better agreement with MCS than is DDK. The agreement is of course reversed deeper in the shield as shown in Figure 38. In both cases, the Monte Carlo data seem to drop more sharply toward the edge of the system.

The corresponding fluxes are shown in Figures 39, 40, and 41 and the comparison is quite similar. The differences noted between currents computed by MCS and 18-0 are well within the error limits.

Relative numbers of radiative capture events in the regions of Configuration A are shown in Figure 42. Data in the second column were computed from DDK 15-group fluxes, using a satellite code which had earlier been prepared for this purpose. Corresponding estimates were then made using the one-dimensional DTK program, in the hope that an inexpensive substitute might be found for lengthy two-dimensional computations of secondary source strength. The comparative results, shown in the third column, assume a radius of 55 cm for use in the DTK radial buckling option. While

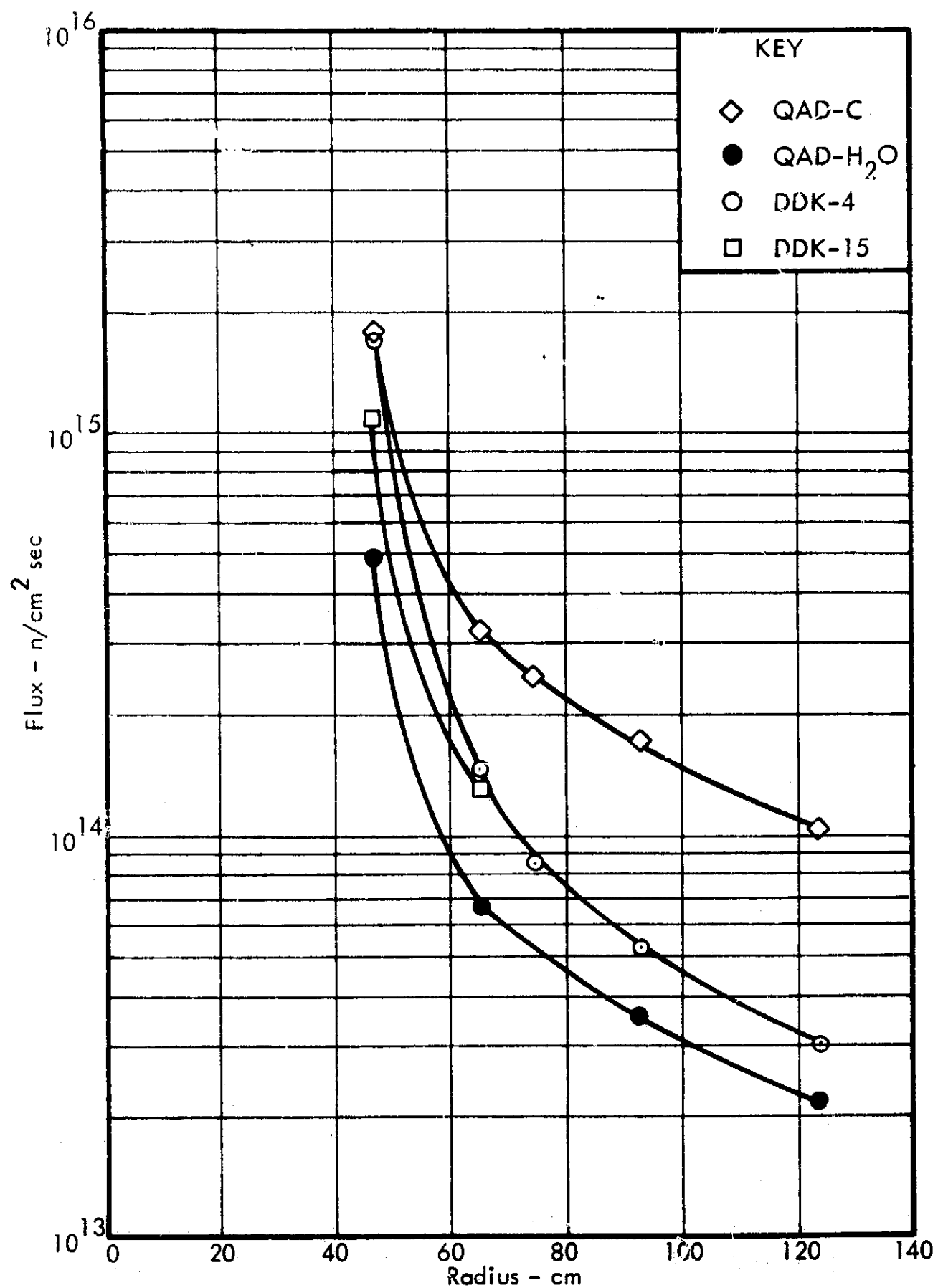


FIGURE 36 NEUTRON FLUX (Z = 93 CM)

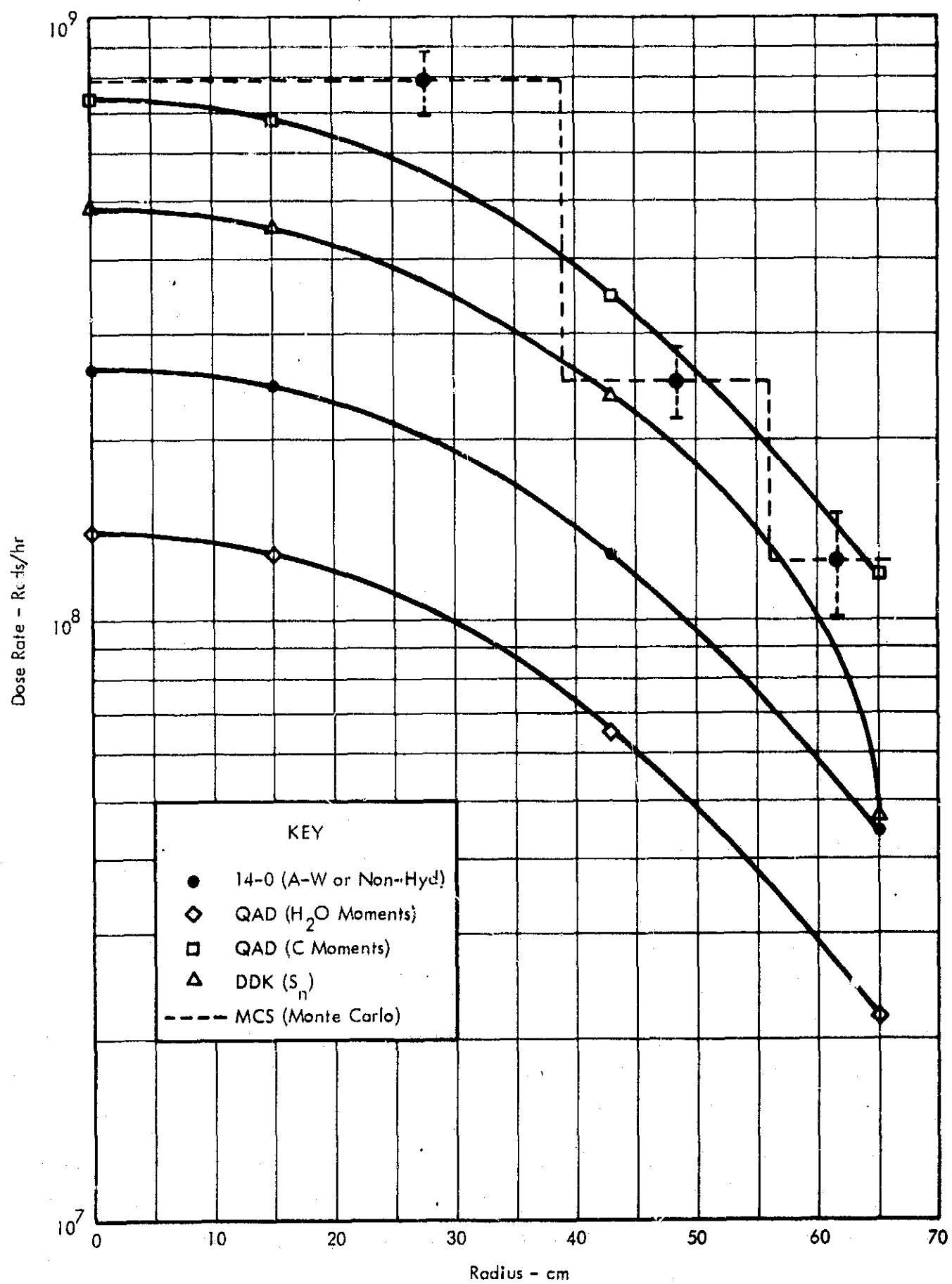


FIGURE 37 NEUTRON DOSE RATE (Z = 164 CM)

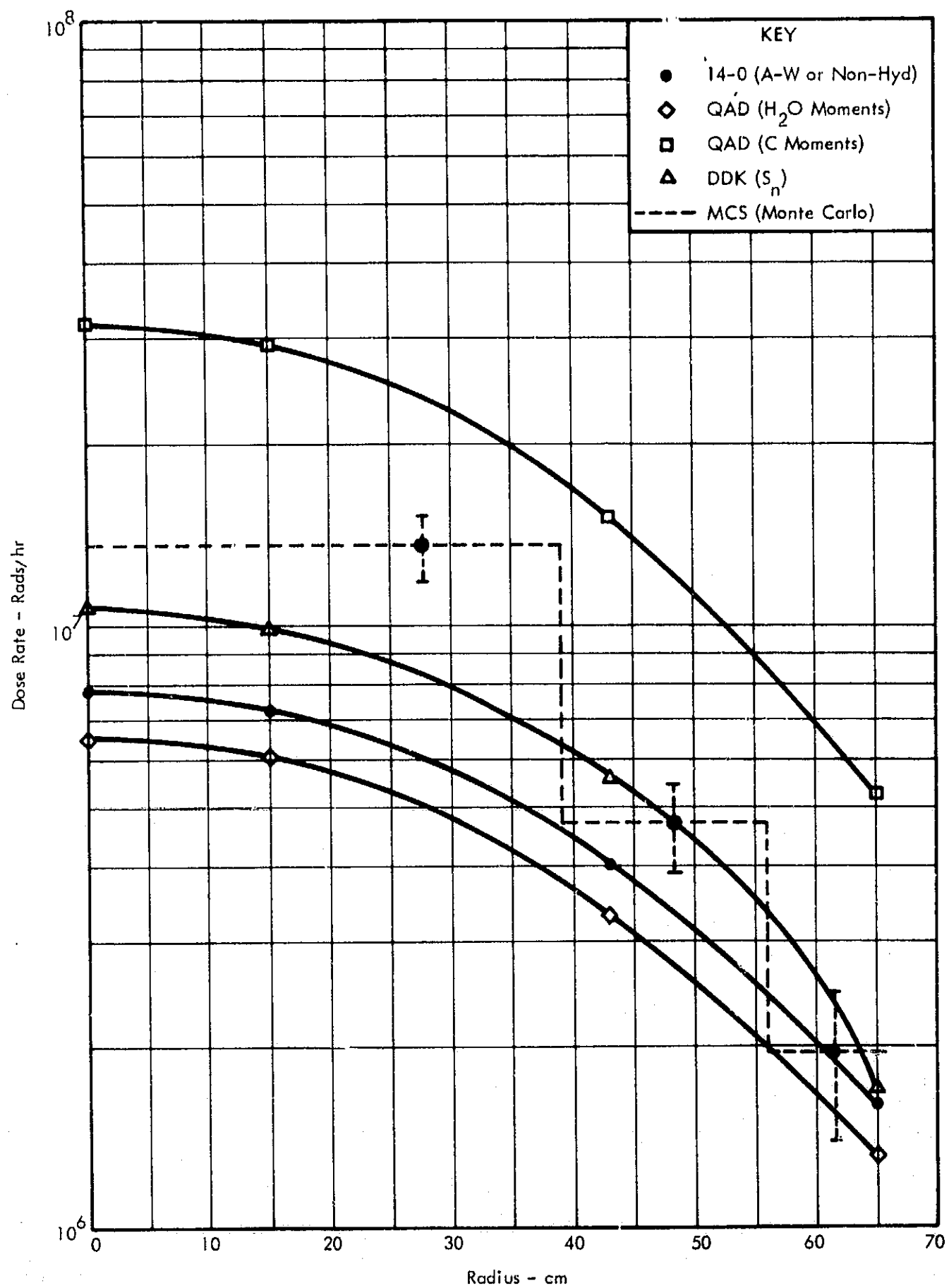


FIGURE 38 NEUTRON DOSE RATE ($Z = 183.9$ CM)

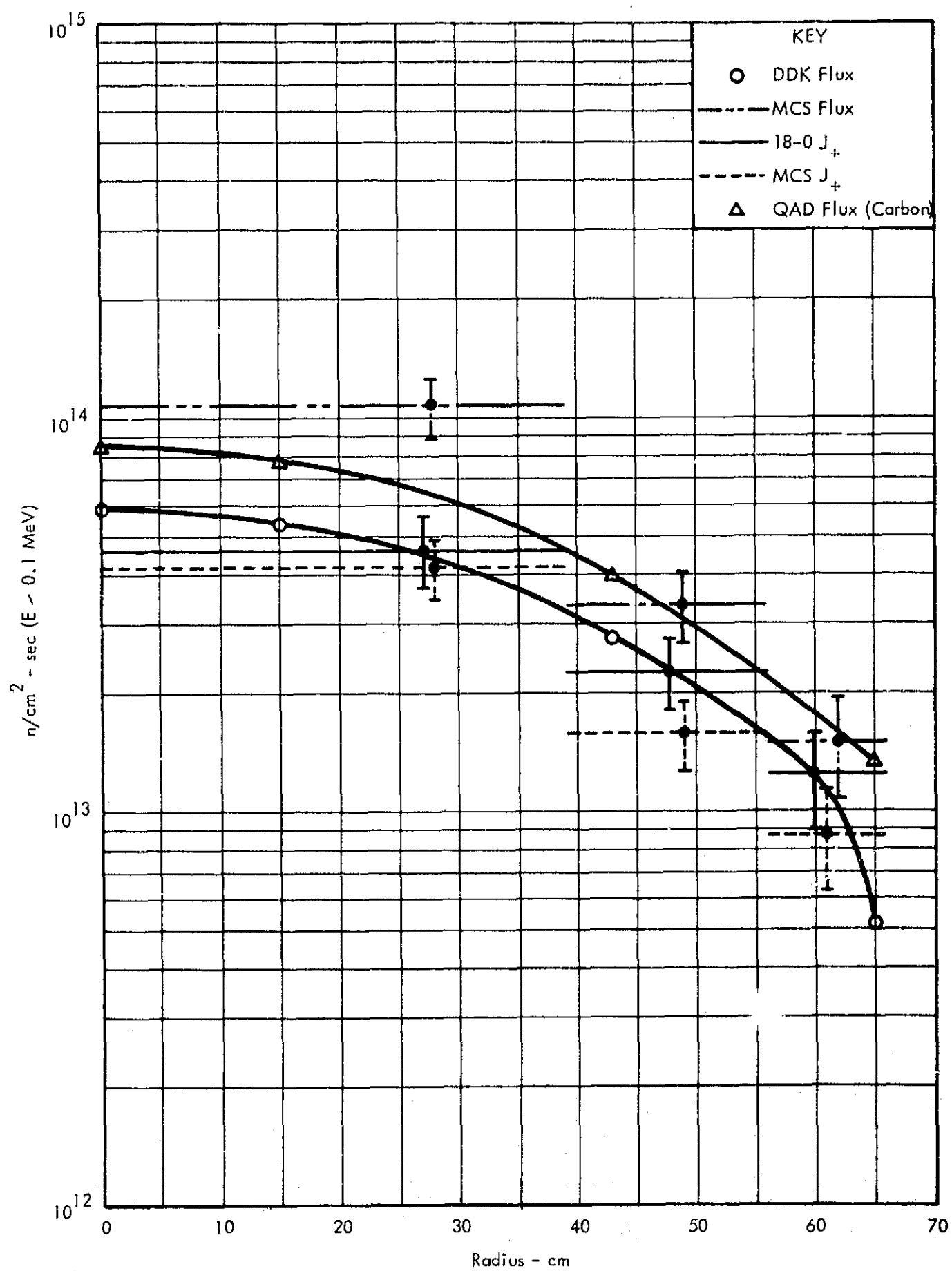


FIGURE 39 NEUTRON FLUX AND FORWARD CURRENT (Z = 165 CM)

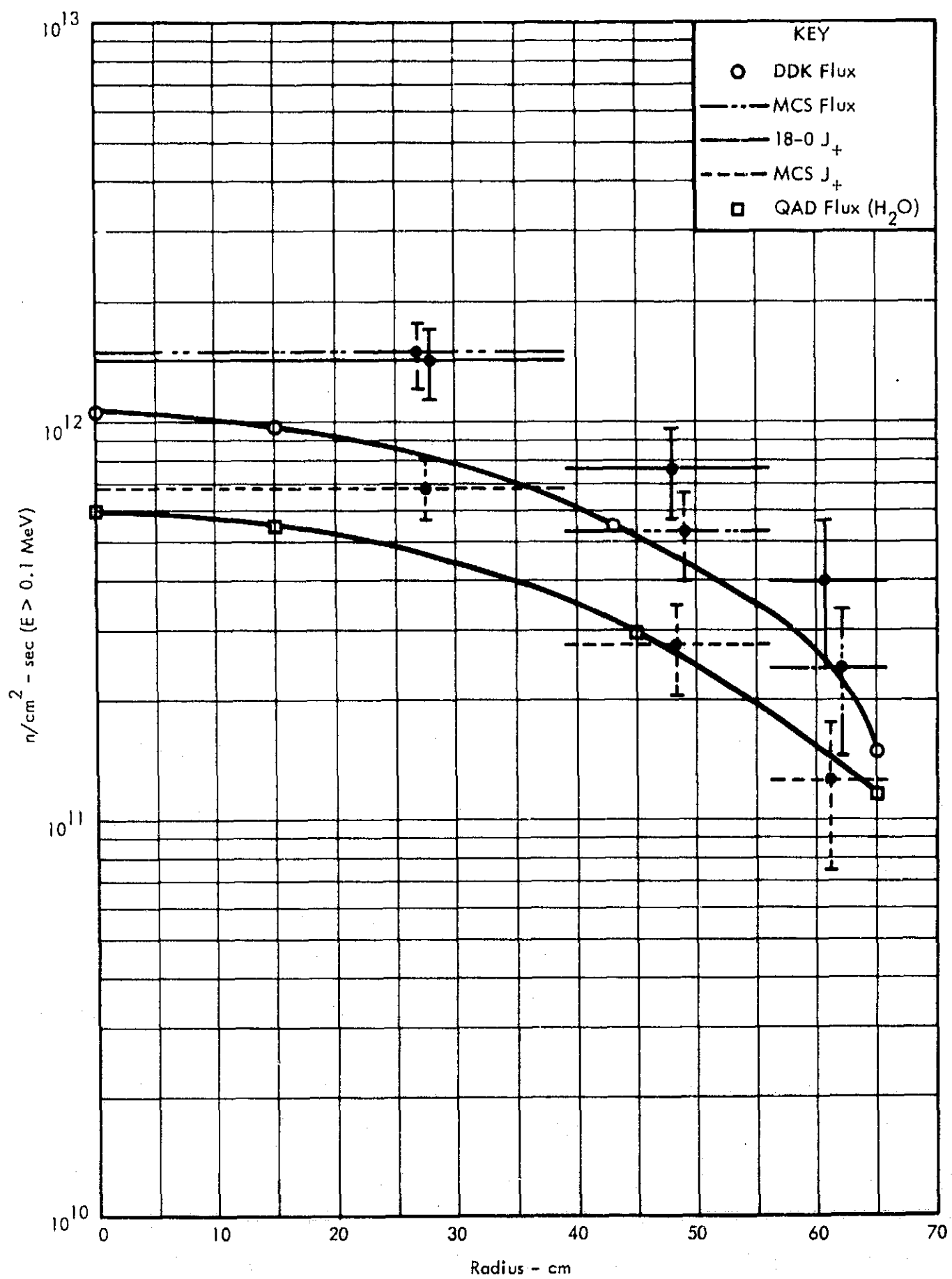


FIGURE 40 NEUTRON FLUX AND FORWARD CURRENT (Z = 183.9 CM)

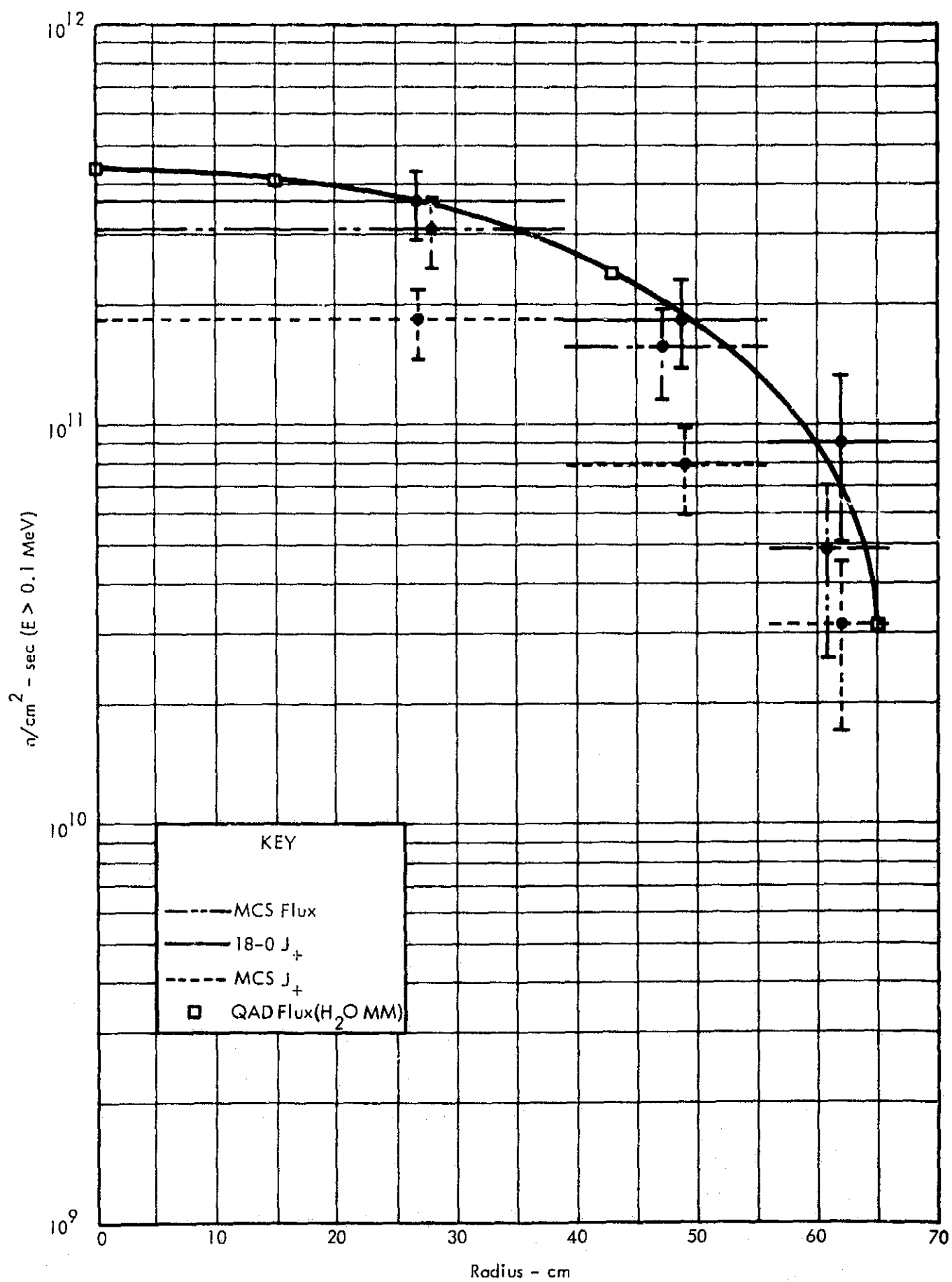


FIGURE 41 NEUTRON FLUX AND FORWARD CURRENT (Z = 192 CM)

REGION	DDK (capt./fiss.)	DTK/DDK
K	6.3 (-7)	.61
C	2.6 (-1)	1.00
CS	1.2 (-2)	.43
P	7.8 (-4)	.46
LS	7.1 (-3)	.48
S	3.1 (-4)	.62
US	2.9 (-6)	.87

FIGURE 42 RADIATIVE CAPTURE EVENTS

a different assumption might improve the present approximation, a more complex system such as Configuration B could hardly be approached with confidence in view of the difficulty with Configuration A.

Neutron dose rates on a traverse through the LiH region of Configuration B are plotted in the next two figures. It will be noted in Figure 43 that there are no DDK data for the region exterior to the boundary. The 4-group computation failed to converge to positive fluxes, over rather large areas of the mesh centering on the stepped boundaries used to represent spherical surfaces. The likely reason is overshoot due to the linear nature of the S_n difference equations.

At the depth in hydrogenous material corresponding to $Z = 194$ cm, the 14-0 and QAD Albert-Welton kernels are identical. Hence, differences in the two estimates are attributable to either the respective source or geometry treatment. Since different source treatments resulted in a trivial error for Configuration A, the 15 to 20% discrepancy found for Configuration B is probably due to approximation of boundaries with 14-0. As shown in Figure 44, the relative error for 18-0 data is of similar magnitude, and comparison of the 18-0 and MCS geometries correspondingly difficult. From the similarity 18-0 to 14-0 and MCS to QAD, it is supposed that such comparison might also disclose a 15 to 20% discrepancy.

The 18-0 data is slightly more in agreement with the carbon-moments data than at 184 cm depth in Configuration A; however, some of the hydride has been replaced by iron. In Figure 45, a flattening of the dose rate profile is apparent, due to the greater shield thickness near the system centerline. In general, the trends observed for the simpler geometry apply also to Configuration B.

A comparison of neutron energy depositions in selected volumes of Configuration A is shown in Figure 46. Each of the other methods shows a significant difference from the Monte Carlo estimate. The carbon-moments data fares best with respect to 18-0,

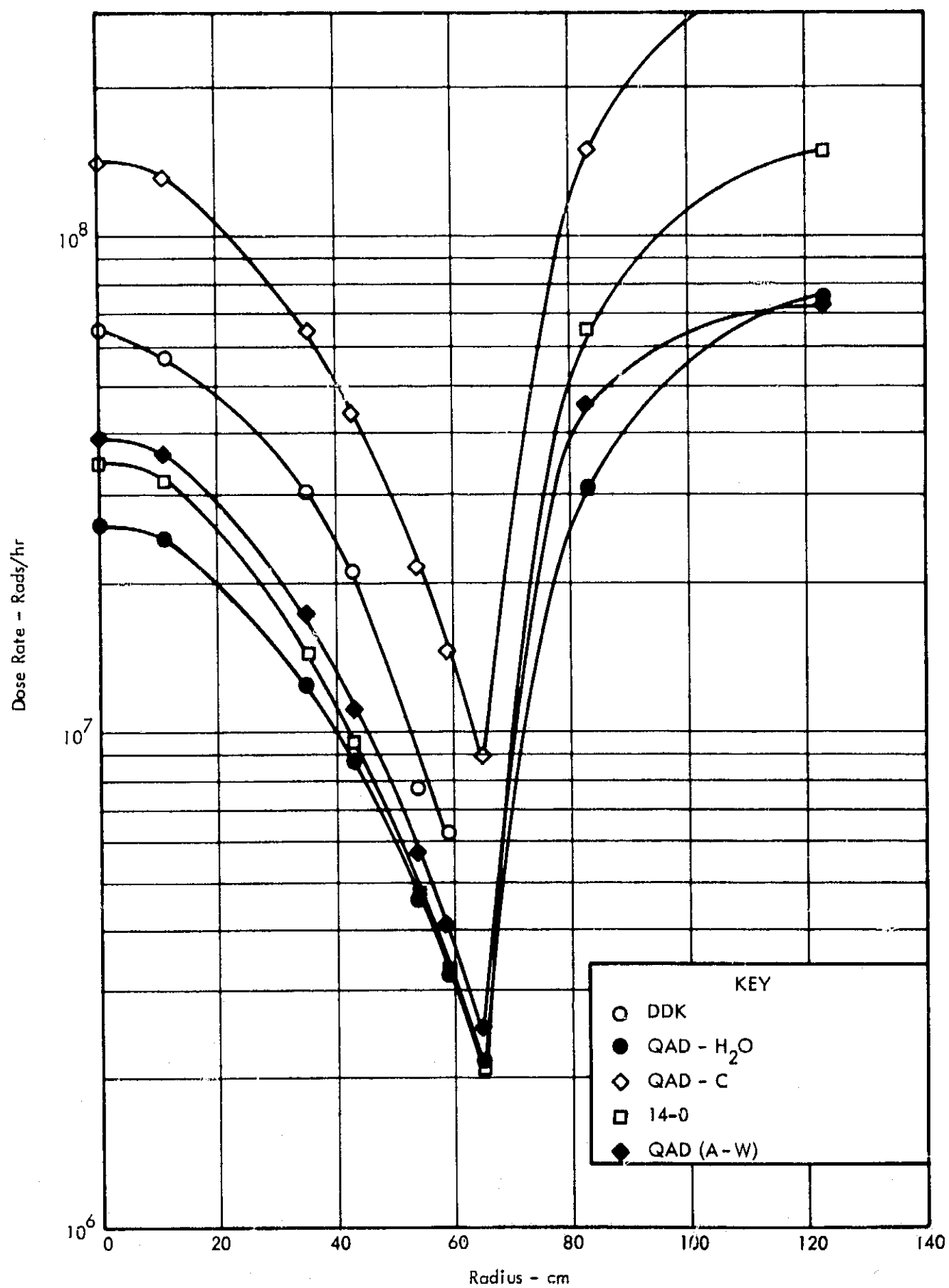


FIGURE 43 CONFIGURATION B, NEUTRON DOSE RATE (Z = 184 CM)

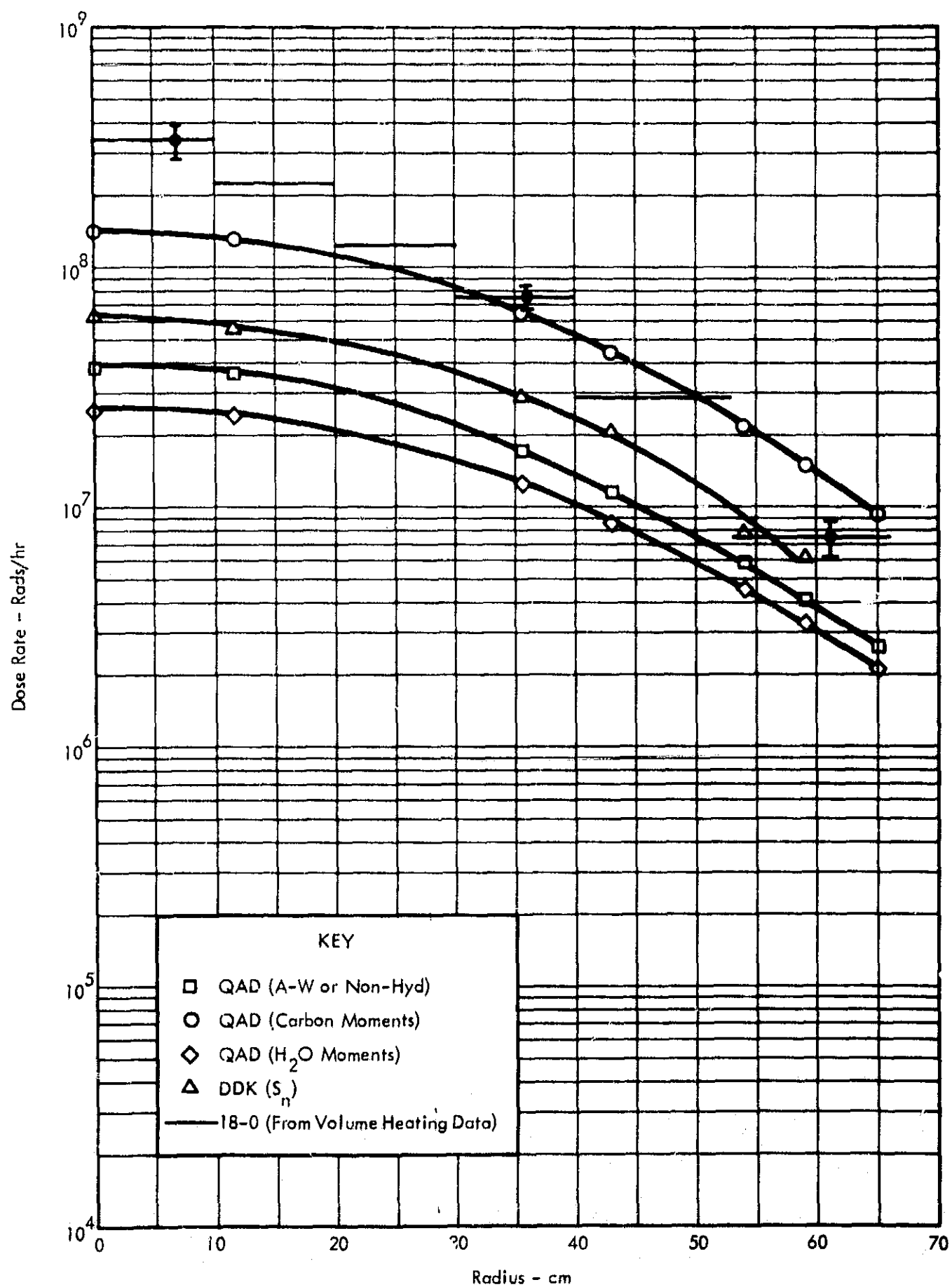


FIGURE 44 CONFIGURATION B, NEUTRON DOSE RATE ($Z = 183.9$ CM)

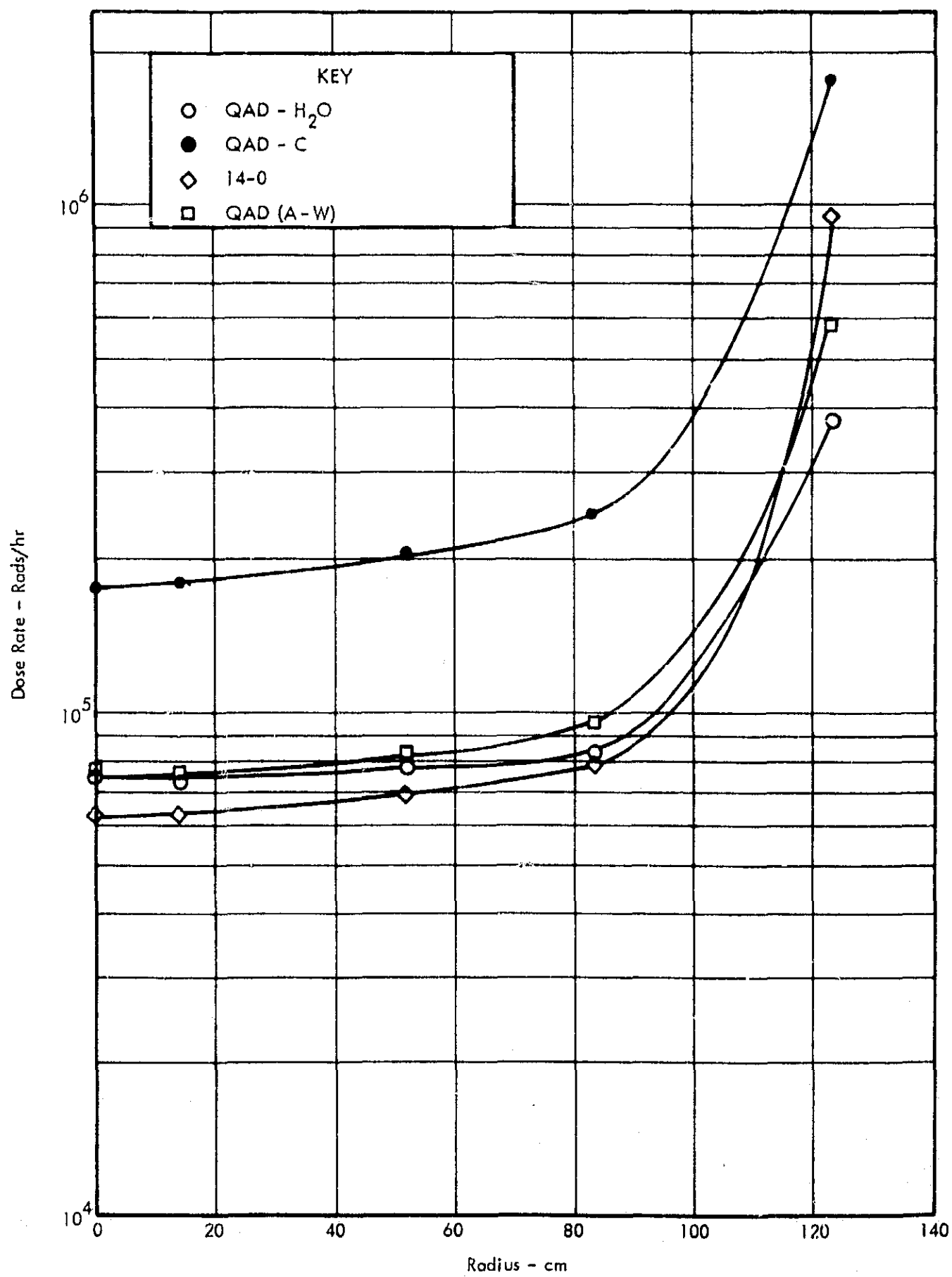


FIGURE 45 CONFIGURATION B, NEUTRON DOSE RATE (Z = 338 CM)

Component	Axial Limits (CM)	Computer Program	Energy Deposition (Watts)					
			Radial Limits (CM)					
			0-39		39-56		56-66	
			Heating	Relative Error %	Heating	Relative Error %	Heating	Relative Error %
Lower Shield Support	155	18-0	7.7(3)	9	4.2(3)	8	1.7(3)	14
	160							
Shield	165	18-0	1.8(4)	8	9.5(3)	12	3.2(3)	14
		14-0 (A-W)	5.6(3)	—	3.6(3)	—	1.4(3)	—
	169	QAD (C)	1.5(4)	—	1.0(4)	—	3.9(3)	—
		DDK	1.0(4)	—	6.7(3)	—	2.5(3)	—
Shield	182	18-0	8.4(2)	22	4.6(2)	20	2.0(2)	21
		14-0 (A-W)	3.0(2)	—	1.9(2)	—	7.7(1)	—
	187	QAD (H ₂ O)	2.6(2)	—	1.6(2)	—	6.6(1)	—
		DDK	4.2(2)	—	2.7(2)	—	1.1(2)	—

A-W - Albert-Welton Kernel C - Carbon Data Moments Method H₂O - Water Data Moments Method

FIGURE 46 SHIELD NEUTRON HEATING, CONFIGURATION A

in regions where applicable. In considering the DDK data, it should be noted that the energy range above 0.1 MeV is represented by only 5 of the 15 energy groups treated. Thus a discrepancy with 18-0, which uses 25 energy intervals above 1 MeV in description of cross sections, is not surprising. The 14-0 data appears low by a factor of 2 to 3.

Monte Carlo spectra, averaged over a section through the shield at $Z = 165$ cm, are shown in Figure 47. Agreement between 18-0 and MCS current is everywhere within the computed standard deviations, which are reasonably small for neutrons carrying most of the total energy. A typical QAD carbon-moments spectrum, computed at the point $Z = 165$ cm suggested by the sketch, is also plotted. Agreement of its shape with that of the Monte Carlo spectra seems surprisingly good considering the inhomogeneity of the system. At the least, no suspicion is cast on the success of the carbon-moments kernel in estimating energy deposition in this region.

A similar comparison is shown in Figure 48, for a disc and point on the bottom of the propellant tank. The point kernel methods agree rather well between themselves, but predict a greater proportion of neutrons below 1.5 MeV than does Monte Carlo. The reason may be the more diffuse angular spread of the less energetic neutrons emitted from the shield, a factor not accounted for in the kernel spectra. In any case, the spectrum computed by 14-0 does not affect the dose rate estimate.

Neutron transmission through the reflector is now considered. Estimates of flux and current across the cylindrical boundary of Configuration A are shown in Figure 49. The low relative error computed for the MCS flux estimate, corroborated by the excellent agreement between 18-0 and MCS currents, inspires confidence in the Monte Carlo flux estimate. The discrete ordinates estimate is about 40% lower at the core midplane, and perhaps 50% lower near the forward end of the reflector. The apparently large discrepancy with the MCS data on the range $Z = 160 \rightarrow 192$ cm is the result of a most unfortunate choice of tally surface. If the slope of the DDK curve is

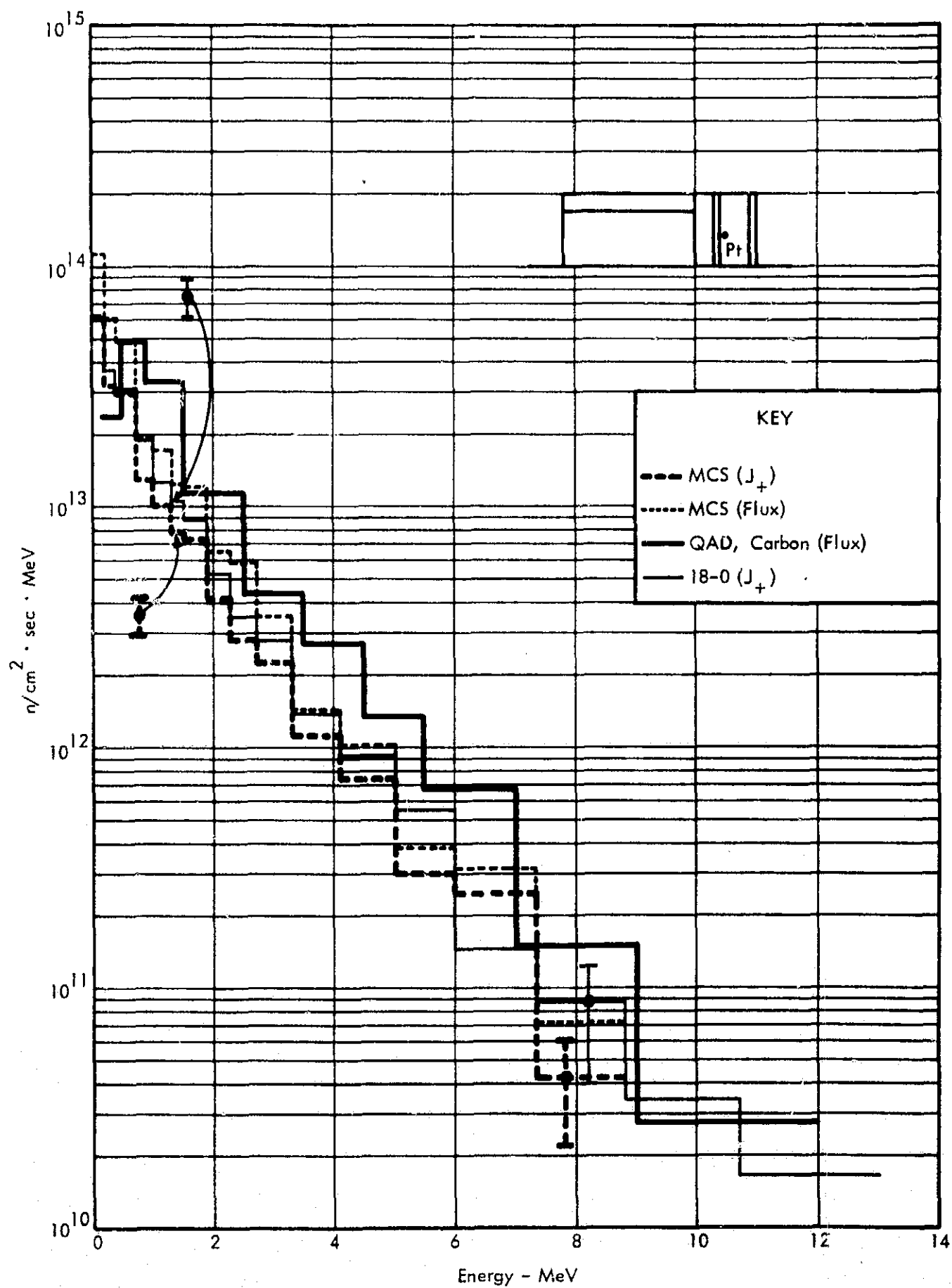


FIGURE 47 NEUTRON SPECTRA

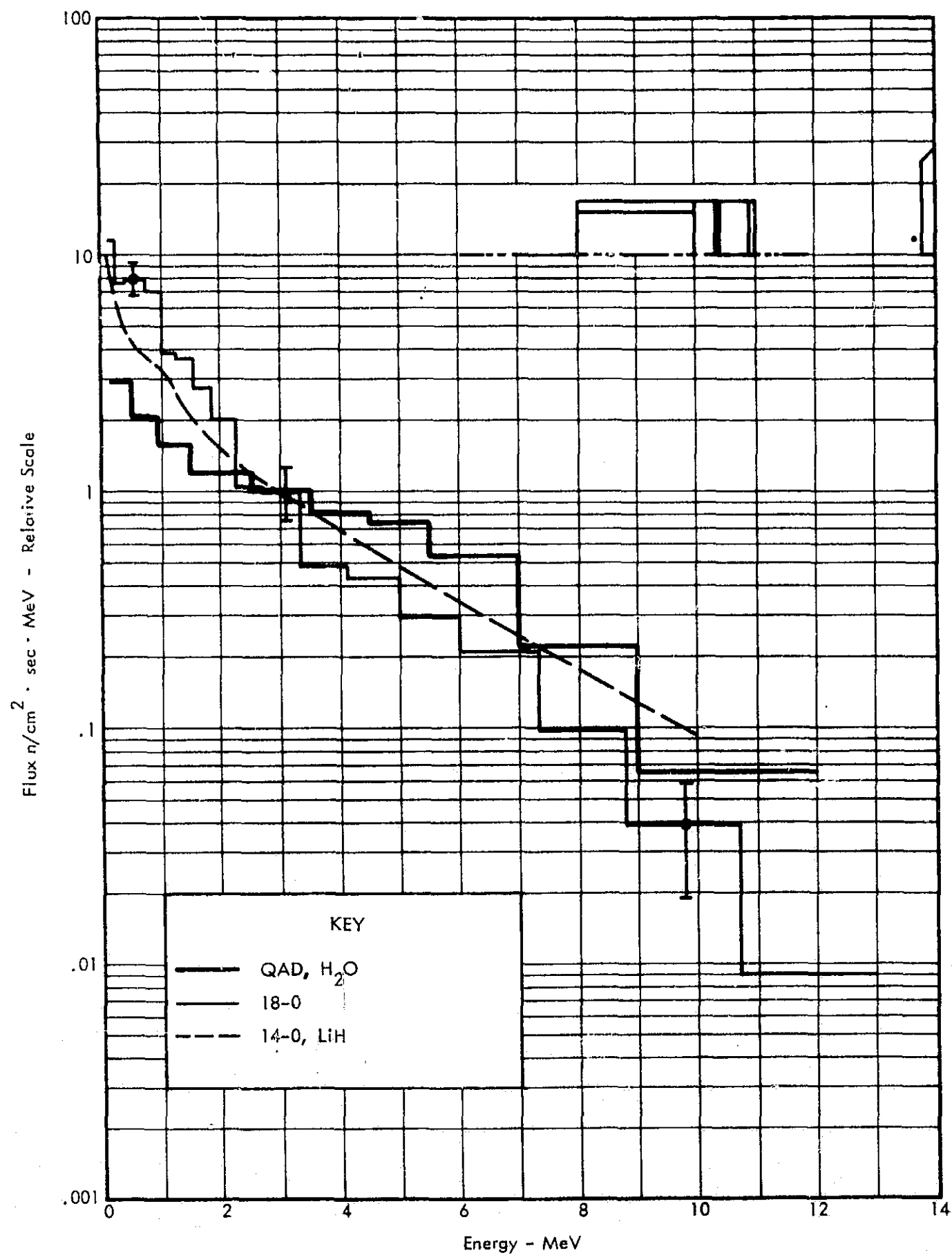


FIGURE 48 NEUTRON SPECTRA NORMALIZED AT 3 MeV

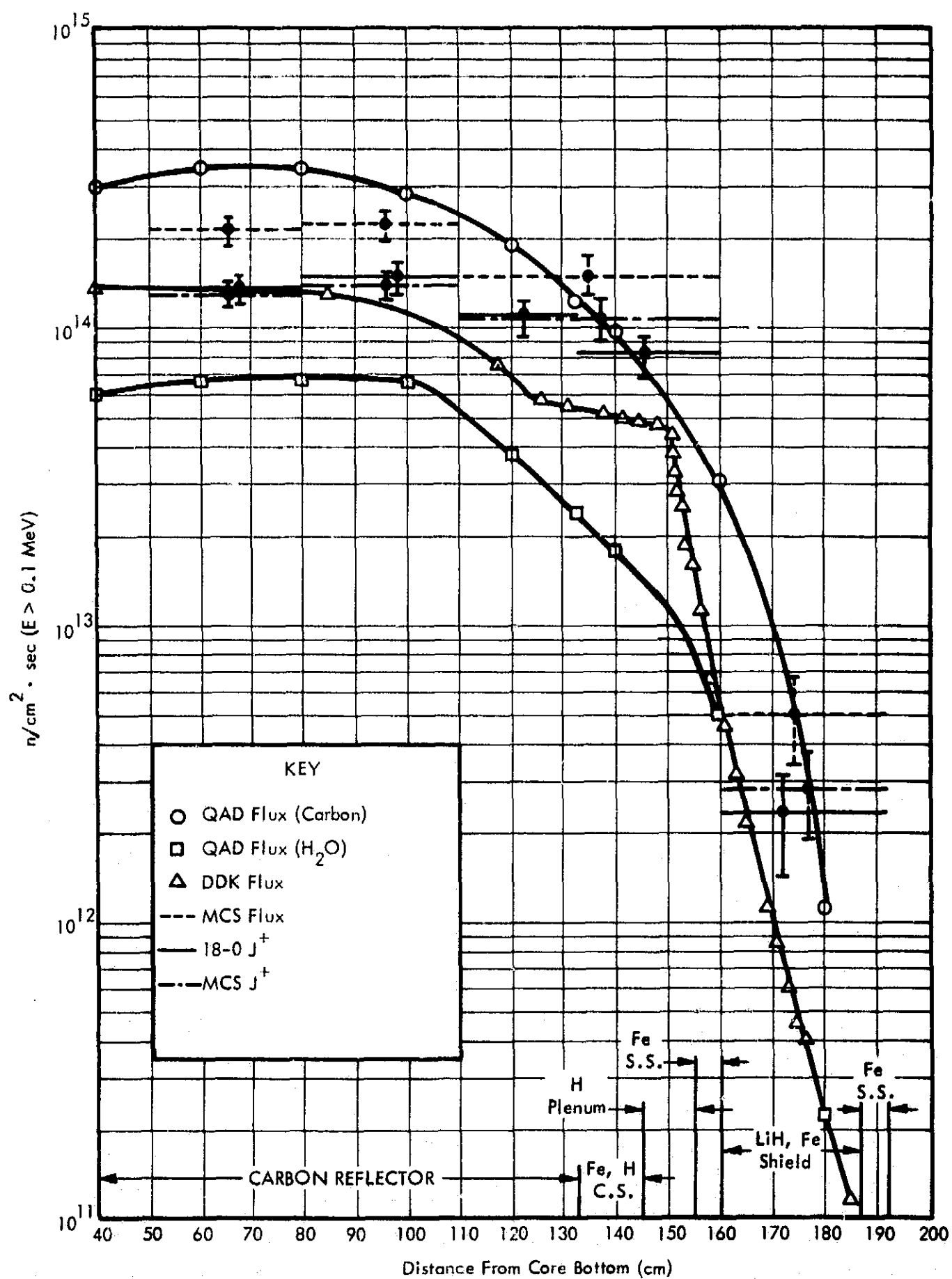


FIGURE 49 NEUTRON FLUX AND CURRENT ON RADIAL BOUNDARY ($R = 66 \text{ CM}$)

accepted, about half of the particles tallied must have escaped on the range $Z = 160 \rightarrow 164$ cm; for a median point of 164 cm the disagreement is only slightly larger than the relative error of the tally. As one possible explanation of the remaining discrepancies between DDK and MCS, we note that a low order discrete-ordinates quadrature is least effective in regions of flux anisotropy, such as on a boundary.

The water-moments kernel data are in excellent agreement with DDK at the only two points where applicable, $Z = 160$ and 180 cm. The carbon-moments kernel data, some 60% higher than MCG, would benefit from the well-known empirical correction factor for the crossing of material-vacuum interfaces. It would, however, be hard to justify omission of a similar correction for the water-moments data.

Some dose rates along an axial traverse 124 cm off the system axis are shown in Figure 50. The 4-group DDK data, completely independent of the 15-group data shown in the previous figure, display a similar plateau. Neutron streaming through the plenum and iron regions is indicated.

Spectra typical of neutrons escaping the reflector are shown in Figure 51. Locations of the Monte Carlo tally surface and point kernel receiver are indicated by the inset. The various data are normalized at 3 MeV. Sampling of neutrons over the energy range appears adequate. Beryllium happens to be the only non-hydrogenous material for which spectral data are available in a form suitable for 14-0.

The remainder of the section treats transmission of neutrons through the propellant tank. Figure 52 shows rate of energy deposition in propellant on the boundary of the tank. The previously noted flexibility of the alternate 14-0 kernels shows to advantage. The water-moments appears relatively low. As shown in Figure 53, however, it progressively approaches the Albert-Welton estimates. As seen later from estimates of dose at the propellant tank top, the curves cross and continue to diverge.

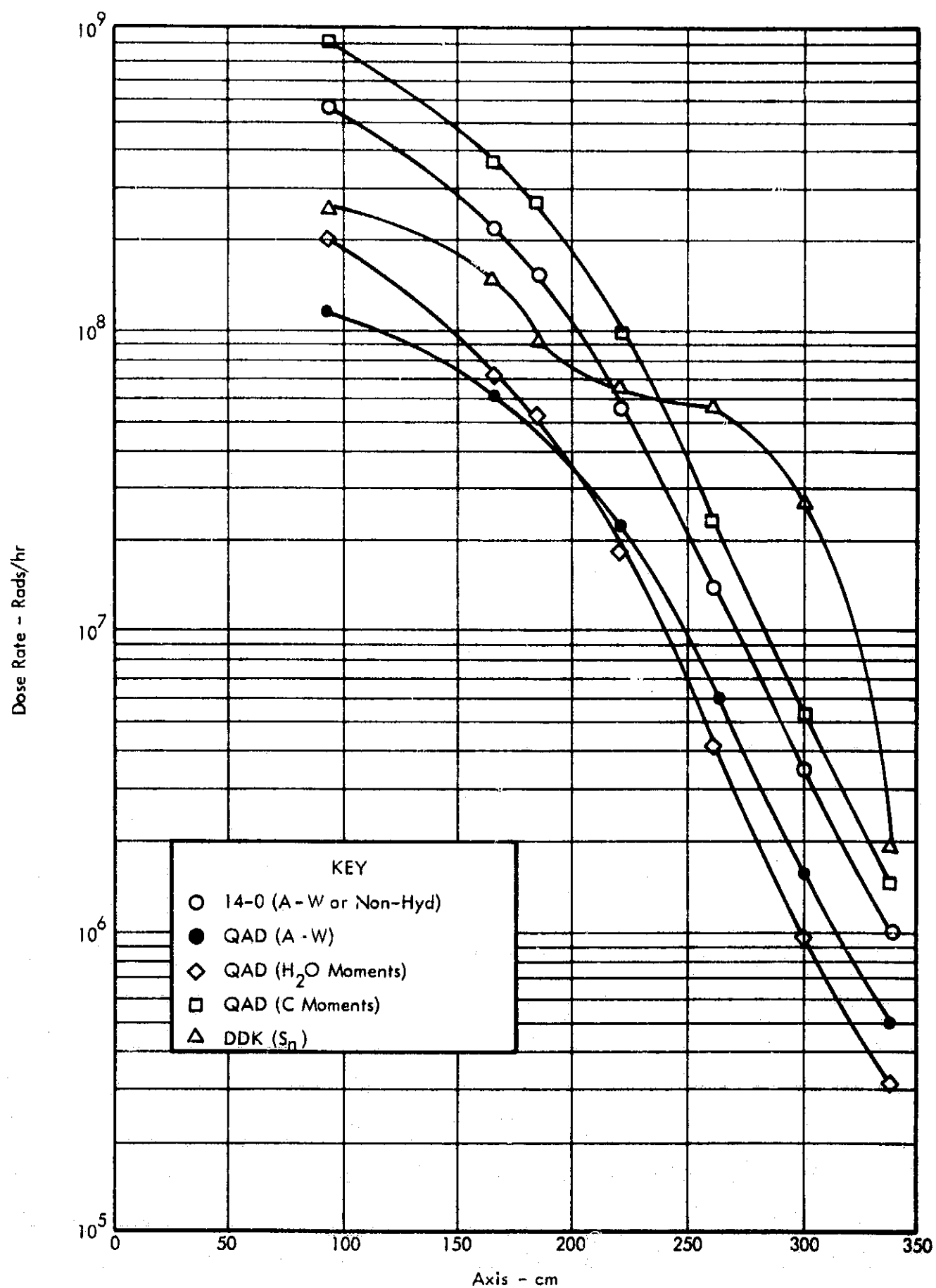


FIGURE 50 NEUTRON DOSE RATE ($R = 124$ CM)

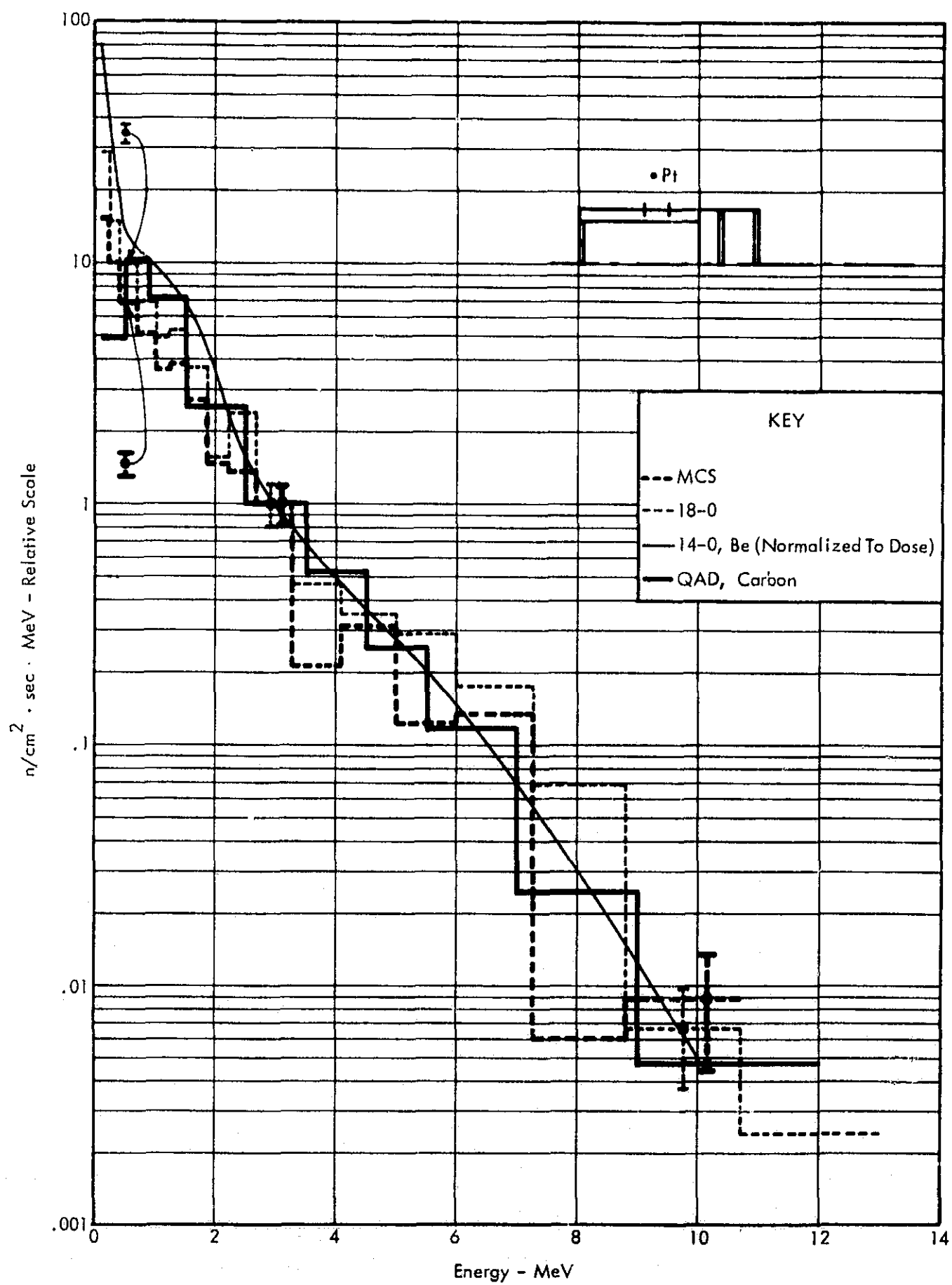


FIGURE 51 NEUTRON SPECTRA NORMALIZED AT 3 MeV

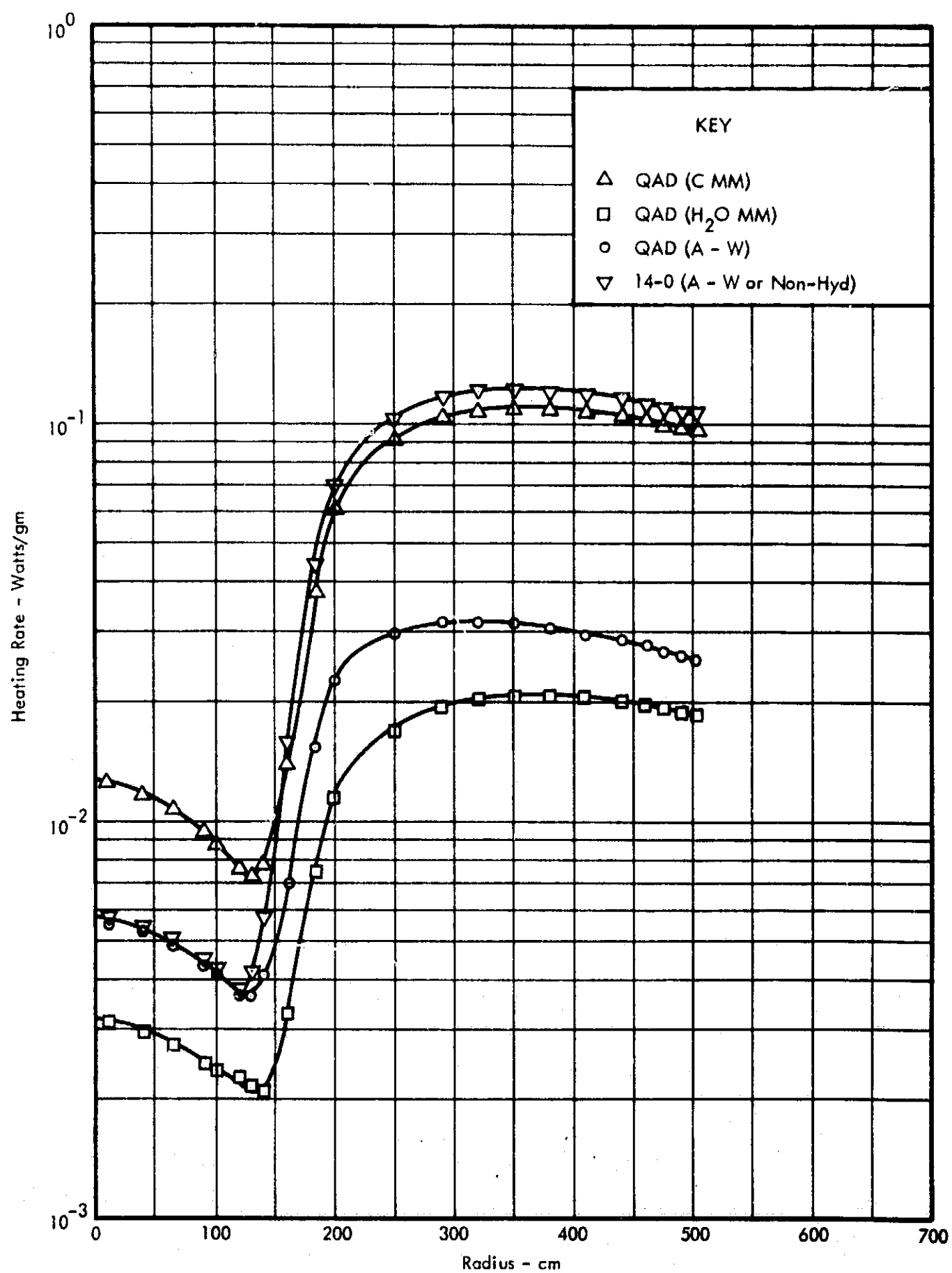


FIGURE 52 NEUTRON HEATING AT PROPELLANT TANK EDGE

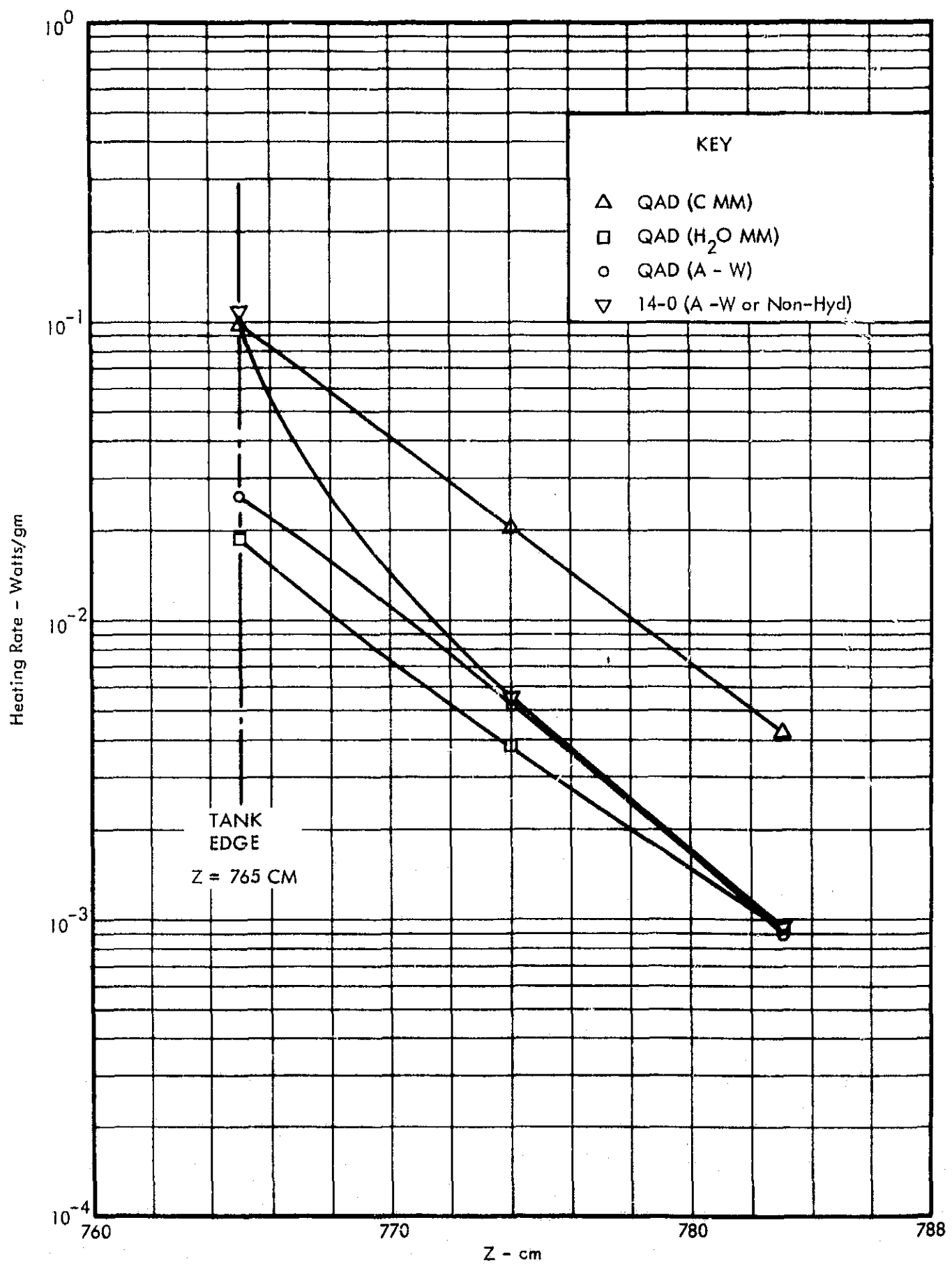


FIGURE 53 NEUTRON HEATING PARALLEL TO TANK AXIS (R = 490 CM)

Neutron energy deposition in propellant is tabulated in Figure 54. Region boundaries are defined in Figure 14. Point kernel methods appear fairly satisfactory for the critical Regions 4 and 5. Correlation is extremely poor in Region 3, however, and contributions to the neutron tally due to either scattering in the reflector or streaming through the plenum may be suspected. The diffuse character of neutrons transmitted through the shield is demonstrated by the energy depositions, in the optically thick Regions 1 through 5, due to axially biased neutrons.

Dose rates at the top of the propellant tank are shown in Figure 55. Liquid level is shown by the broken line in Figure 14. The discrepancy between point kernel and Monte Carlo estimates appears significant, particularly in view of the expected similarity of dose rate on the three tally surfaces. The most plausible cause of the difficulty is neutron scattering around the bulk of propellant, which in the present instance does not cover the conical portion of the tank bottom. While some scattering may occur in the thin edge of the propellant mass, the 0.25 cm thick iron propellant tank appears a more likely culprit. This excellent neutron scattering material is exposed to a high flux escaping through the reflector, and over 99% of the dose rate at the tank top is attributable to radially biased neutrons.

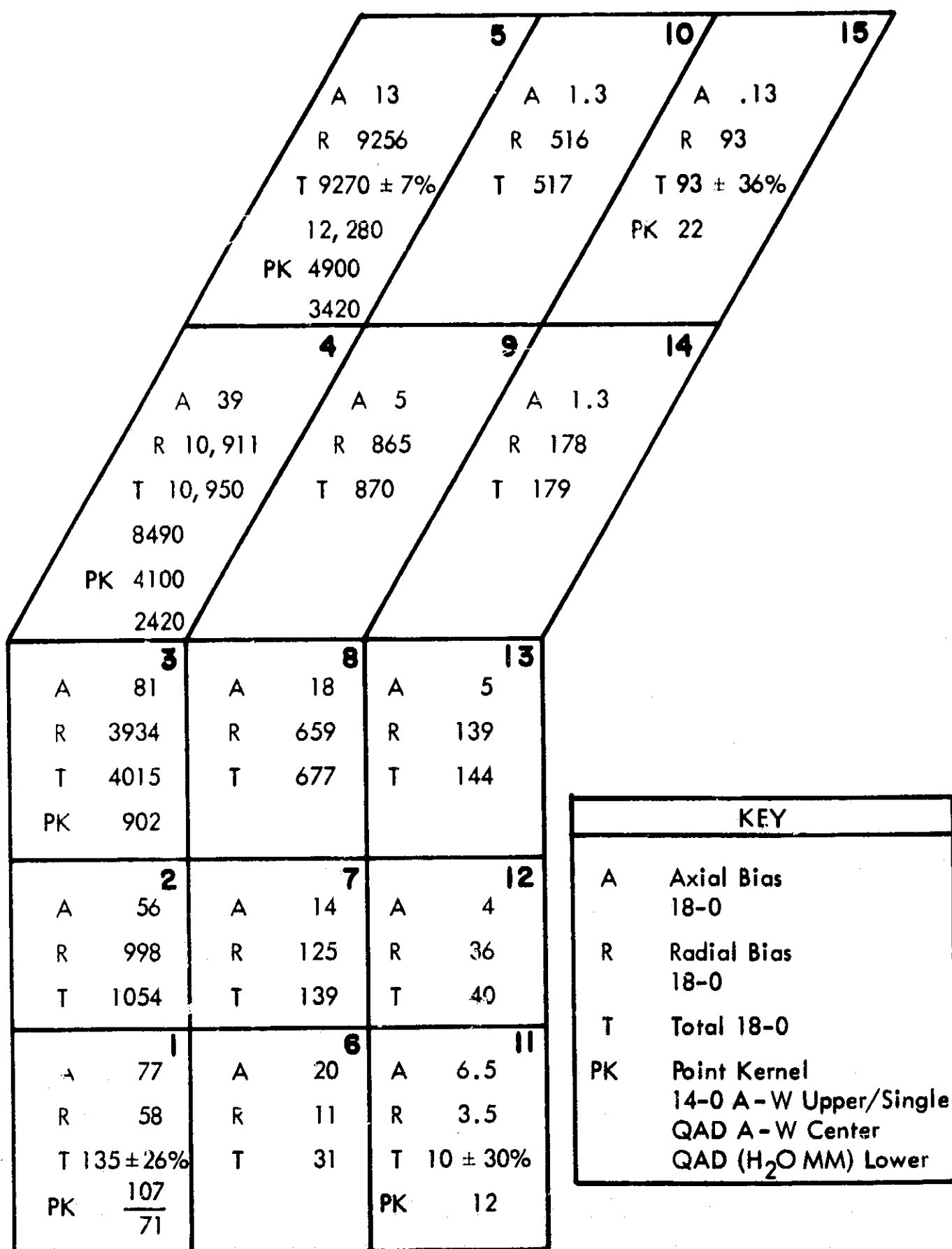


FIGURE 54 PROPELLANT NEUTRON ENERGY DEPOSITION (WATTS)

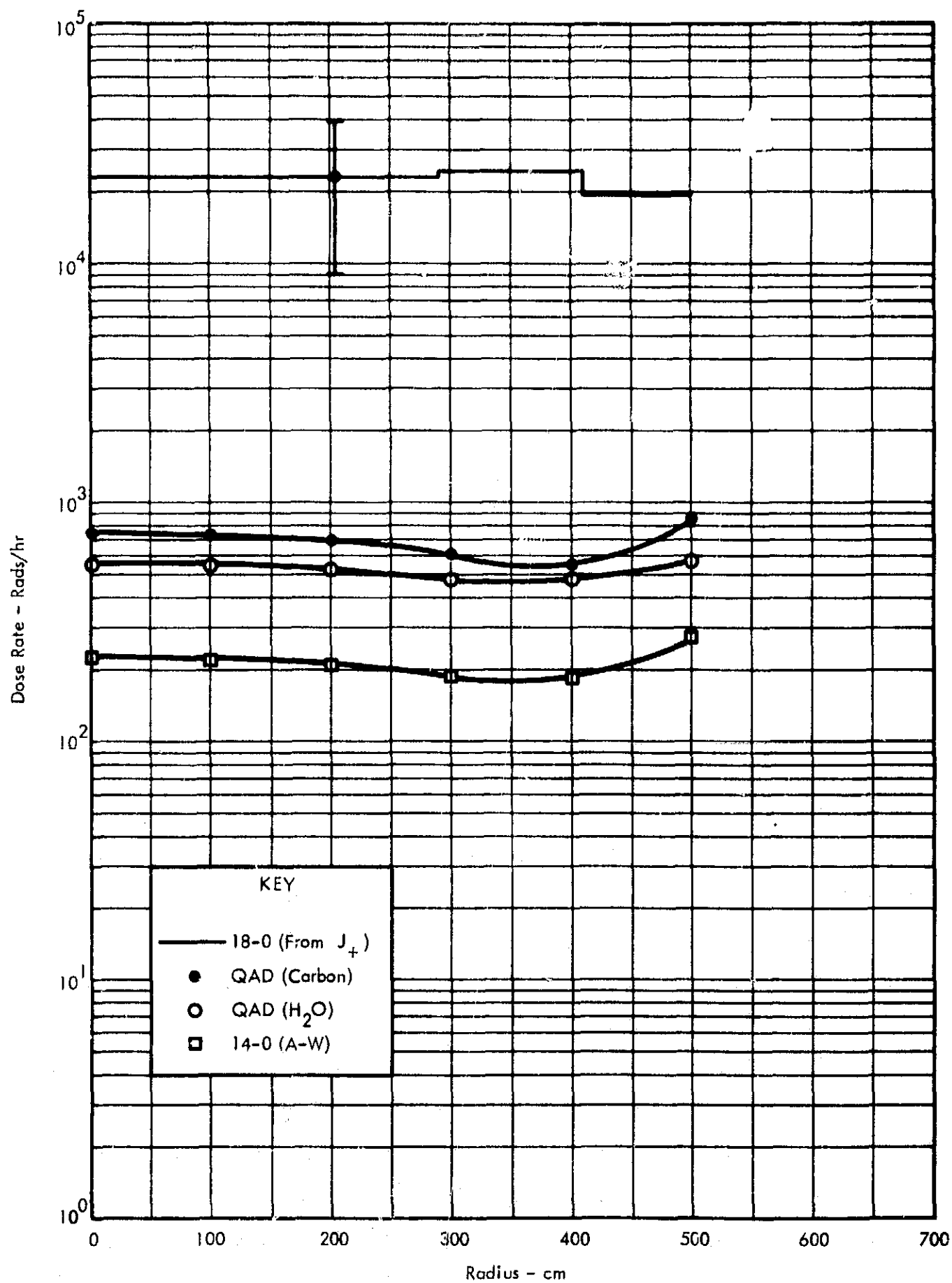


FIGURE 55 NEUTRON DOSE RATE, PROPELLANT TANK TOP ($Z = 1729$ CM)

4.0 SUMMARY

Computer programs based on three radiation transport models are compared and critically evaluated for usefulness in predicting radiation intensities required in analysis and design of nuclear rocket systems. The QAD-P5, QAD-IV and 14-0 point kernel programs, the DDK and DTK discrete ordinates (S_n) programs, and the MCS, MCG and 18-0 Monte Carlo programs are quantitatively compared. The 14-1 and C-17 point kernel programs and O5R Monte Carlo program are considered qualitatively.

Comparison and evaluation is based on preliminary survey of program features and specifications and a series of computations of radiation intensity throughout two configurations representative of a nuclear rocket system. Computation is directed toward comparison of accuracy and computational efficiency in the estimation of neutron and gamma flux and energy deposition or dose, for vehicular regions below, within and above the propellant tank. Treatment of spectra and of events within the shield are treated extensively as a guide to interpretation of the above data.

Each of the point kernel and Monte Carlo programs treated quantitatively can (considering MCS and MCG jointly) compute estimates in useful form of the intensities of interest up to the propellant tank top. The discrete ordinates programs are limited to neutron estimates in the reactor-shield assembly and regions immediately adjacent. Point kernel estimates of gamma intensity vary from the corresponding Monte Carlo data by factors up to two. Point kernel neutron estimates, by the best methods which might later be chosen a priori, show corresponding discrepancies of up to a factor of four. The ratio between discrete ordinates and Monte Carlo neutron intensity is typically 1.5 within the shield, a factor which might be reduced by inclusion of additional energy groups in the former. Computer time requirements typically increase with the sophistication of the model assumed, from point kernel, through discrete ordinates, to Monte Carlo.

5.0 CONCLUSIONS

- (1) Each method considered has its place in nuclear rocket design analysis:
 - Point kernel, for preliminary parametric studies;
 - Monte Carlo, for design point verification;
 - Discrete Ordinates, for estimation of fission and radiative capture distributions over the reactor-shield assembly.
- (2) Parametric point kernel neutron estimates should always be compared with a representative Monte Carlo computation performed simultaneously, and adjusted as required.
- (3) Neutron scattering in propellant and/or tank wall appears sufficient to invalidate point kernel neutron estimates at the tank top.
- (4) Transmission through the reflector, including angular distribution of at least neutrons, is an important design consideration.
- (5) Performance of separate Monte Carlo computations emphasizing reflector and shield leakage is highly desirable for propellant tank analysis.
- (6) With judicious use of available variance reduction techniques, Monte Carlo design analyses with computed statistical errors of 10 to 20% appear feasible for intensities at or below the propellant tank top.
- (7) The flexible MCS/MCG programs are preferable to the specialized 18-0, on the basis of variance reduction techniques, latent particle storage capacity and geometric description. (Qualitatively, O5R appears comparable with MCS and includes much greater flexibility for cross section description.)

- (8) The two-dimensional DDK should be used in preference to the much faster one-dimensional DTK, except for the crudest of preliminary investigations.
- (9) Each of the point kernel programs studied has advantages which make it preferable for special types of computation; relative neutron accuracy depends on the problem.
- QAD-IV is fastest for gamma computations.
 - QAD-P5 is most accurate for neutrons in non-hydrogenous media, in computing neutron spectra, and in geometric description.
 - 14-0 has the best neutron kernel for mixed hydrogenous and non-hydrogenous media, and can treat multiple source regions and gamma spectra.
- (10) Estimation of gamma intensities in manned modules on stages above the tank top appears feasible with MCG or similar Monte Carlo programs; preliminary point kernel estimates might be useful. Feasibility of comparable estimates of neutron intensity appears questionable with the programs studied.
- (11) Assessment of differences in test-stand and deep-space radiation environments over the nuclear stage appears marginally feasible with the programs studied, but only with a multiplicity of computations of separate radiation components. These include surface and air scattering of neutrons and gamma radiation, and production of inelastic and capture gamma radiation.

6.0 RECOMMENDATIONS

- (1) Since Monte Carlo is the implied standard of accuracy used here, one such program should be evaluated absolutely by detailed comparison with the available experimental data most representative of a nuclear rocket configuration.
- (2) Effects due to angular distribution of neutrons transmitted through the reflector should be investigated further.
- (3) A quantitative assessment of problems in estimating manned module environment should be made.
- (4) A scheme for systematic treatment of radiation components comprising test-stand environment should be developed, leading to preparation of a program system.
- (5) QAD-P5 should be modified to incorporate desirable features of 14-0.

APPENDIX A

PRECEDING PAGE BLANK NOT FILMED.

APPENDIX A

BASIC CROSS SECTION DATA

The following tabulations list the "standard" neutron and gamma cross section points utilized as primary input for the averaging and/or interpolating techniques of the Monte Carlo programs and the DDK program (neutron only). Energy values (MeV) are separated by commas and listed following the variable name, ESUB. Corresponding cross section values (barns/atom) are listed following the variable name, CS. An entry such as 1/-7 is interpreted as 1×10^{-7} . Each cross section value for gamma absorption is the sum of photoelectric and pair production cross sections. All other entries are self-explanatory.

The listed neutron cross section data were compiled principally from three sources:

- BNL 325 (second edition) 1958;
- UCRL-5226 and 5351, 1958; and
- AWRE 0-28/60 (United Kingdom) 1960.

Gamma cross sections with the exception of lithium were compiled from NBS circular 583, 1957. Lithium data were computed and interpolated from data given in XDC 59-10-19, 1959.

PRECEDING PAGE BLANK NOT FILMED.

NEUTRON CROSS SECTIONS (BARN/ATOM)

9 *****

9 HYDROGEN ELASTIC,

3ESUB,2.50/-8,5/-8,7.5/-8,1/-7,2/-7,4/-7,6/-7,8/-7,1/-6,7/-6,1/-3,1/-2,
 .02,.03,.04,.05,.06,.07,.08,.1,.15,.2,.25,.3,.4,.5,.6,.7,.8,.9,1.1,1.5,2,
 2.5,3,3.5,4,5,6,7,8,9,10,11,12,13,14,

3CS,35,29,27.5,26,24,23,22,21,2,21,20.5,20,19,18,17,16,15.5,14.8,14.3,
 13.5,12.5,10.8,9.6,8.6,7.9,6.9,6.1,5.61,5.15,4.8,4.5,4.25,3.4,2.95,
 2.55,2.26,2.1,1.9,1.6,1.4,1.24,1.13,1.03,.94,.86,.79,.73,.69,

9 *****

9 HYDROGEN N,GAMMA

3ESUB,2.50/-8,5/-8,7.5/-8,1/-7,2/-7,4/-7,6/-7,8/-7,1/-6,3/-6,7/-6,1/-5,
 3/-5,7/-5,1/-4,3/-4,7/-4,1/-3,3/-3,7/-3,1/-2,.02,.03,.04,.05,.06,.07,
 .08,.09,.1,.15,.2,.3,.4,.5,.6,.7,.8,.9,1.1,1.5,2,2.5,3,4,5,6,7,8,9,10,11,
 12,13,14,

3CS,3.4/-1,2.4/-1,1.85/-1,1.7/-1,1.2/-1,8.5/-2,7.7/-2,6/-2,5.4/-2,
 3.1/-2,2.05/-2,1.7/-2,9.9/-3,6.4/-3,5.4/-3,3.1/-3,2.05/-3,1.7/-3,
 9.9/-4,6.4/-4,5.4/-4,3.8/-4,3.1/-4,2.7/-4,2.4/-4,2.2/-4,2.05/-4,1.9/-4,
 1.8/-4,1.7/-4,1.4/-4,1.2/-4,9.9/-5,8.5/-5,7.6/-5,7.0/-5,6.4/-5,6/-5,
 5.7/-5,5.4/-5,4.4/-5,3.8/-5,3.4/-5,3.1/-5,2.7/-5,2.4/-5,2.2/-5,2.05/-5,
 1.7/-5,1.8/-5,1.7/-5,1.62/-5,1.55/-5,1.5/-5,1.44/-5,

9 *****

9 HYDROGEN TOTAL

3ESUB,2.50/-8,5/-8,7.5/-8,1/-7,2/-7,4/-7,6/-7,8/-7,1/-6,7/-6,1/-3,1/-2,
 .02,.03,.04,.05,.06,.07,.08,.1,.15,.2,.25,.3,.4,.5,.6,.7,.8,.9,1.1,1.5,2,
 2.5,3,3.5,4,5,6,7,8,9,10,11,12,13,14,

3CS,35,29,27.5,26,24,23,22,21,2,21,20.5,20,19,18,17,16,15.5,14.8,14.3,
 13.5,12.5,10.8,9.6,8.6,7.9,6.9,6.1,5.61,5.15,4.8,4.5,4.25,3.4,2.95,
 2.55,2.26,2.1,1.9,1.6,1.4,1.24,1.13,1.03,.94,.86,.79,.73,.69,

9 *****

9 *****

9 LITHIUM(NATURAL)ELASTIC,

3ESUB,2.5/-8,1/-7,3/-3,7/-3,1/-2,.1,.15,.18,.2,.22,.24,.2575,.27,.3,.33,
 .4,.5,1,2,2.5,3,4,4.4,5,6,7,8,9,10,14,

3CS,1.4,1.12,1.12,1.05,.93,.97,1.05,1.4,1.8,2.7,5,11,6.6,2.96,1.99,1.27,
 1.11,1.33,1.54,1.75,1.7,2.18,2.22,2.22,1.79,1.55,1.33,1.22,1.17,1.12,

9 *****

9 LITHIUM NATURAL N,GAMMA

3ESUB,2.5-8,2-7,6-7,2-6,7-6,2-5,7-5,3-4,14,

3CS,.029,.012,.006,.004,.002,.001,.001,0,0,

9 *****

9 LITHIUM(NATURAL) N,NPRIME

3ESUB,1/-8,.5,.544,.6,.8,.9,1,1.5,2.5,4,4.5,6,8,9,10,12,14,

3CS,0,0,.012,.025,.08,.11,.16,.2,.09,.11,.23,.35,.5,.514,.45,.395,.3,

9 *****

9 LITHIUM NATURAL N,ALPHA,

3ESUB,2.5/-8,5/-8,7.5/-8,1/-7,2/-7,4/-7,6/-7,8/-7,1/-6,3/-6,7/-6,1/-5,
 3/-5,7/-5,1/-4,3/-4,7/-4,1/-3,3/-3,7/-3,.01,.05,.08,.1,.14,.18,.2,.23,
 .26,.29,.32,.62,1,2,3,4,10,20,

3CS,71,49,41,35,24,3,16,8,13,5,11,6,10,3,5,9,3,7,3,03,1,6,1,0,.8,.4,.3,
 .16,.1,.1,.1,.07,.066,.068,.082,.108,.16,.23,.246,.202,.047,.037,.028,
 .0195,.013,.010,.004,.0018,

PRECEDING PAGE BLANK NOT FILLED.


```

9*****
9LITHIUM(NATURAL)TOTAL,
3ESUB,2.5/-8.5/-8.7.5/-8.1/-7.2/-7.4/-7.6/-7.8/-7.1/-6.3/-6.7/-6.1/-5,
3/-5.7/-5.1/-4.3/-4.7/-4.1/-3.3/-3.7/-3.01.01.12.145.163.206,
.2175.2575.299.326.405,
.5.71.1.1.5.2.2.5.3.3.5.4.5.8.55.11.2.14.15,
3CS,72.50.42.36.25.5.17.9.14.7.12.8.11.4.7.4.9.4.15.2.7.2.1.1.9.1.5.1.4,
1.3.1.2.1.2.1.2.1.04.1.03.1.06.1.17,
2.3.2.7.11.3.2.2.05.1.35.1.15.1.35.1.5.1.63.1.73.1.85.2,
2.2.2.3.2.45.1.75.1.63.1.5.1.44,
9*****
9*****
9CARBON ELASTIC
3ESUB,1/-8.1/-7.1/-6.1/-5.1/-4.1/-3.1/-2.1/-1.2.3.4.5.6.7.8.9,
1.1.1.1.3.1.5.1.7.1.75.1.9.1.95.2.2.1.2.12.2.15.2.25.2.4.2.5.2.65.2.78,
2.85.2.9.2.95.3.3.07.3.11.3.3.3.4.3.78.3.9.4.05.4.17.4.32.4.4.5.5.25,
5.36.6.6.3.6.5,
6.6.7.7.3.7.8.8.8.2.8.3.8.5.8.8,
9.2.9.7.10.4.11.11.5.12.13.14,
3CS,5.4.9.4.8.4.7.4.6.4.6.4.7.4.55.4.21.3.9.3.7.3.5.3.3.3.2.87.2.7.2.7,
2.6.2.2.2.1.75.1.8.1.8.1.7.1.82.5.1.8.1.6.1.6.1.5.1.5.1.7.1.8.2.1.2.45,
3.05.1.3.1.1.1.3.2.2.2.2.2.35.2.1.86.1.9.2.1.1.9.1.1.1.1.1.4,
.85.1.9.70,
.42.6.8.1.5.1.35.1.25.1.0.9.83,
.75.81.67.88.95.94.8.62,
9*****
9 CARBON ABSORPTION INCLUDES (N,NPRIME+3ALPHA)
3ESUB,1/-8.8.10.1.11.12.12.9.14.1.15.16.17.18.19.20,
3CS,0.01.03.05.1.19.23.29.31.31.305.28.275,
9*****
9 CARBON N,NPRIME INCLUDES (N,NPRIME), (N,2N)
3ESUB,2.5/-8.1.4.4.8.5.5.2.5.6.6.2.6.30.6.4.6.45.6.5.6.6.6.8.7.2,
7.4.7.6.7.7.8.8.8.2.8.4.8.8.9.2.10.11.12.13.14,
3CS,C,0.0.01.05.03.11.25.45.32.3.3.35.20.20,
.35.35.35.52.45.55.3.28.34.39.43.47.50.50,
9*****
9CARBON TOTAL
3ESUB,1/-8.1/-7.1/-6.1/-5.1/-4.1/-3.1/-2.1/-1.2.3.4.5.6.7.8.9.1,
1.1.1.3.1.5.1.7.1.75.1.9.1.95.2.2.1.2.12.2.15.2.25.2.4.2.5.2.65.2.78,
2.85.2.9.2.95.3.3.07.3.11.3.3.3.4.3.78.3.9.4.05.4.17.4.32.4.4.4.65.5,
5.25.5.36.5.45.5.6.5.8.6.6.1.6.25.6.3.6.5.6.6.6.7.6.8.7.7.2.7.3.7.4,
7.5.7.7.7.80.8.8.4.8.5.8.8.9.2.9.7.10.4.11.15.11.6.12.12.5.13.14.15.20,
3CS,5.4.9.4.8.4.7.4.6.4.6.4.7.4.55.4.21.3.9.3.7.3.5.3.3.3.2.87.2.7.2.7,
2.6.2.2.2.1.75.1.8.1.8.1.7.1.82.5.1.8.1.6.1.6.1.5.1.5.1.7.1.8.2.1.2.45,
3.05.1.3.1.1.1.3.2.2.2.2.2.35.2.1.86.1.9.2.1.1.9.1.5.1.2.1.13.1.5.1.4,
1.25.1.1.1.1.1.3.1.4.2.4.1.1.64.8.82.84.92.1.1.1.55.1.65.1.7.2,
1.88.1.3.1.2.1.1.1.1.1.2.1.12.1.42.1.5.1.51.1.49.1.44.1.35.1.3.1.45,
9*****
9*****
9IRON ELASTIC
3ESUB,2.5/-8.1/-6.1/-4.3/-4.7/-4,
1-3.2-3.3.2-3,
3.8/-3.4.5/-3.6/-3.6.5/-3.7/-3.1/-2.2/-2.2.3/-2.025.028.032,
.04.05.054.056.068.07.072.08.083.09.1,
.12.128.135.14.15.163.165.17.182.185.19.213.218.22.24,

```

```

.25,.27,.275,.29,
.31,.32,.35,.36,.375,.385,.4,.5,.6,.65,.7,.76,.79,.8,.86,
.9,.94,.96,1,1.06,1.09,1.11,1.13,1.15,1.17,1.19,1.21,1.23,1.29,1.3,
1.32,1.34,1.36,1.38,1.4,1.45,1.5,2,3,4,5,5.5,6,7,8,9,10,11,12,14,
3CS,11,11.4,11.4,11.9,
9,6,7,5,
6,7,4,7,13,5,12,26,6,8,2,1,2,.1,80,11,5,
5,5,4,5,9,4,2,6,1,3,23,1,2,24,5,4,
1,11,.8,15,5,4,1,11,4,.3,12,7,1,5,8,3,5,2,5,3,1,5,7,2,
1,5,2,1,3,5,1,5,5,8,4,5,3,2,5,2,5,2,73,4,45,4,2,8,2,6,
1,94,1,3,2,31,1,81,2,9,1,8,2,15,1,85,1,85,1,6,1,6,1,7,2,45,2,2,2,1,
2,45,1,9,1,8,1,8,1,8,2,7,1,85,2,15,1,85,2,2,2,3,2,25,2,25,2,14,
2,1,78,1,7,1,52,1,35,1,2,
9*****
9 IRON (N,P),
3ESUB,2,5/-8,6,7,8,10,12,14,
3CS,0,0,.026,.041,.07,.1,.11,
9*****
9 IRON N,NPRIME INCLUDES (N,NPRIME), (N,2N),
3ESUB,1/-8,.86,.87,1,2,1,77,2,5,4,4,7,7,11,3,14,3,
3CS,0,0,.29,.5,.73,1,04,1,42,1,38,1,39,1,268,1,2,
9*****
9 IRON N,GAMMA
3ESUB,2,5/-8,5/-8,1/-7,1/-6,1/-3,3/-3,7/-3,1/-2,.015,.029,.03,.04,.05,
.06,.07,.09,.1,.15,.2,.3,.4,.6,1,2,5,4,7,8,10,12,14,
3CS,2,53,1,.8,.1,.025,.0031,.011,.015,.008,.015,.016,.016,.0115,.0076,
.0084,.0098,.009,.0075,.006,.0054,.0047,.0043,.0031,.0017,.0042,.0009,
.82/-3,.7/-3,.58/-3,.46/-3,
9*****
9IRON TOTAL
3ESUB,1/-8,6/-8,1/-7,1/-6,1/-5,1/-4,3/-4,6/-4,8/-4,1/-3,2/-3,3,2/-3,
3,8/-3,4,5/-3,6/-3,6,5/-3,7/-3,1/-2,2/-2,2,3/-2,.025,.028,.032,
.04,.05,.054,.056,.068,.07,.072,.08,.083,.09,.1,
.12,.128,.135,.14,.15,.163,.165,.17,.182,.185,.19,.213,.216,.22,.24,
.25,.27,.275,.29,
.31,.32,.35,.36,.375,.385,.4,.5,.6,.65,.7,.76,.79,.8,.86,.9,.94,.96,1,
1,06,1,09,1,11,1,13,1,15,1,17,1,19,1,21,1,23,1,29,1,3,1,32,1,34,1,36,
1,38,1,4,1,45,1,5,2,3,
4,5,5,5,6,7,8,9,10,11,12,14,15,20,
3CS,14,5,12,3,12,11,5,11,4,11,4,11,1,10,3,9,7,9,6,7,5,
6,7,4,7,13,5,12,26,6,8,2,1,2,.1,80,11,5,
5,5,4,5,9,4,2,6,1,3,23,1,2,24,5,4,
1,11,.8,15,5,4,1,11,4,.3,12,7,1,5,8,3,5,2,5,3,1,5,7,2,
1,5,2,1,3,5,1,5,5,8,4,5,3,2,5,2,5,2,73,4,45,4,2,8,2,6,2,85,1,6,2,7,2,3,
3,4,2,3,2,7,2,3,2,3,2,1,2,1,2,2,3,2,7,2,6,3,2,5,2,4,2,4,2,4,3,3,2,5,3,
3,17,
3,6,3,7,3,7,3,7,3,6,3,4,3,2,3,1,2,9,2,7,2,5,2,4,2,2,
9*****
9*****
9 URANIUM 235 ELASTIC,
3ESUB,2,5/-8,5/-8,7,5/-8,1/-7,2/-7,6/-7,1/-6,3/-6,10/-6,30/-6,7/-5,
1/-4,6,74/-2,.183,.25,.30,
.4,.5,.6,.7,.8,.9,1,1,5,2,2,5,3,4,5,6,7,8,1,
9,10,11,9,13,14,1,
3CS,17,5,16,5,16,15,1,15,14,5,14,12,3,11,11,10,10,10,3,

```

8.2,7.5,6.85,6.2,5.5,
 4.75,4.5,4.15,4.1,3.88,3.65,3.85,4.3,4.45,4.5,4.13,3.95,3.60,3.23,3.14,
 3.09,3.0,2.98,3.03,
 9*****
 9 U 235 FISSION INCLUDES (FISSION), (N,NPRIME+FISSION) AND (N,2N+FISSION)
 3ESUB,1./-8,2.5/-8,1./-7,2./-7,2.9/-7,6./-7,8./-7,1./-6,1.1/-6,1.35/-6,
 1.85/-6,2.05/-6,2.2/-6,2.7/-6,3.1/-6,3.3/-6,3.6/-6,4./-6,4.5/-6,
 4.9/-6,5.1/-6,5.6/-6,6./-6,6.2/-6,6.3/-6,6.6/-6,6.9/-6,7./-6,
 7.1/-6,7.25/-6,7.8/-6,8.4/-6,8.8/-6,9.1/-6,9.2/-6,9.3/-6,1./-5,
 1.015/-5,1.075/-5,1.1/-5,1.25/-5,1.3/-5,1.41/-5,1.5/-5,1.55/-5,1.59/-5,
 1.65/-5,1.7/-5,1.95/-5,2.03/-5,
 2.15/-5,2.2/-5,2.4/-5,2.45/-5,2.55/-5,2.75/-5,3/-5,3.25/-5,3.56/-5,
 3.65/-5,3.8/-5,3.99/-5,4.15/-5,4.25/-5,4.65/-5,5.2/-5,5.55/-5,
 5.85/-5,6.4/-5,6.7/-5,8/-5,1/-4,3/-4,1/-3,3/-3,.01,.1,.2,.5,1,
 2,2.5,3,4,5,6,6.5,7,7.5,8,8.5,9,9.5,10,10.5,
 11,11.5,12,12.5,13,13.5,14,14.5,15,20,
 CS,940.,570.,250.,175.,195.,63.,54.,60.,105.,22.,14.,25.,13.,8.6,43.,
 18.,85.,5.,4.,119.,6.,14.,19.,45.,320.,9.,13.,33.,110.,5.,3.,20.,570.,
 90.,90.,90.,28.,50.,19.,14.,180.,30.,65.,20.,30.,20.,35.,22.,600.,45.,
 90,20,68,50,50,29,14,70,160,30,25,35,30,30,35,70,60,
 30,12,45,25,20,17,8,5,6,3,4,1,78,1,5,1,26,1,25,
 1,33,1,31,1,29,1,22,1,15,1,15,1,4,1,56,1,7,1,8,1,85,1,87,1,86,1,83,1,8,
 1,8,1,87,2,02,2,17,2,23,2,24,2,22,2,21,2,18,2,1,
 9*****
 9 U 235 N,NPRIME INCLUDES (N,NPRIME), (N,2N), (N,3N)
 3ESUB,2.50/-8,.02,.03,.04,.05,.06,.07,.08,.1,.15,.2,.25,.3,.4,.45,.5,
 .55,.6,.7,.3,.9,1,1.5,2,2.5,3,4,5,
 6,7,8,9,10,11,12,13,14,
 3CS,0,0,.02,.05,.06,.09,.13,.23,.29,.45,.55,.66,.74,.88,.93,.97,1.00,
 1.06,1.2,1.3,1.35,1.4,1.60,1.73,1.83,1.94,2.0,2.0,
 1.85,1.35,1.10,1.04,1.03,1.03,.83,.62,.55,
 9*****
 9 URANIUM 235 N,GAMMA,
 3ESUB,1./-8,2.5/-8,1./-7,2./-7,2.9/-7,6./-7,8./-7,1./-6,1.1/-6,1.35/-6,
 1.85/-6,2.05/-6,2.2/-6,2.7/-6,3.1/-6,3.3/-6,3.6/-6,4./-6,4.5/-6,
 4.9/-6,5.1/-6,5.6/-6,6./-6,6.2/-6,6.3/-6,6.6/-6,6.9/-6,7./-6,
 7.1/-6,7.25/-6,7.8/-6,8.4/-6,8.8/-6,9.1/-6,9.2/-6,9.3/-6,1./-5,
 1.015/-5,1.075/-5,1.1/-5,1.25/-5,1.3/-5,1.41/-5,1.5/-5,1.55/-5,1.59/-5,
 1.65/-5,1.7/-5,1.95/-5,2.03/-5,
 2.15/-5,2.2/-5,2.4/-5,2.45/-5,2.55/-5,2.75/-5,3/-5,3.25/-5,3.56/-5,
 3.65/-5,3.8/-5,3.99/-5,4.15/-5,4.25/-5,4.65/-5,5.2/-5,5.55/-5,
 5.85/-5,6.4/-5,6.7/-5,8/-5,1/-4,3/-4,1/-3,3/-3,7/-3,.01,.02,.03,.05,
 .07,.1,.175,
 .3,.5,.6,.9,1,2,3,4,5,6,7,14,
 3CS,190.,108.,45.,40.,55.,13.,8.,16.,35.,8.,3.,62.,4.5,1.5,35.,4.5,73.,
 1.,3.8,70.,4.5,5.5,14.5,43.5,219.,10.,15.,56.,98.,10.,4.,4.,319.,49.,
 49.,59.,4.,9.,3.,2.,320.,5.,45.,9.,39.,5.,50.,7.,390.,13.,
 114,5,80,60,40,21,5,60,200,20,5,55,20,50,5,50,10,
 40,18,25,5,10,8,9,8,3,5,8,1,3,1,.84,.66,.54,.45,.25,
 .2,.15,.14,.104,.1,.09,.07,.04,.02,.01,0,0,
 9*****
 9 URANIUM 235, TOTAL, COMPARISON.
 3ESUB,1./-8,2.5/-8,1./-7,2./-7,2.9/-7,6./-7,8./-7,1./-6,1.1/-6,1.35/-6,
 1.85/-6,2.05/-6,2.2/-6,2.7/-6,3.1/-6,3.3/-6,3.6/-6,4./-6,4.5/-6,
 4.9/-6,5.1/-6,5.6/-6,6./-6,6.2/-6,6.3/-6,6.6/-6,6.9/-6,7./-6,
 7.1/-6,7.25/-6,7.8/-6,8.4/-6,8.8/-6,9.1/-6,9.2/-6,9.3/-6,1./-5,
 1.015/-5,1.075/-5,1.1/-5,1.25/-5,1.3/-5,1.41/-5,1.5/-5,1.55/-5,1.59/-5,
 1.65/-5,1.7/-5,1.95/-5,2.03/-5,
 2.15/-5,2.2/-5,2.4/-5,2.45/-5,2.55/-5,2.75/-5,3/-5,3.25/-5,3.56/-5,
 3.65/-5,3.8/-5,3.99/-5,4.15/-5,4.25/-5,4.65/-5,5.2/-5,5.55/-5,
 5.85/-5,6.4/-5,6.7/-5,8/-5,1/-4,3/-4,1/-3,3/-3,7/-3,.01,.02,.03,.05,
 .07,.1,.175,
 .3,.5,.6,.9,1,2,3,4,5,6,7,14,
 3CS,190.,108.,45.,40.,55.,13.,8.,16.,35.,8.,3.,62.,4.5,1.5,35.,4.5,73.,
 1.,3.8,70.,4.5,5.5,14.5,43.5,219.,10.,15.,56.,98.,10.,4.,4.,319.,49.,
 49.,59.,4.,9.,3.,2.,320.,5.,45.,9.,39.,5.,50.,7.,390.,13.,
 114,5,80,60,40,21,5,60,200,20,5,55,20,50,5,50,10,
 40,18,25,5,10,8,9,8,3,5,8,1,3,1,.84,.66,.54,.45,.25,
 .2,.15,.14,.104,.1,.09,.07,.04,.02,.01,0,0,
 9*****

7.1/-6.7.25/-6.7.8/-6.8.4/-6.8.8/-6.9.1/-6.9.2/-6.9.3/-6.1./-5.
 1.015/-5.1.075/-5.1.1/-5.1.25/-5.1.3/-5.1.41/-5.1.5/-5.1.55/-5.1.59/-5.
 1.65/-5.1.7/-5.1.95/-5.2.03/-5.
 2.15/-5.2.2/-5.2.4/-5.2.45/-5.2.55/-5.2.75/-5.3/-5.3.25/-5.3.56/-5.
 3.65/-5.3.8/-5.3.99/-5.4.15/-5.4.25/-5.4.65/-5.5.2/-5.5.55/-5.
 5.85/-5.6.4/-5.6.7/-5.8/-5.1/-4.3/-4.1/-3.3/-3.6/-3.01.01.03.06.
 1.1.5.1.7.2.2.5.3.4.4.4.5.6.7.05.8.67.10.74.20.
 3CS.1150.695.310.230.265.90.76.90.155.43.30.100.30.23.
 90.35.170.17.5.19.200.22.31.45.100.550.30.40.100.220.
 26.18.35.900.150.150.160.42.70.32.27.510.45.120.40.
 80.35.96.40.1000.68.
 215.35.160.120.100.60.29.140.370.60.40.100.60.90.50.130.80.
 80.40.80.40.40.35.28.25.20.15.12.3.9.2.7.2.
 6.6.6.65.6.75.7.7.55.7.8.7.8.7.65.7.35.6.95.6.5.6.05.5.9.5.8.
 9 *****

GAMMA CROSS SECTIONS (BARN/ATOM)

```

*****
DATA HL,3, HYDROGEN
DTYPEC,3, COMPTON
BESUS,1,15,2,3,4,5,6,8,1,0,1.5,2,0,3,0,4,0,5,0,6,0,8,0,10,15,
CCS,462,444,407,354,317,282,258,235,211,1716,1464,1151,076,
.0328,0732,0552,0510,0377,
DTYPEC,3, ABSORPTION
BESUS,1,15,2,3,4,5,6,8,1,0,1.5,2,0,3,0,4,0,5,0,6,0,8,0,10,15,
CCS,0,0,0,0,0,0,0,0,0,1.8-4,5,2-4,6,7-4,1,1-3,1,5-3,2,2-3,2,7-3,
1,3-3,
*****
DATA HL,3, LITHIUM
DTYPEC,3, COMPTON
BESUS,1,15,2,3,4,5,6,7,8,9,1,1.5,2,3,4,5,6,8,10,15,
CCS,1.4797,1.3308,1.2240,1.0622,0.927,0.8663,0.803,0.7546,0.7074,0.667,0.6336,
0.6148,0.4722,0.4487,0.333,0.2434,0.2190,0.1797,0.153,0.1132,
DTYPEC,3, ABSORPTION
BESUS,1,15,2,3,4,5,6,7,8,9,1,1.5,2,3,4,5,6,8,10,15,
CCS,0,0,0,0,0,0,0,0,0,1,3-3,2,3-3,4,2-3,7,2-3,1,2-2,1,03-2,1,06-2,
2,04-2,3,12-2,
*****
DATA HL,3, CARBON
DTYPEC,3, COMPTON
BESUS,1,15,2,3,4,5,6,8,1,0,1.5,2,0,3,0,4,0,5,0,6,0,8,0,10,15,
CCS,2.76,2.86,2.45,2.12,1.9,1.735,1.605,1.41,1.267,1.03,0.878,0.691,0.576,
0.47,0.403,0.352,0.306,0.226,
DTYPEC,3, ABSORPTION
BESUS,1,15,2,3,4,5,6,8,1,0,1.5,2,0,3,0,4,0,5,0,6,0,8,0,10,15,
CCS,0.17,0.14,0.11,0.09,0.07,0.05,0.03,0.018,0.03,0.04,0.049,0.065,
0.03,0.05,
*****
DATA HL,3, IRON
DTYPEC,3, COMPTON
BESUS,1,15,2,3,4,5,6,8,1,0,1.5,2,0,3,0,4,0,5,0,6,0,8,0,10,15,
CCS,12.83,11.53,10.37,9.19,8.23,7.52,6.96,6.11,5.49,4.46,3.31,2.99,2.5,
2.13,1.701,1.357,1.226,0.81,
DTYPEC,3, ABSORPTION
BESUS,1,15,2,3,4,5,6,8,1,0,1.5,2,0,3,0,4,0,5,0,6,0,8,0,10,15,
CCS,19.1,15.4,12.27,0.66,0.29,0.16,0.1,0.05,0.03,0.022,0.12,0.35,0.561,0.752,
0.15,1.13,1.41,1.54,
*****
DATA HL,3, URANIUM
DTYPEC,3, COMPTON
BESUS,1,1163,15,2,3,4,5,6,8,1,1.5,2,3,4,5,6,8,10,15,
CCS,43.3,43.7,40.3,37.4,22.5,22.1,26.6,24.8,21.6,19.42,13.79,12.47,
11.59,8.82,7.62,6.74,5.51,4.62,3.47,
DTYPEC,3, ABSORPTION
BESUS,1,1162,1162,15,2,3,4,5,6,8,1,1.5,2,3,4,5,6,8,10,15,
CCS,274,237,1790,215,425,140,73,2,42,1,22,2,16,10,5,5.87,5.65,
0.99,8.56,10,11,23,13,43,13,52,19,7,
*****

```

PRECEDING PAGE BLANK NOT FILMED.

REFERENCES

1. Martin, J. T., Yalch, J. P., Edwards, W. E., "Shielding Computer Programs 14-0 and 14-1, Reactor Shield Analysis, " XDC 59-2-16, 23 January 1959.
2. Edwards, W. E., et al, "Reactor and Shield Physics, " APEX 918, 31 May 1962.
3. Capo, M. A., "Gamma Ray Absorption Coefficients for Elements and Mixtures, " APEX 628, August 1961.
4. Capo, M. A., "Polynomial Approximation of Gamma Ray Buildup Factors for a Point Isotropic Source, " APEX 510, November 1958.
5. Peterson, D. M., Los Alamos Scientific Laboratories; Private Communication Including Unnumbered Internal Documents, "QAD Notes, " obtained August 1964.
6. Lee, C. E., "The Discrete S_n Approximation to Transport Theory, " LA 2595, 9 March 1962.
7. Anderson, Ralph, Los Alamos Scientific Laboratories; Private Communication Including an Unnumbered Internal Document, "DDK Operating Instructions, " 7 August 1963.
8. Maskewitz, Betty, Oak Ridge Radiation Shielding Information Center; Private Communication.
9. MacDonald, J. E., Martin, J. T., and Yalch, J. P., "Specialized Reactor-Shield Monte Carlo Program 18-0, " GEMP-102, October 1961.

PRECEDING PAGE BLANK NOT FILMED.

10. Yalch, J. P. and MacDonald, J. E., "Program 20-2, A Program for Approximating Cross Section Dependence on Energy, " GEMP-113, June 1962.
11. Yalch, J. P. and MacDonald, J. E., "Program 20-3, A Program for Computation of Total Macroscopic Cross Section and Collision Probabilities for Specified Material Composition, " GEMP-114, June 1962.
12. Yalch, J. P. and MacDonald, J. E., "Program 20-4, A Program for Averaging Differential Scattering Cross Sections, " GEMP-115, June 1962.
13. Yalch, J. P. and MacDonald, J. E., "Program 20-5, A Program for Preparation of Spectrum Tables from Evaporation Model, " GEMP-116, June 1962.
14. Yalch, J. P. and MacDonald, J. E., "Program 20-6, A Program for Computing Nuclear Excitation and Transition Probabilities from Measured Gamma Ray Intensities, " GEMP-117, June 1962.
15. Martin, J.T., "Shield Region Data Converter Program 20-7, " APEX-605, April 1961.
16. MacDonald, J. E. and Martin, J. T., "Shielding Computer Program 20-0, " APEX-610, May 1961.
17. Yalch, J. P. and MacDonald, J. E., "Program 20-8, A Program for Interpreting Program 18-0 Source and Escape Particle Tapes, " GEMP-123, July 1962.
18. Hill, C. W., et al, "Computer Programs for Shielding Problems in Manned Space Vehicles, " ER 6643, January 1964.
19. Johnston, R. R., "A General Monte Carlo Neutronics Code, " LAMS 2856, 13 May 1963.

20. Carlson, B. G., Kazek, C. S., Lee, C. E., "FLOCO II Manual, " LAMS 2339, 13 October 1959.
21. Cashwell, E. D., Neengard, J. R., Los Alamos Scientific Laboratories; Private Communication Including an Unnumbered Internal Document, "General Monte Carlo for Gammas (MCG), " 23 September 1964.
22. Irving, D. C., et al, "O5R, A General Purpose Monte Carlo Neutron Transport Code, " ORNL-3622, February 1965.